EFI-09-10, MIFP-09-20

Electroweak Baryogenesis, CDM and Anomaly-free Supersymmetric $U(1)'$ Models

Junhai Kang, Paul Langacker[a], Tianjun Li[b,c] and Tao Liu[d]

[a] School of Natural Science, Institute for Advanced Study,
Einstein Drive, Princeton, NJ 08540, USA
[b] Key Laboratory of Frontiers in Theoretical Physics,
Institute of Theoretical Physics, Chinese Academy of Sciences,
Beijing 100190, P. R. China
[c] George P. and Cynthia W. Mitchell Institute for Fundamental Physics,
Texas A&M University, College Station, TX 77843, USA
[d] Enrico Fermi Institute, University of Chicago,
Chicago, IL 60637, USA

Abstract

We construct two anomaly-free supersymmetric $U(1)'$ models with a secluded $U(1)'$-breaking sector. For the one with E_6 embedding we show that there exists a strong enough first order electroweak phase transition for electroweak baryogenesis (EWBG) because of the large soft trilinear terms in the Higgs potential. Unlike the Minimal Supersymmetric Standard Model (MSSM), the stop masses can be very heavy. We then discuss possible CP violation in the Higgs sector, which can be both spontaneous and explicit, even at tree level. The spontaneous violation provides a direct source for baryogenesis, while its magnitude is mediated by an explicit phase from the secluded sector. These new CP sources do not introduce significant new contributions to electric dipole moments. EWBG in the thin wall (τ leptons) and thick wall regimes (top squarks, charginos and top quarks) are systematically discussed. We find that the CP-violating stop and chargino currents are very different from those obtained in the MSSM. Due to the space-dependence of the relevant CP phases, they do not require a variation of $\tan\beta$ in the bubble wall to have a non-trivial structure at the lowest order of Higgs insertion. In addition to τ leptons, top squarks and charginos, we find that top quarks can also play a significant role. Numerical results show that the baryon asymmetry is large enough to explain the cosmological observation today. We illustrate that EWBG and neutralino cold dark matter can be accommodated in the same framework, *i.e.*, there exists parameter space where a strong enough first order EWPT, large CP phase variations across the bubble wall, a reasonable baryon asymmetry as well as an acceptable neutralino dark matter relic density can be achieved simultaneously.

Contents

1 Introduction

The baryon asymmetry of the Universe (BAU) has been precisely measured by WMAP. Combining their five year results with other CMB and large scale structure results, they obtain [1]

$$\Omega_b h^2 \;=\; 0.02265 \pm 0.00059 \;, \tag{1}$$

in excellent agreement with the 95% C.L. range $0.017 - 0.024$ obtained from big bang nucleosynthesis [2]. This implies

$$\frac{n_B}{n_\gamma} \;=\; (6.21 \pm 0.16) \times 10^{-10} \;, \tag{2}$$

$$\frac{n_B}{s} \;=\; (8.82 \pm 0.23) \times 10^{-11} \;, \tag{3}$$

for the ratios of baryon density (n_B) to photon density (n_γ) and entropy (s).

To generate the baryon asymmetry, the Sakharov criteria [3] must be satisfied: (1) Baryon number (B) violation; (2) C and CP violation; (3) a departure from thermal equilibrium (or CPT violation). The first criterion is obvious. The second is required because if C and CP are exact symmetries, no net baryon number can be produced. Moreover, the equilibrium average of B is zero in thermal equilibrium by CPT, so the third criterion is necessary.

There are several baryogenesis scenarios: Grand Unified Theory (GUT) baryogenesis [4, 5, 6], Affleck-Dine baryogenesis [7], leptogenesis [8, 9], electroweak baryogenesis (EWBG) [10, 11, 12], etc. (For reviews, see [13, 14, 15, 16].) We will concentrate on EWBG, where the Sakharov criteria can be satisfied. Baryon number violation is induced by the anomalous sphaleron process, which violates $B + L$ but preserves $B - L$ at temperatures higher than the critical temperature T_c of the electroweak (EW) phase transition (EWPT) [17, 18, 19]. In addition, C is violated because the left- and right-handed fermions transform differently under $SU(2)_L \times U(1)_Y$. CP can be violated in the Standard Model (SM) and Minimal Supersymmetric Standard Model (MSSM) and their extensions by the Yukawa interactions, μ term, and soft supersymmetry breaking terms. Non-equilibrium processes may be obtained through the expansion of bubbles containing the true vacuum after the EWPT.

However, to preserve the generated baryon asymmetry after the EWPT, one needs a strong first order EWPT so that the sphaleron effects in the bubbles of true vacuum are shut down quickly. This requirement can be expressed as[1]

$$\frac{v(T_c)}{T_c} \gtrsim 1 \;, \tag{4}$$

where in the SM $v(T)$ is the vacuum expectation value of the Higgs field H^0 at temperature T and T_c is the critical temperature of the EWPT. Similarly, in the

[1]Some authors impose the weaker constraint $\sqrt{2}v(T_c)/T_c \gtrsim 1$.

MSSM

$$v(T) = \sqrt{v_1(T)^2 + v_2(T)^2}\ , \tag{5}$$

where $v_1(T)$ and $v_2(T)$ are respectively the VEVs of the two neutral Higgs fields H_d^0 and H_u^0. Our normalization is such that $v(0) \sim 174$ GeV.

In the SM, the EWPT can be strongly first order only if the Higgs mass is lighter than 40 GeV, which is inconsistent with the lower bound of 114.4 GeV from LEP [20] (recently, it was noticed that this tension can be relaxed in the SM, with an extra singlet introduced [21]). Furthermore, the CP violation from the CKM matrix is too small to generate a sufficient baryon asymmetry during the EWPT. In the MSSM there may be a small parameter space for EWBG [22]-[41]. There are additional sources of CP violation associated with the phases of the μ and supersymmetry breaking parameters. However, a strong enough first order EWPT requires that the lightest stop quark mass be smaller than the top quark mass $\sim$ 173 GeV, called the light stop scenario [28, 29, 30, 31, 32] (for recent work, also see [33, 34, 36, 37, 38, 39]). Also, the mass of the lightest CP-even Higgs must be smaller than 125 GeV, which leaves a small window above the current limit. In the Next-to-Minimal Supersymmetric Standard Model (NMSSM) [42] there is a trilinear term $A_h h S H_u H_d$ in the Higgs potential, where S is a singlet under the SM gauge group. This allows a strong enough first order EWPT [43, 44, 45, 46]. In the best-motivated versions of the NMSSM (motivated by the μ problem [47]), the effective μ parameter is given by $h\langle S\rangle$ (for recent studies, see [48]). However, the original versions involve a discrete Z_3 symmetry and serious cosmological domain wall problems [49]. These can be avoided by introducing an elementary bilinear μ term in the superpotential (or linear or quadratic terms in S), but at the cost of reintroducing the μ (or analogous) problems [44, 45]. The domain wall problem can also be avoided in an alternative version of the NMSSM [50], and in the nearly Minimal Supersymmetric Standard Model (nMSSM) [51, 52, 53], using a different discrete symmetry broken by a loop-induced tadpole. (For reviews, see [54].)

On the other hand, the possibility of an extra $U(1)'$ gauge symmetry [55] is well-motivated in superstring constructions [56], in grand unified theories [57], in models of dynamical symmetry breaking [58], and in little Higgs models [59]. In supersymmetric models, an extra $U(1)'$ can provide an elegant solution to the μ problem [60, 61], with an effective μ parameter generated by the VEV of the Standard Model singlet field S which breaks the $U(1)'$ symmetry. This is somewhat similar to the effective μ parameter in the NMSSM [42]. However, with a $U(1)'$ there are no extra discrete symmetries or domain wall problems. A closely related feature is that the MSSM upper bound of M_Z on the tree-level mass of the lightest Higgs scalar is relaxed, both in models with a $U(1)'$ and in the NMSSM, because of the hSH_uH_d term in the superpotential and the $U(1)'$ D-term [63]. Light Higgs masses lower than those allowed in the MSSM are also allowed experimentally because of possible mixings among the Higgs doublets and singlets [64, 65]. For specific $U(1)'$ charge assignments for the ordinary and exotic fields in some theories one can simultaneously ensure

the absence of anomalies; that all fields of the TeV-scale effective theory are chiral, avoiding a generalized μ problem; consistency with gauge coupling unification; and the absence of dimension-4 proton decay operators [66].

There are stringent limits on an extra Z' from direct searches from the Tevatron [67] and from indirect precision tests at the Z-pole, at LEP 2, and from weak neutral current experiments [68]. The constraints depend on the particular Z' couplings, but in typical models one requires $M_{Z'} > (800 - 1000)$ GeV and the $Z - Z'$ mixing angle $\alpha_{Z-Z'}$ to be smaller than a few $\times 10^{-3}$. (The specific parameters considered here yield a Z' mass of around 1 TeV.) Thus, explaining the $Z - Z'$ mass hierarchy without fine-tuning is non-trivial. Two of us with J. Erler proposed a supersymmetric $U(1)'$ model with a secluded $U(1)'$-breaking sector (sMSSM) in which the squark and slepton spectra can mimic those of the MSSM, the EW symmetry breaking is driven by relatively large A terms, and a large Z' mass can be generated by the VEVs of additional SM singlet fields that are charged under the $U(1)'$ but do not directly contribute to the effective μ parameter [69]. If these fields are only weakly coupled to the SM fields, *i.e.*, by $U(1)'$ interactions and possibly soft SUSY-breaking terms, then the scale of VEVs in this sector is only weakly linked to the EW scale. In particular, we consider the situation in which there is an almost F and D flat direction involving these secluded fields, with the flatness lifted by a small Yukawa coupling λ. For a sufficiently small value for λ, the Z' mass can be arbitrarily large.

In this paper, we systematically study EWBG and its correlation with neutralino CDM in the sMSSM (for a discussion on EWBG in the thin wall regime in the sMSSM, also see [70]). We construct two explicit anomaly-free models. In Model I, we embed the $SU(3)_C \times SU(2)_L \times U(1)_Y \times U(1)'$ gauge symmetry into a subgroup of E_6. We consider three families of the SM fermions as arising from three fundamental **27** representations of E_6. The **27**'s also contain candidates for the Higgs doublets, SM singlets (needed to break the $U(1)'$), and additional exotic fields. Additional vector-like pairs from $\mathbf{27} + \mathbf{27}^*$ representations can also exist at low energy without introducing anomalies. Consistency with gauge coupling unification is achieved by introducing one pair of vector-like Higgs-type doublets from $\mathbf{27} + \mathbf{27}^*$ [71][2], while the necessary $U(1)'$ breaking and the generation of masses for the exotic fermions is achieved by introducing three pairs of vector-like SM singlets from two pairs of $\mathbf{27} + \mathbf{27}^*$. The spectrum of exotics is rather complicated in Model I. In contrast, in Model II we add the minimal number of exotic particles with rational $U(1)'$ charges to cancel the $U(1)'$ anomalies. This model has the minimal exotic particle content but does not respect the simplest form of gauge coupling unification. We present the general superpotential and the supersymmetry breaking soft terms for both models.

For concreteness, we will work in Model I (the E_6 embedding). First, we discuss the one-loop effective potential at finite temperature in the 't Hooft-Landau gauge in the $\overline{MS}$-scheme. We calculate the gauge boson, Higgs, neutralino, chargino, squark, and slepton mass matrices, and those for the scalar components of the exotic chiral

[2]These are in addition to those in the three **27**'s. It is not important for our purposes which ones correspond to the two MSSM Higgs doublets.

superfields. We also calculate the temperature dependent masses for the Higgs fields, the longitudinal components of the gauge bosons, squarks, sleptons, and the scalar components of the exotic chiral superfields. There are two relevant phase transitions as the temperature decreases: the $U(1)'$ symmetry is broken at about 1 TeV, and the EW symmetry at the weak scale. We show that there exists strong enough first order EWPT because of the large trilinear term $A_h h S H_u H_d$ in the tree-level Higgs potential. Thus, unlike the MSSM, the stop masses can be very heavy compared to the top quark mass. The EWPT features in model II or the other possible anomaly-free embeddings are similar, because the exotic particles' contributions to the one-loop effective potential at finite temperature are suppressed by their heavy masses.

Subsequently, we discuss possible CP violation introduced by the extended Higgs sector of the sMSSM. As first pointed out in [70], unlike the MSSM in which there is no CP-violation in the Higgs sector at tree level, both explicit and spontaneous violation (denote them as ECPV and SCPV) can occur. There are five complex parameters in the supersymmetry breaking soft terms and only four gauge-independent Higgs phase degrees of freedom, which implies that one of these complex phases cannot be removed by field redefinition. The CP-symmetry of this tree-level potential can therefore be explicitly broken. In addition, as a result of balancing different terms in the minimization of the tree-level neutral Higgs potential, the phases of the Higgs fields can obtain non-trivial VEVs, which implies that CP symmetry can also be spontaneously broken. With loop corrections included, there may coexist vacua at finite temperature with broken and unbroken EW symmetry. The values of the spontaneous CP phases are usually different in these vacua.

In this work SCPV provides a direct source for baryogenesis, while its magnitude is mediated by an explicit phase from the secluded sector[3]. These new CP sources do not introduce significant new contributions to the electric dipole moments (EDMs) of the electron and neutron. After proper field redefinitions, the CP-violation phases will only appear in the Higgs mass matrix through soft masses associated with singlet components. Numerical estimates show that, for typical parameter values, their contributions to EDMs will be about six or seven orders of magnitude smaller than the experimental upper limits. These contributions disappear completely in the limit with a trivial explicit CP phase, where the spontaneous CP phases are absent in the true vacuum but not where EWBG occurs.

In the early Universe the first order EWPT is realized by nucleating bubbles of the broken phase. The dynamical properties of these bubbles, such as the wall profile and expansion velocity, can have important influences on the production of the baryon asymmetry. We also study their physics in detail. The VEVs of the Higgs fields (including both their magnitudes and phases) are space-dependent, as one crosses the bubble wall. The bubble wall thickness is estimated by minimizing

[3]We turn off all CP-violating sources beyond the Higgs sector, e.g., the ones from soft gaugino and sfermion masses, which are generally used for EWBG in supersymmetric models. Though they may provide non-trivial contributions to EWBG, these CP phases usually suffer strong constraints from electric dipole moments.

the action under the kink ansatz [72, 73, 74]. Numerical results show that it varies from 3 T_c^{-1} to 30 T_c^{-1} as an approximately monotonically increasing function of the phase changes of the Higgs fields. In addition, we argue that the wall velocity in the sMSSM cannot be larger than that in the MSSM under the same phase transition condition and thus should be non-relativistic. This fact implies that EW sphaleron processes have more time to occur and hence will enhance the final baryon asymmetry.

We then systematically study non-local EWBG in both the thin wall and thick wall regimes. Non-local baryogenesis has a great advantage over the local one [75]: the baryon number violation processes take place in an effective volume extending from the wall surface to a region in the symmetric phase, and thus we may expect an enhancement in the generation of the baryon asymmetry. According to the bubble wall profile, we calculate the contribution from τ leptons in the thin wall regime, and the ones from stop, charginos and top quarks in the thick wall regime. We find that the CP-violating currents induced by stops and charginos are very different from those obtained in the MSSM: (1) the current of the $v_1\partial v_2 - v_2\partial v_1$ type (in our formalism, the concrete expression is a little different) never requires $\partial \tan\beta \neq 0$ in the bubble wall due to the variance of the relevant CP phases crossing the wall[4]; (2) there is a new type of CP-violating current at the leading order which is proportional to $v_i v_i$ with $i = 1, 2$ and is absent in the MSSM. The CP-violating current of the new type has important influence on the EWBG. First, the stop contribution can be quadratically enhanced by a large soft A_{h_t} parameter. Second, in addition to τ leptons, top squarks and charginos, top quarks can also play a significant role in the EWBG. All of these features are results of the SCPV-driven EWBG, so they are not sensitive to the concrete embeddings of the sMSSM. Numerical calculations show that the produced baryon asymmetry is large enough to explain the cosmological observation today. Though the EWBG is directly driven by SCPV, there is no dilution problem between matter and anti-matter bubbles. Such a dilution is caused by a Z_2 discrete symmetry which usually exists in the SCPV scenarios. In our work, however, this symmetry has been explicitly broken at tree level by the explicit CP-violating phase.

We also study the correlation between EWBG and cold dark matter (CDM) in the sMSSM. Large trilinear soft parameters (used for strong enough first order EWPT) more often arise from gravity-mediated SUSY breaking, where the lightest supersymmetric particle (LSP) is usually the lightest neutralino. We study the possibility of describing the EWBG and neutralino CDM in the same framework. Though we do not scan the whole parameter space, we find that there indeed exist some regions where strong enough first order EWPT, large CP phase variations across the bubble wall, reasonable baryon asymmetry, as well as acceptable neutralino LSP relic density can be achieved simultaneously. The relevant neutralino mass $m_{\chi_1^0}$ is close to

[4]In the MSSM, there also exists a CP-violating current of the $v_1\partial v_2 + v_2\partial v_1$ type for charginos which arises from a resummation of corrections associated with higher order Higgs insertions or multiple scattering effects in the bubble wall. Though not suppressed by $\partial \tan\beta$, the current of this type is usually subdominant unless $\partial \tan\beta$ is suppressed (in our model it is always subdominant). For relevant or more general discussions, see [76, 77, 26, 27, 29, 30, 31, 32]. We will therefore not discuss the currents of this type.

$M_Z/2$. Finally, we comment briefly on possible cosmological signals: superconducting cosmic strings and gravitational waves (GWs). We expect that particle emission from the decays of cosmic strings and GWs from EWPT may be observed within the foreseeable future.

This paper is organized as follows. We briefly review the tree-level Higgs potential in the sMSSM and construct two anomaly-free embeddings in Section 2. The one-loop effective potential at finite temperature is considered in Section 3. In Section 4, we show that the EWPT is strongly first order. We study CP violation in Section 5 and the bubble wall physics in Section 6. In Section 7, we systematically study non-local EWBG in both the thin wall and thick wall regimes, and discuss the contributions from leptons, squarks, charginos and quarks in detail. In Section 8, we illustrate that there exists common parameter space where the baryon asymmetry and the CDM can both be explained by EWBG and neutralino LSP, respectively. Some simple comments on the cosmological signals of cosmic string decays and GWs are given in Section 9. The last section is our discussion and conclusions.

2 Two Anomaly-free $U(1)'$ Models

Let us briefly review the sMSSM [69]. There are one pair of Higgs doublets, H_u and H_d, and four SM singlets, S, S_1, S_2, and S_3. The $U(1)'$ charges for the Higgs fields satisfy

$$Q'_{H_d} + Q'_{H_u} + Q'_S = 0, \quad Q'_S = -Q'_{S_1} = -Q'_{S_2} = \frac{1}{2} Q'_{S_3}. \tag{6}$$

The superpotential for the Higgs is

$$W_H \;=\; hSH_uH_d + \lambda S_1 S_2 S_3 \;, \tag{7}$$

where the Yukawa couplings h and λ are respectively associated with the effective μ term and with an (almost) F and D-flat direction. For simplicity, we assume that terms such as $S_1^2 S_3, S_2^2 S_3$ and their associated soft terms are absent, and that there are no bilinears $SS_{1,2}$ in W_H. The existence of a number of SM singlets and the non-diagonal nature of the superpotential is in part motivated by explicit superstring constructions [78]. The corresponding F-term scalar potential is

$$\begin{aligned} V_F \;=\; & h^2 \left(|H_d^0|^2 |H_u^0|^2 + |S|^2 |H_d^0|^2 + |S|^2 |H_u^0|^2 \right) \\ & + \lambda^2 \left(|S_1|^2 |S_2|^2 + |S_2|^2 |S_3|^2 + |S_3|^2 |S_1|^2 \right) \;. \end{aligned} \tag{8}$$

The D-term scalar potential for the neutral fields is

$$\begin{aligned} V_D \;=\; & \frac{G^2}{8} \left(|H_u^0|^2 - |H_d^0|^2 \right)^2 \\ & + \frac{1}{2} g_{Z'}^2 \left(Q'_S |S|^2 + Q'_{H_d} |H_d^0|^2 + Q'_{H_u} |H_u^0|^2 + \sum_{i=1}^{3} Q'_{S_i} |S_i|^2 \right)^2 \;, \end{aligned} \tag{9}$$

where $G^2 = g_1^2 + g_2^2$; g_1, g_2, and $g_{Z'}$ are the coupling constants for $U(1)$, $SU(2)_L$ and $U(1)'$; and Q'_ϕ is the $U(1)'$ charge of the field ϕ.

In addition, one introduces the supersymmetry breaking soft terms

$$\begin{aligned} V_{soft}^H &= m_{H_d}^2 |H_d^0|^2 + m_{H_u}^2 |H_u^0|^2 + m_S^2 |S|^2 + \sum_{i=1}^{3} m_{S_i}^2 |S_i|^2 \\ &\quad - \left(A_h h S H_d^0 H_u^0 + A_\lambda \lambda S_1 S_2 S_3 + m_{SS_1}^2 S S_1 \right. \\ &\quad \left. + m_{SS_2}^2 S S_2 + m_{S_1 S_2}^2 S_1^\dagger S_2 + \text{H.C.} \right) \ . \end{aligned} \tag{10}$$

$m_{SS_i}^2, i = 1, 2$ are needed to break two unwanted global $U(1)$ symmetries (for a recent discussion of such global symmetries, see [79]). There is an almost F and D flat direction involving S_i, with the flatness lifted by a small Yukawa coupling λ. For a sufficiently small value of λ, the Z' mass can be arbitrarily large. For example, if $h \sim 10\lambda$, one can generate a $Z - Z'$ mass hierarchy in which the Z' mass is of order 1 TeV. The dimensional parameters in V_{soft}^H are specified in arbitrary units, and then rescaled after the (effective) potential is minimized so that the EW scale is $v = \sqrt{v_1^2 + v_2^2} \sim 174$ GeV, with $v_1 = \langle H_u^0 \rangle$ and $v_2 = \langle H_d^0 \rangle$.

In [69], $m_{S_1 S_2}^2$ was set to 0 for simplicity. In that case, the fields can be defined so that A_h, A_λ, $m_{SS_1}^2$, and $m_{SS_2}^2$ are all real and positive. The minimum then occurs at a point at which all of the fields are real and positive, i.e., there is no CP violation in the tree-level Higgs potential. For $m_{S_1 S_2}^2 \neq 0$, however, there will in general be CP violation.

The $U(1)'$ charges for the fermions and the anomaly cancellations were not discussed in Ref. [69], so in the following two subsections we construct two anomaly-free models, one of which is consistent with minimal gauge coupling unification.

2.1 Model I: sMSSM with E_6 Embedding

$U(1)'$ models necessarily imply that new fermions are needed for anomaly cancellations [55, 66]. Since all complete representations of E_6 are anomaly-free, it is convenient and conventional to simply consider the $U(1)'$ charge assignment and exotic particle content of E_6 as an example of an anomaly-free construction. We are not considering a full E_6 grand unified theory, because a light Z' would prevent a large doublet-triplet splitting, leading to rapid proton decay if the E_6 Yukawa relations were enforced. (Detailed studies of E_6 theories with broken Yukawa relations may be found in [80].)

The E_6 gauge group can be broken as [81, 82]

$$E_6 \to \ SO(10) \times \ U(1)_\psi \to \ SU(5) \times \ U(1)_\chi \times \ U(1)_\psi \ . \tag{11}$$

The $U(1)_\psi$ and $U(1)_\chi$ charges for the E_6 fundamental **27** representation are given in Table 1. The $U(1)'$ in Model I is one linear combination of the $U(1)_\chi$ and $U(1)_\psi$

$$Q' \ = \ \cos\theta \ Q_\chi + \sin\theta \ Q_\psi \ , \tag{12}$$

Table 1: Decomposition of the E_6 fundamental **27** representation under $SO(10)$, $SU(5)$, and the $U(1)_\chi$, $U(1)_\psi$ and $U(1)'$ charges.

$SO(10)$	$SU(5)$	$2\sqrt{10}Q_\chi$	$2\sqrt{6}Q_\psi$	$2\sqrt{15}Q$
16	10 $(u, d, \bar{u}, \bar{e})$	–1	1	$-1/2$
	$\bar{5}$ $(\bar{d}, \nu, e)$	3	1	4
	$1\bar{N}$	–5	1	–5
10	5 (D, H'_u)	2	–2	1
	$\bar{5}$ $(\bar{D}, H'_d)$	–2	–2	$-7/2$
1	1 S_L	0	4	$5/2$

where the angle θ will be chosen to ensure the needed $U(1)'$ charges for the SM singlets. For simplicity, we assume that the other $U(1)$ gauge symmetry from the orthogonal linear combination of the $U(1)_\chi$ and $U(1)_\psi$ is absent or broken at a high scale.

We assume three **27**s, which include three families of the SM fermions, one pair of Higgs doublets (H_u and H_d), and a number of SM singlets, extra Higgs-like doublets, and other exotics. The embeddings of the SM fermions are obvious. For definiteness, we assume that the Higgs doublets (H_u and H_d) are the doublets in **10** (or **5** and $\bar{\mathbf{5}}$) in the third **27**. (Of course, the exact identification of the H_u, H_d and S with specific **27**s is irrelevant.) In addition, we assume that the four SM singlets S, S_1, S_2, S_3 are the S_L, S_L^*, S_L^* and $\bar{N}^*$, respectively, in two (partial) pairs of **27** and $\mathbf{27}^*$. To cancel the $U(1)'$ anomalies, we introduce X and X_3, which are S_L and $\bar{N}$, respectively, in the two pairs. Thus, (S, S_1), (X, S_2) and (X_3, S_3) are three pairs of vector-like SM singlets and will not introduce any anomalies. To be consistent with minimal gauge coupling unification, we introduce one pair of vector-like doublets H'_u and $\bar{H}'_u$ from a pair of $\mathbf{27}+\mathbf{27}^*$ [71]. For simplicity, we assume that the other particles in the $\mathbf{27}+\mathbf{27}^*$ pairs are absent or are very heavy and decouple at low energy. From the requirement $Q_S = \frac{1}{2}Q_{S3}$, *i.e.*, $Q_{S_L} = \frac{1}{2}Q_{\bar{N}^*}$, we obtain

$$\tan\theta \;=\; \frac{\sqrt{15}}{9}\;. \tag{13}$$

The exotic particles in Model I are D_i, $\bar{D}_i$, S_L^i, $\bar{N}_i$, where $i = 1, 2, 3$; $H_u'^k$ and $\bar{H}_d'^k$, where $k = 1, 2$; X, X_3; and H'_u and $\bar{H}'_u$. The $U(1)'$ charges for the Standard Model fermions and exotic particles are also given in Table 1.

The general superpotential is $W_H + W_Y$, where

$$\begin{aligned} W_Y \;=\;& \alpha S X X_3 + \alpha^N_{ij} S S^i_L \bar{N}_j + \mu' \bar{H}'_u H'_u + h^u_{ij} Q_i H_u \bar{u}_j + h^d_{ij} H_d Q_i \bar{d}_j + h^e_{ij} H_d L_i \bar{e}_j \\ & + h^N_{ij} H_u L_i \bar{N}_j + \alpha^D_{ij} S D_i \bar{D}_j + \alpha^{H'}_{kl} S H'^k_u H'^l_d + \lambda^u_{ij} Q_i H'_u \bar{u}_j \\ & + \lambda^N_{ij} H'_u L_i \bar{N}_j + \lambda^1_{ijm} D_i \bar{u}_j \bar{e}_m + \lambda^2_{ijm} \bar{D}_i Q_j L_m + \lambda^3_{ijm} D_i \bar{d}_j \bar{N}_m \\ & + \lambda^4_{ijm} D_i Q_j Q_m + \lambda^5_{ijm} \bar{D}_i \bar{u}_j \bar{d}_m + \lambda^6_{ki} \phi S_k S^i_L + M_\phi \phi^2 \;, \end{aligned} \tag{14}$$

with $Q_i = (u_i, d_i)$, $L_i = (\nu_i, e_i)$, and $i, j, m = 1, 2, 3$ while $k, l = 1, 2$. For simplicity, we will assume that the Yukawa couplings h^u_i, h^d_{ij}, h^e_{ij} and h^N_{ij} and those associated with the exotics are diagonal in the numerical calculations. In addition, to explain the neutrino masses and mixings, we introduce a SM singlet ϕ which is neutral under $U(1)'$. Integrating out ϕ, we obtain the non-renormalizable terms $S_k S_l S^i_L S^j_L / M_\phi$, and then Majorana mass terms for $S^i_L S^j_L$ will appear after $U(1)'$ breaking. Thus, the light neutrino masses and mixings in Model I can be generated via a double-see-saw mechanism naturally [83, 84]. We see from Eq. (14) that all of the exotics except $\bar{H}'_u$ and H'_u can have masses generated by the VEV of S. The latter can be given a supersymmetric mass μ'. This reintroduces a form of the μ problem, though not for the Higgs fields associated with EW symmetry breaking, and is clearly a flaw of the specific construction. However, this segment of the model is only loosely connected with the issue of concern in this paper, *i.e.*, EWBG, so we will tolerate it rather than going to a more complicated model.

The new scalar supersymmetry breaking soft terms (in addition to Eq. (10)) are

$$\begin{aligned} V^A_{soft} \;=\; & -A_\alpha \alpha S X X_3 - A_{\alpha^N_{ij}} \alpha^N_{ij} S S^i_L \bar{N}_j - B_{\mu'} \mu' \bar{H}'_u H'_u - A_{h^u_{ij}} h^u_{ij} Q_i H_u \bar{u}_j \\ & - A_{h^d_{ij}} h^d_{ij} H_d Q_i \bar{d}_j - A_{h^e_{ij}} h^e_{ij} H_d L_i \bar{e}_j - A_{h^N_{ij}} h^N_{ij} H_u L_i \bar{N}_j - A_{\alpha^D_{ij}} \alpha^D_{ij} S D_i \bar{D}_j \\ & - A_{\alpha^{H'}_{kl}} \alpha^{H'}_{kl} S H'^k_u H'^l_d - A_{\lambda^u_{ij}} \lambda^u_{ij} Q_i H'_u \bar{u}_j - A_{\lambda^N_{ij}} \lambda^N_{ij} H'_u L_i \bar{N}_j \\ & - A_{\lambda^1_{ijm}} \lambda^1_{ijm} D_i \bar{u}_j \bar{e}_m - A_{\lambda^2_{ijm}} \lambda^2_{ijm} \bar{D}_i Q_j L_m - A_{\lambda^3_{ijm}} \lambda^3_{ijm} D_i \bar{d}_j \bar{N}_m \\ & - A_{\lambda^4_{ijm}} \lambda^4_{ijm} D_i Q_j Q_m - A_{\lambda^5_{ijm}} \lambda^5_{ijm} \bar{D}_i \bar{u}_j \bar{d}_m - A_{\lambda^6_{ki}} \lambda^6_{ki} \phi S_k S^i_L \\ & - B_\phi M_\phi \phi^2 + \text{ H.C.}, \end{aligned} \tag{15}$$

$$\begin{aligned} V^m_{soft} \;=\; & \sum_{i=1}^{3} \Big(m^2_{\tilde{Q}_i} |\tilde{Q}^2_i| + m^2_{u^i_R} |\tilde{\bar{u}}_i|^2 + m^2_{d^i_R} |\tilde{\bar{d}}_i|^2 + m^2_{\tilde{L}_i} |\tilde{L}^2_i| + m^2_{e^i_R} |\tilde{\bar{e}}_i|^2 \\ & + m^2_{\tilde{\bar{N}}_i} |\tilde{\bar{N}}_i|^2 + m^2_{S^i_L} |S^i_L|^2 + m^2_{\tilde{D}_i} |\tilde{D}_i|^2 + m^2_{\tilde{\bar{D}}_i} |\tilde{\bar{D}}_i|^2 \Big) \\ & + \sum_{k=1}^{2} \Big(m^2_{H'^k_u} |H'^k_u|^2 + m^2_{H'^k_d} |H'^k_d|^2 \Big) + m^2_\phi |\phi|^2 \\ & + m^2_{\tilde{X}} |\tilde{X}|^2 + m^2_{\tilde{X}_3} |\tilde{X}_3|^2 + m^2_{H'_u} |H'_u|^2 + m^2_{\bar{H}'_u} |\bar{H}'_u|^2, \end{aligned} \tag{16}$$

where we have assumed that the mass-squared terms are diagonal. We assume that only $S,\ S_1,\ S_2,\ S_3,\ H^0_u$, and H^0_d acquire VEVs.

The vector-like particles H'_u and $\bar{H}'_u$ can decay via the Yukawa λ^u_{ij} and λ^N_{ij} terms in Eq. (14). In addition, the charged exotic particles D_i and $\bar{D}_i$ can decay through the Yukawa λ^n_{ijm} terms with $n = 1,\ 2, ...,\ 5$ in Eq. (14) [82, 85]. However, to avoid the proton decays via dimension-5 operators, we must forbid some of the Yukawa λ^n_{ijm} terms. For example, we can choose $\lambda^n_{ijm} = 0$ either for $n = 1,\ 2,\ 3$ or for $n = 4,\ 5$.

2.2 Model II: Minimal Anomaly-free Model

In this subsection, we consider the minimal sMSSM in which all the particles have rational $U(1)'$ charges. In order to cancel the gauge and gauge-gravity mixed anomaly due to the $U(1)'$ gauge symmetry, we introduce the exotic particles D_1, $\bar{D}_1$, D_2, $\bar{D}_2$, V, $\bar{V}$, X_1, $\bar{X}_1$, X_2, $\bar{X}_2$, X_3, $\bar{X}_3$, X_4, and $\bar{X}_4$. The quantum numbers under $SU(3)_C \times SU(2)_L \times U(1)_Y \times U(1)'$ for the SM fermions, Higgs fields and extra exotic particles are given in Table 2. If one allowed irrational $U(1)'$ charges, only $\bar{D}_1$, D_2, $\bar{D}_2$, V, and $\bar{V}$ would be needed.

With the $U(1)'$ charge assignments for the particles in Table 2, the conditions for $[SU(3)_C]^2U(1)'$ and $[\text{Gravity}]^2U(1)'$ are automatically satisfied, and the condition for $[SU(2)_L]^2U(1)'$ is the same as that for $[U(1)_Y]^2U(1)'$. The anomaly-free conditions for $[SU(2)_L]^2U(1)'$, $U(1)_Y[U(1)']^2$ and $[U(1)']^3$, respectively, are

$$c_1 + c_2 + 3(a+3b) = 0 \ , \tag{17}$$

$$\begin{aligned} &-3a^2 + 3b^2 + 3(a+c_1)^2 - 6(b+c_2)^2 + 3(b+c_1)^2 - c_1^2 + c_2^2 \\ &-d_1^2 + (s+d_1)^2 - d_2^2 + (2s+d_2)^2 - d_3^2 + (2s+d_3)^2 = 0 \ , \end{aligned} \tag{18}$$

$$\begin{aligned} &6a^3 - 3(a+c_2)^3 - 3(a+c_1)^3 + 18b^3 - 9(b+c_2)^3 - 9(b+c_1)^3 \\ &+3d_1^3 - 3(s+d_1)^3 + 3d_2^3 - 3(2s+d_2)^3 + d_3^3 - (2s+d_3)^3 \\ &+2d_4^3 - (d_4-s)^3 - (d_4+s)^3 + 7s^3 + 2c_1^3 + 2c_2^3 = 0 \ . \end{aligned} \tag{19}$$

The simplest solution is $c_1 = 9/10$, $c_2 = 9/10$, $s = -9/5$, $a = -18/5$, $b = 1$, $d_1 = -2$, $d_2 = -1/5$, $d_3 = 9/5$, $d_4 = 27/10$, $d_5 = 9/10$, and $d_6 = -3$.

The general superpotential in Model II is

$$\begin{aligned} W \ = \ & \alpha_1 S D_1 \bar{D}_1 + \alpha_2 S_3 D_2 \bar{D}_2 + \alpha_3 S_3 V \bar{V} + \alpha_4 S_1 X_1 \bar{X}_1 + \alpha_5 S_2 X_1 \bar{X}_1 \\ & + \alpha_6 S X_2 \bar{X}_2 + \alpha_7 S_1 X_3 \bar{X}_3 + \alpha_8 S_2 X_3 \bar{X}_3 + \alpha_9 S X_4 \bar{X}_4 \\ & + \alpha'_1 S_1 X_1 X_1 + \alpha'_2 S_1 \bar{X}_1 \bar{X}_1 + \alpha'_3 S_2 X_1 X_1 + \alpha'_4 S_2 \bar{X}_1 \bar{X}_1 \\ & + h^u_{ij} Q_i H_u \bar{u}_j + h^d_{ij} H_d Q_i \bar{d}_j + h^e_{ij} H_d L_i \bar{e}_j + h^N_{ij} H_u L_i \bar{N}_j \\ & + \lambda^1_{ij} D_1 Q_i Q_j + \lambda^2_{ij} \bar{D}_2 \bar{u}_i \bar{d}_j + \lambda^3_i V \bar{e}_i X_1 + \lambda^4_i V \bar{e}_i \bar{X}_1 \ . \end{aligned} \tag{20}$$

All of the exotics can be made massive by $U(1)'$ breaking.

The charged exotic particles (D_i, $\bar{D}_i$), and (V, $\bar{V}$) can decay through the Yukawa λ^1_{ij}, λ^2_{ij}, λ^3_i and λ^4_i terms in Eq. (20) [82, 85], where we have assumed that $m_V > m_{X_1}$. After the $U(1)'$ breaking, the vector-like particles (X_i, $\bar{X}_i$) are neutral. There is no discrete symmetry after $U(1)'$ breaking, so the vector-like particles (X_i, $\bar{X}_i$) can decay via higher dimensional operators.

Table 2: Minimal Anomaly-free Model. Quantum numbers under $SU(3)_C \times SU(2)_L \times U(1)_Y \times U(1)'$ for the left-chiral Standard Model fermions (Q_i, $\bar{u}_i$, $\bar{d}_i$, L_i, $\bar{N}_i$, $\bar{e}_i$), Higgs fields (H_u, H_d, S, S_1, S_2, S_3), and extra exotic particles (D_1, $\bar{D}_1$, D_2, $\bar{D}_2$, V, $\bar{V}$, X_1, $\bar{X}_1$, X_2 and $\bar{X}_2$).

Particles	Quantum Numbers	Particles	Quantum Numbers
L_i	$(1;\, 2;\, -1/2;\, a)$	Q_i	$(3;\, 2;\, 1/6;\, b)$
$\bar{N}_i$	$(1;\, 1;\, 0;\, -(a+c_2))$	$\bar{u}_i$	$(\bar{3};\, 1;\, -2/3;\, -(b+c_2))$
$\bar{e}_i$	$(1;\, 1;\, 1;\, -(a+c_1))$	d_i	$(\bar{3};\, 1;\, 1/3;\, -(b+c_1))$
H_d	$(1;\, 2;\, -1/2;\, c_1)$	H_u	$(1;\, 2;\, 1/2;\, c_2)$
S	$(1;\, 1;\, 0;\, s)$	S_3	$(1;\, 1;\, 0;\, 2s)$
S_1	$(1;\, 1;\, 0;\, -s)$	S_2	$(1;\, 1;\, 0;\, -s)$
D_1	$(3;\, 1;\, -1/3;\, d_1)$	$\bar{D}_1$	$(\bar{3};\, 1;\, 1/3;\, -(s+d_1))$
D_2	$(3;\, 1;\, -1/3;\, d_2)$	$\bar{D}_2$	$(\bar{3};\, 1;\, 1/3;\, -(2s+d_2))$
V	$(1;\, 1;\, -1;\, d_3)$	$\bar{V}$	$(1;\, 1;\, 1;\, -(d_3+2s))$
X_1	$(1;\, 1;\, 0;\, d_4)$	X_1	$(1;\, 1;\, 0;\, -(d_4-s))$
X_2	$(1;\, 1;\, 0;\, d_5)$	X_2	$(1;\, 1;\, 0;\, -(d_5+s))$
X_3	$(1;\, 1;\, 0;\, d_6)$	X_3	$(1;\, 1;\, 0;\, -(d_6-s))$
X_4	$(1;\, 1;\, 0;\, d_6)$	X_4	$(1;\, 1;\, 0;\, -(d_6+s))$

3 One-Loop Effective Potential at Finite Temperature

In the 't Hooft-Landau gauge and in the $\overline{MS}$-scheme, the one-loop effective potential at finite temperature is [86]

$$V_{\rm eff}(\phi,T) \;=\; V_0(\phi) + V_1(\phi,0) + \Delta V_1(\phi,T) + \Delta V_{\rm daisy}(\phi,T)\;, \tag{21}$$

where $V_0(\phi)$ is the tree-level potential, $V_1(\phi,0)$ is the one-loop zero temperature correction, $\Delta V_1(\phi,T)$ is the temperature dependent one-loop correction, and $\Delta V_{\rm daisy}(\phi,T)$ is the multi-loop daisy correction. The explicit expressions for $V_0(\phi)$, $V_1(\phi,0)$, $\Delta V_1(\phi,T)$ and $\Delta V_{\rm daisy}(\phi,T)$ are

$$V_0(\phi) \;=\; V_F + V_D + V_{soft}^H\;, \tag{22}$$

$$V_1(\phi,0) \;=\; \sum_i \frac{n_i}{64\pi^2} m_i^4(\phi)\left[\log\frac{m_i^2(\phi)}{Q^2} - C_i\right]\;, \tag{23}$$

$$\Delta V_1(\phi,T) \;=\; \frac{T^4}{2\pi^2}\left\{\sum_i n_i\, J_i\left[\frac{m_i^2(\phi)}{T^2}\right]\right\}\;, \tag{24}$$

$$\Delta V_{\rm daisy}(\phi,T) \;=\; -\frac{T}{12\pi}\sum_{i=\rm bosons} n_i\left[\mathcal{M}_i^3(\phi,T)-m_i^3(\phi)\right]\;, \tag{25}$$

where $m_i(\phi)$ are field-dependent masses, n_i are the number of degrees of freedom, and C_i are constants dependent on the regularization scheme: in the $\overline{MS}$-scheme that we are assuming, $C_i = 5/6$ for the gauge bosons and $3/2$ for scalars and fermions[5]. The function J_i comes from the one-loop corrections to the effective potential at finite temperature [86]. For bosons

$$J_B(m^2(\phi)/T^2) = \int_0^\infty dx\; x^2 \log\left[1-e^{-\sqrt{x^2+\frac{m^2(\phi)}{T^2}}}\right]\;. \tag{26}$$

At relatively high temperature, $\frac{m(\phi)}{T} < 2.2$, one can expand [86]

$$\begin{aligned} J_B(m^2(\phi)/T^2)^{HT} \;=\; & -\frac{\pi^4}{45}+\frac{\pi^2}{12}\frac{m^2(\phi)}{T^2}-\frac{\pi}{6}\left(\frac{m^2(\phi)}{T^2}\right)^{3/2} \\ & -\frac{1}{32}\frac{m^4(\phi)}{T^4}\log\frac{m^2(\phi)}{a_b T^2}-2\pi^{7/2}\sum_{\ell=1}^{\infty}(-1)^\ell \\ & \frac{\zeta(2\ell+1)}{(\ell+1)!}\Gamma\left(\ell+\frac{1}{2}\right)\left(\frac{m^2(\phi)}{4\pi^2T^2}\right)^{\ell+2}\;, \end{aligned} \tag{27}$$

where $a_b = 16\pi^2\exp(3/2-2\gamma_E)$ ($\log a_b = 5.4076$) and ζ is the Riemann ζ-function. At relatively low temperature, $\frac{m(\phi)}{T} > 2.2$, we can expand [87]

$$\begin{aligned} J_B(m^2(\phi)/T^2)^{LT} \;=\; & -\frac{\pi^4}{45}+\left(\frac{\pi}{2}\right)^{1/2}\left(\frac{m(\phi)}{T}\right)^{3/2}e^{-m(\phi)/T} \\ & \left[1+\frac{15}{8}\frac{T}{m(\phi)}+...\right]\;. \end{aligned} \tag{28}$$

The function J_F for fermion ψ with mass m is [86]

$$J_F(m^2(\psi)/T^2) = \int_0^\infty dx\; x^2\log\left[1+e^{-\sqrt{x^2+\frac{m^2(\psi)}{T^2}}}\right]\;, \tag{29}$$

For $\frac{m(\psi)}{T} < 1.8$, one finds [86]

$$\begin{aligned} J_F(m^2(\psi)/T^2)^{HT} \;=\; & \frac{7\pi^4}{360}-\frac{\pi^2}{24}\frac{m^2(\psi)}{T^2}-\frac{1}{32}\frac{m^4(\psi)}{T^4}\log\frac{m^2(\psi)}{a_f T^2} \\ & -\frac{\pi^{7/2}}{4}\sum_{\ell=1}^{\infty}(-1)^\ell\frac{\zeta(2\ell+1)}{(\ell+1)!}\left(1-2^{-2\ell-1}\right) \\ & \Gamma\left(\ell+\frac{1}{2}\right)\left(\frac{m^2(\psi)}{\pi^2T^2}\right)^{\ell+2}\;, \end{aligned} \tag{30}$$

[5]For the $\overline{DR}$-scheme, C_i in Eq. (23) is $3/2$ for gauge bosons, scalars, and fermions. Our discussions and conclusions do not depend on the scheme.

where $a_f = \pi^2 \exp(3/2 - 2\gamma_E)$ ($\log a_f = 2.6351$). At low temperature, $\frac{m(\psi)}{T} > 1.8$ [87],

$$J_F(m^2(\psi)/T^2)^{LT} = \frac{7\pi^4}{360} + \left(\frac{\pi}{2}\right)^{1/2} \left(\frac{m(\psi)}{T}\right)^{3/2} e^{-m(\psi)/T} \left[1 + \frac{15}{8}\frac{T}{m(\psi)} + ...\right] . \quad (31)$$

The $m(\phi)$ and $m(\psi)$ are the Higgs field dependent masses from the eigenvalues of the mass matrices. Thus, we need the mass matrices for all the particles in the models. The tree-level mass matrices[6] for the particles in Model I are presented in Appendix A. (Those for the ordinary and exotic fermions are trivial.)

There are small discontinuities between the $J_B(m^2(\phi)/T^2)^{HT}$ and $J_B(m^2(\phi)/T^2)^{LT}$ at $\frac{m(\phi)}{T} \sim 2.2$, and between the $J_F(m^2(\phi)/T^2)^{HT}$ and $J_F(m^2(\phi)/T^2)^{LT}$ at $\frac{m(\phi)}{T} \sim 1.8$. When we numerically calculate the minimum of the potential, we need smooth interpolations for $J_B(m^2(\phi)/T^2)$ and $J_F(m^2(\phi)/T^2)$. Thus, in our numerical calculation we use the following approximation

$$J_B(m^2(\phi)/T^2) = \frac{\tanh(-m_i^2(\phi)/T^2 + 2.2^2) + 1}{2} \times J_B(m^2(\phi)/T^2)^{HT} + \frac{\tanh(m_i^2(\phi)/T^2 - 2.2^2) + 1}{2} \times J_B(m^2(\phi)/T^2)^{LT} , \quad (32)$$

$$J_F(m^2(\phi)/T^2) = \frac{\tanh(-m_i^2(\phi)/T^2 + 1.8^2) + 1}{2} \times J_F(m^2(\phi)/T^2)^{HT} + \frac{\tanh(m_i^2(\phi)/T^2 - 1.8^2) + 1}{2} \times J_F(m^2(\phi)/T^2)^{LT} . \quad (33)$$

The temperature dependent scalar mass-squared $\mathcal{M}_i^2(\phi, T)$ is obtained from the $m_i^2(\phi)$ by adding the leading temperature dependent self-energy contributions $\Pi_\Phi(T)$,

$$\mathcal{M}^2(\phi, T) = m^2(\phi) + \Pi_\Phi(T) , \quad (34)$$

where $\Pi_\Phi(T)$ is proportional to T^2 [88]. For the gauge bosons, only the longitudinal components receive such contributions. The $\Pi_\Phi(T)$'s for the particles in Model I are presented in Appendix B. The daisy corrections are of higher order, but important at high temperature.

[6]The use of tree-level mass matrices leads to a slight inconsistency when they are evaluated at the minimum of the full one-loop effective potential. In particular, the tree-level approximations to the Goldstone Boson masses are sometimes shifted slightly from zero. We avoid singularities by setting slightly negative mass-squares to zero. We have checked that these small shifts have negligible effects on the phase structure, as should be apparent from the formula (27) relevant for small $\frac{m(\phi)}{T}$.

Table 3: Three sets of typical parameter values. The energy units are 69 GeV, 92 GeV and 120 GeV, corresponding to $m^2_{H^0_d} = 5.0$, 9.0 and 13.0, respectively. In this paper, we will denote them as cases a, b and c. Note that the soft mass squares in the superpotential are relatively small, *i.e.*, the symmetry breaking is A-term dominant. M'_1, M_1 and M_2 denote the three neutral gaugino soft masses.

h	A_h	λ	A_λ	$m^2_{SS_1}$	$m^2_{SS_2}$	$m^2_{S_1S_2}$	$m^2_{H^0_d}$
0.8	4.2	0.06	3.3	0.02	0.1	4.8 $\times 10^{-4}$	5.0 / 9.0 / 13.0
$m^2_{H^0_u}$	m^2_S	$m^2_{S_1}$	$m^2_{S_2}$	$m^2_{S_3}$	M'_1	M_1	M_2
-0.1	0.5	0.03	0.03	0.03	1.5	1.5	3.0
$m^2_{\tilde{Q}_3}$	$m^2_{\tilde{u}^3_R}$	$m^2_{\tilde{d}^3_R}$	$m^2_{\tilde{Q}_{1,2}}$	$m^2_{\tilde{u}^{1,2}_R}$	$m^2_{\tilde{d}^{1,2}_R}$	$m^2_{\tilde{l}^{1,2,3}_L}$	$m^2_{\tilde{l}^{1,2,3}_R}$
8	8	25	25	25	25	25	25

4 The Electroweak Phase Transition

Generally, the EWPT in the sMSSM is more complicated than those in the SM, MSSM, and NMSSM due to the secluded $U(1)'$-breaking sector. The temperature dependent corrections to the effective potential are a function of the masses $\mathcal{M}_i(\phi, T)$. At low temperature, the temperature dependent corrections are negligible, while at very high temperature they are dominant. At the critical temperature, the temperature dependent corrections are comparable to the effective potential at zero temperature. Our one-loop effective potential is a function of 10 physical variables (the complex VEVs of the six neutral Higgs fields[7] minus two gauge degrees of freedom). There might exist local minima near the critical temperature. In our analysis we always choose the global minimum (at one-loop level plus daisy correction).

Because the Z' mass is assumed to be of order 1 TeV, the VEVs of the SM singlets S_1, S_2, and S_3 are about an order of magnitude larger than those of the Higgs doublets and S [69]. There are therefore two phase transitions: the $U(1)'$ symmetry breaking at TeV scale and the EW symmetry breaking at the weak scale.

In Figure 1, we plot the Higgs VEVs versus temperature for the given parameters values in case b (see Table 3). From the figure, one can see that the $U(1)'$ phase transition occurs just below 1200 GeV, and the EWPT at about 120 GeV. We are interested in whether the EWPT is strongly first order. From the figure, we also see that the VEVs of H^0_d, H^0_u and S all experience a first order transition due to their discontinuity at the weak scale. The magnitudes of the VEVs of the Higgs fields are plotted at the global minimum of the potential for the given temperature. There is an abrupt change in the S_i VEVs at temperatures around 400–450 GeV because another

[7]We ignore the possibility of charge or color breaking minima.

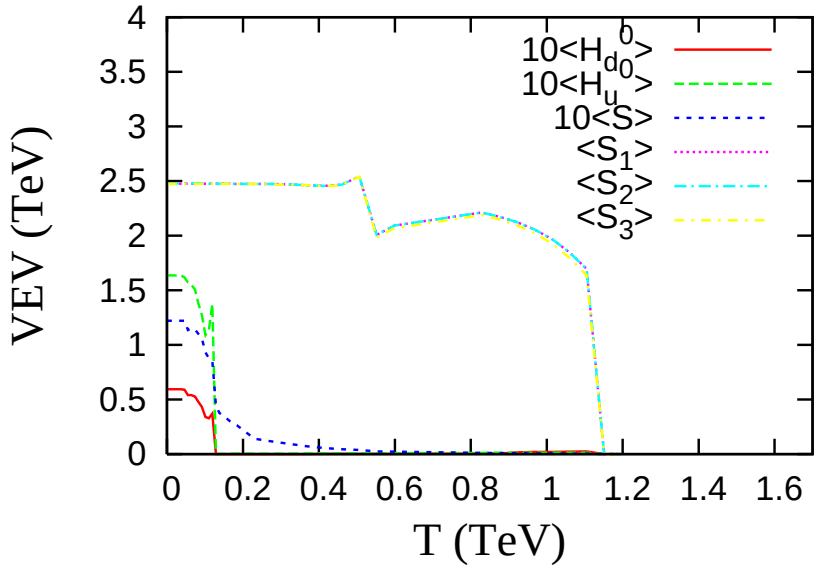

Figure 1: The Higgs VEVs vs. temperature T. The VEVs of $H^0_{u,d}$ and S are multiplied by 10. The VEVs of S_1, S_2 and S_3 are indistinguishable.

local minimum becomes the global one[8].

After the $U(1)'$ symmetry is broken, S_1, S_2, and S_3 have non-zero VEVs of order 2 TeV, while the VEVs for H^0_d and H^0_u are still zero. The supersymmetry breaking soft terms $m^2_{SS_1}SS_1$ and $m^2_{SS_2}SS_2$ generate a linear term for S in the potential after the $U(1)'$ symmetry breaking, which induces a non-zero VEV for S. At high temperature, $\langle S\rangle$ is tiny because $m^2_{SS_1}$ and $m^2_{SS_2}$ are small and the temperature dependent corrections to the S mass are large. At lower temperature, $\langle S\rangle$ becomes larger, as can be seen from Figure 1. At the EWPT the term $A_h h S H_u H_d$ induces a first order phase transition in the VEV of S as well.

The first order EWPT can be strong because of the trilinear term $A_h h S H_u H_d$ in the tree-level potential. Unlike in the MSSM [30, 31, 32], in which the phase transition is associated with loop effects, there is no upper bound on the lightest stop mass. This feature is independent of the concrete embeddings of the sMSSM, though we are using an effective potential of finite temperature in Model I as an illustration. This feature is also shared by the NMSSM [43, 44, 45, 46], the nMSSM [51, 52], the $U(1)'$ models with no secluded sector [89], and the singlet extensions of the SM [21].

In Table 4, we calculate $v(T_c)/T_c$ versus the stop soft mass square $m^2_{\tilde{Q}_3}$, $m^2_{\tilde{u}^3_R}$ and A_h while the other parameters are fixed to the values given by Table 3 with the

[8]In a real transition the fields would most likely remain in the same minimum, but that would have little effect on our conclusions. Detailed investigations of issues such as these are very model dependent and beyond the scope of this investigation.

Table 4: $v(T_c)/T_c$ versus the stop soft mass squares $m^2_{\tilde{Q}_3}$, $m^2_{\tilde{u}^3_R}$ and A_h, where the other parameters are fixed to the values in case b (see Table 3). For simplicity, we assume $m^2_{\tilde{Q}_3} = m^2_{\tilde{u}^3_R}$. The scales are different for different points, but typically they are about 100 GeV. The slashes in the table mean that there is no first order EWPT.

$m^2_{\tilde{Q}_3} = m^2_{\tilde{u}^3_R} \backslash A_h$	2.0	3.0	4.0	5.0
4.0	/	1.29	1.59	2.06
8.0	0.91	1.02	1.21	1.50
12.0	/	0.56	1.03	1.22
16.0	/	/	/	1.37

choice $m^2_{H^0_d} = 9.0$. The scales are different for different points, but typically they are about 100 GeV. As expected, when A_h decreases (with fixed $m^2_{\tilde{Q}_3}$ and $m^2_{\tilde{u}^3_R}$), $v(T_c)/T_c$ decreases. The first order EWPT is not strong enough when $A_h \leq 2 - 3$. This table also displays the dependence of $v(T_c)/T_c$ on $m^2_{\tilde{Q}_3}$ and $m^2_{\tilde{u}^3_R}$. For fixed A_h, the strength of the first order EWPT usually becomes weaker as $m^2_{\tilde{Q}_3}$ increases. Unlike the MSSM, even for heavy stop soft masses (or physical masses) one can still have a strong enough first order EWPT.

For simplicity, we did not turn on any CP phases for the discussion in this section. We will see later that the results obtained in this section are insensitive to these phases.

5 Generation of CP Violation

5.1 CP Violation at Tree Level

One nice feature of the sMSSM is that both ECPV and SCPV can happen in the Higgs sector at tree level [70]. This model involves six complex neutral fields. To study the CP-violation, we define

$$\begin{aligned} &H^0_d \equiv |H^0_d| e^{i\theta_1} \ , \ H^0_u \equiv |H^0_u| e^{i\theta_2} \ , \ S \equiv |S| e^{i\alpha} \ , \\ &S_1 \equiv |S_1| e^{i\alpha_1} \ , \ S_2 \equiv |S_2| e^{i\alpha_2} \ , \ S_3 \equiv |S_3| e^{i\alpha_3} \ . \end{aligned} \tag{35}$$

Among these six phase degrees of freedom, only four of them, which are given by

$$\begin{aligned} \beta_1 = \alpha + \alpha_1 \ , \ \beta_2 = \alpha + \alpha_2, \\ \beta_3 = \alpha + \theta_1 + \theta_2 \ , \ \beta_4 = \alpha_1 + \alpha_2 + \alpha_3 \ . \end{aligned} \tag{36}$$

are invariant under the $U(1)_Y$ and $U(1)'$ gauge transformations. The two remaining degrees of freedom

$$\Sigma_i Y_{\phi_i}\theta_{\phi_i}\ ,\ \Sigma_i Q'_{\phi_i}\theta_{\phi_i}\ , \tag{37}$$

correspond to Goldstone bosons associated with the two spontaneously broken gauge symmetries, and decouple from the Higgs sector. Here, Y_{ϕ_i} and Q'_{ϕ_i} are the $U(1)_Y$ and $U(1)'$ charges for ϕ_i, θ_{ϕ_i} is the phase of ϕ_i, and the index "ϕ_i" runs over all six complex Higgs fields. The complex phases of the Higgs fields θ_{ϕ_i} are linear combinations of the gauge-invariant and gauge-dependent components. Of course, physical consequences only depend on the gauge-invariant components.

There are five supersymmetry breaking complex parameters in the tree-level Higgs potential Eq (8-10), $A_h h$, $A_\lambda \lambda$, $m^2_{SS_1}$, $m^2_{SS_2}$ and $m^2_{S_1S_2}$. Four of the five complex phases can be resolved by $\beta_{1,2,3,4}$. Without loss of generality, we assume that

$$m^2_{S_1S_2} \ = \ |m^2_{S_1S_2}|e^{i\gamma}\ . \tag{38}$$

is complex and the other parameters are real and positive. If γ is not equal to zero or π, there will be ECPV at the tree level. Unlike the MSSM, SCPV can also occur at tree level in this model. Let us rewrite the supersymmetry breaking soft terms for the neutral Higgs bosons as

$$\begin{aligned} V^H_{soft} \ = \ & m^2_{H^0_d}|H^0_d|^2 + m^2_{H^0_u}|H^0_u|^2 + m^2_S|S|^2 + \sum_{i=1}^{3} m^2_{S_i}|S_i|^2 \\ & -2A_h h|S||H^0_d||H^0_u|\cos\beta_3 - 2A_\lambda\lambda|S_1||S_2||S_3|\cos\beta_4 \\ & -2m^2_{SS_1}|S||S_1|\cos\beta_1 - 2m^2_{SS_2}|S||S_2|\cos\beta_2 \\ & -2|m^2_{S_1S_2}||S_1||S_2|\cos(-\beta_1+\beta_2+\gamma). \end{aligned} \tag{39}$$

It is easy to see that a mildly dominant $m^2_{S_1S_2}$ soft term will make β_1 or $\beta_2 \neq 0, \pi$ for $\gamma \neq 0, \pi$ and hence lead to SCPV. Meanwhile, the strength of SCPV can be controlled by the explicit CP phase γ.

5.2 CP Violation at Finite Temperature

Explicit CP phases from soft parameters beyond the Higgs sector could also contribute to EWBG. However, it is advantageous to turn off these phases and use the spontaneous CP phases as the source for baryogenesis. To implement the EWPT, we need to include radiative corrections to the Higgs potential, as discussed in Section 3. At finite temperature there may coexist multiple vacua, in which spontaneous CP phases usually have different values. If the phase transition between two vacua is realized through bubble nucleation, as in a first order EWPT, these CP phases are space-dependent as one crosses the bubble wall. In the next sections we will see that the generated baryon asymmetry depends on these variations.

To make this more explicit, it is convenient to write the particle interactions during EWBG using the individual Higgs phases. We define the two gauge-dependent phases as A and B, given by

$$\begin{aligned} Y_{H_d^0}\theta_1 + Y_{H_u^0}\theta_2 + Y_S\alpha + \Sigma_i Y_{S_i}\alpha_i = A \ , \\ Q'_{H_d}\theta_1 + Q'_{H_u}\theta_2 + Q'_S\alpha + \Sigma_i Q'_{S_i}\alpha_i = B \ . \end{aligned} \tag{40}$$

Inverting Eq. (36) and Eq. (40), we obtain

$$\begin{aligned} \theta_1 &= -\frac{1}{5}\beta 1 - \frac{1}{5}\beta_2 + \frac{7}{15}\beta_3 + \frac{2}{15}\beta_4 - \frac{11}{25}A - \frac{4}{15}B \ , \\ \theta_2 &= -\frac{1}{5}\beta 1 - \frac{1}{5}\beta_2 + \frac{7}{15}\beta_3 + \frac{2}{15}\beta_4 + \frac{14}{25}A - \frac{4}{15}B \ , \\ \alpha &= \frac{2}{5}\beta 1 + \frac{2}{5}\beta_2 + \frac{1}{15}\beta_3 - \frac{4}{15}\beta_4 - \frac{3}{25}A + \frac{8}{15}B \ , \\ \alpha_1 &= \frac{3}{5}\beta 1 - \frac{2}{5}\beta_2 - \frac{1}{15}\beta_3 + \frac{4}{15}\beta_4 + \frac{3}{25}A - \frac{8}{15}B \ , \\ \alpha_2 &= -\frac{2}{5}\beta 1 + \frac{3}{5}\beta_2 - \frac{1}{15}\beta_3 + \frac{4}{15}\beta_4 + \frac{3}{25}A - \frac{8}{15}B \ , \\ \alpha_3 &= -\frac{1}{5}\beta 1 - \frac{1}{5}\beta_2 + \frac{2}{15}\beta_3 + \frac{7}{15}\beta_4 - \frac{6}{25}A + \frac{16}{15}B \ , \end{aligned} \tag{41}$$

where we have used the rescaled $U(1)_Y$ and $U(1)'$ charges for the Higgs particles in Model I

$$Y_{H_d^0} = -Y_{H_u^0} = -1 \ , \ Y_S = Y_{S_1} = Y_{S_2} = Y_{S_3} = 0 \ ; \tag{42}$$

$$Q'_{H_d} = \frac{-7}{20} \ , \ Q'_{H_u} = \frac{1}{10} \ , \ Q'_S = -Q'_{S_1} = -Q'_{S_2} = \frac{1}{2}Q'_{S_3} = \frac{1}{4} \ . \tag{43}$$

Because A and B correspond to the Goldstone bosons of the $U(1)_Y$ and $U(1)'$ breaking, they can be rotated away by gauge transformations.

The variations of the Higgs phases crossing the bubble wall are given by

$$\Delta\langle\theta_{\phi_i}\rangle = \langle\theta_{\phi_i}\rangle_t - \langle\theta_{\phi_i}\rangle_f, \tag{44}$$

where $\langle\theta_{\phi_i}\rangle_{f,t}$ are the values of the Higgs phases in the false and true vacua, respectively. More explicitly,

$$\begin{aligned} \Delta\theta_1 &= \Delta\theta_2 = -\frac{1}{5}\Delta\beta_1 - \frac{1}{5}\Delta\beta_2 + \frac{7}{15}\Delta\beta_3 + \frac{2}{15}\Delta\beta_4 \\ \Delta\alpha &= \frac{2}{5}\Delta\beta 1 + \frac{2}{5}\Delta\beta_2 + \frac{1}{15}\Delta\beta_3 - \frac{4}{15}\Delta\beta_4 \ , \\ \Delta\alpha_1 &= \frac{3}{5}\Delta\beta 1 - \frac{2}{5}\Delta\beta_2 - \frac{1}{15}\Delta\beta_3 + \frac{4}{15}\Delta\beta_4 \ , \\ \Delta\alpha_2 &= -\frac{2}{5}\Delta\beta 1 + \frac{3}{5}\Delta\beta_2 - \frac{1}{15}\Delta\beta_3 + \frac{4}{15}\Delta\beta_4 \ , \\ \Delta\alpha_3 &= -\frac{1}{5}\Delta\beta 1 - \frac{1}{5}\Delta\beta_2 + \frac{2}{15}\Delta\beta_3 + \frac{7}{15}\Delta\beta_4. \end{aligned} \tag{45}$$

These quantities are not uniquely defined, due to the uncertainties in the winding numbers of the $\langle\beta_i\rangle_{f,t}$. If there is a large difference between the winding numbers of $\langle\beta_i\rangle_f$ and $\langle\beta_i\rangle_t$, then $\Delta\theta_{\phi_i}$ can be large, and hence the variation of θ_{ϕ_i} in the bubble wall is also large. However, the nucleation rate for a phase transition between two such vacua is generically small [70], so we will require $|\beta_i| < \pi$.

Let us consider how $\Delta\theta_{\phi_i}$ is affected by the behavior of the related field variables in the wall. For a qualitative discussion, we neglect all loop as well as finite temperature corrections, even though they are important for the complete physical picture. Due to $h \gg \lambda$, the $|S_i|$ are fixed to almost the same large VEVs in both the symmetric and broken phases, which leads to $\langle\beta_4\rangle_{f,t} = 0$ and $\Delta\beta_4 = 0$. The change in β_3, however, is subtle. For the unbroken phase, $v_1 = v_2 = 0$ and hence β_3 is not fixed. But for non-local EWBG the relevant scattering processes mainly occur in the bubble wall where $v_{1,2}$ do not vanish, so we can understand β_3 in the unbroken phase as its asymptotic value as v_1 and v_2 approach zero. From the tree-level potential Eq. (39), it is easy to see that the non-vanishing Higgs VEVs lead to $\beta_3 = 0$ inside the bubble wall except the boundary region between the wall and the false vacuum. We simply assume $\Delta\beta_3 = 0$. The phase changes of the Higgs fields therefore are mainly due to $\Delta\beta_1$ and $\Delta\beta_2$. To illustrate how to obtain large $\Delta\beta_1$ and $\Delta\beta_2$, let us consider their first order differential equations from the tree-level potential Eq. (39),

$$\begin{aligned}
\left(m^2_{SS_1}|S||S_1|\cos\beta_1 + |m^2_{S_1S_2}||S_1||S_2|\cos(-\beta_1+\beta_2+\gamma)\right)\Delta\beta_1 \\
-|m^2_{S_1S_2}||S_1||S_2|\cos(-\beta_1+\beta_2+\gamma)\Delta\beta_2 = -m^2_{SS_1}|S_1|\sin\beta_1\Delta|S| \\
\left(m^2_{SS_2}|S||S_2|\cos\beta_2 + |m^2_{S_1S_2}||S_1||S_2|\cos(-\beta_1+\beta_2+\gamma)\right)\Delta\beta_2 \\
-|m^2_{S_1S_2}||S_1||S_2|\cos(-\beta_1+\beta_2+\gamma)\Delta\beta_1 = -m^2_{SS_2}|S_2|\sin\beta_2\Delta|S|. \qquad (46)
\end{aligned}$$

Obviously, large $\Delta\theta_{\phi_i}$ or large $\Delta\beta_1$ and $\Delta\beta_2$ requires large $\Delta|S|$, and also depends significantly on γ.

Let us consider a parameter subspace: $100|m_{S_1S_2}|^2 > m^2_{SS_1} \sim 0.1 m^2_{SS_2} > 10|m_{S_1S_2}|^2$. Assume that $\langle S\rangle/\langle S_{1,2,3}\rangle$ is small (~ 0.01) in the false vacuum and large (~ 0.1) in the true vacuum. In the broken phase, the $m^2_{SS_1}$ and $m^2_{SS_2}$ terms will dominate over the $m^2_{S_1S_2}$ term in the tree-level potential and thus favor small β_1 and β_2. In the symmetric phase, the dominant terms change to $m^2_{SS_2}$ and $m^2_{S_1S_2}$ due to the sharp decrease of the VEV of S. For $\gamma \sim \pi$, β_1 is pushed to a large value in this region. A large $\Delta\beta_1$ is then generated. We will follow this line to generate large $\Delta\theta_{\phi_i}$ in our analyses. In Figure 2, we illustrate the γ-dependence of β_1 and β_2, in the false and true vacua respectively. The relevant γ-dependence of $\Delta\theta_{\phi_i}$ is illustrated in Figure 3. For both of them, the parameter values are from case b (see Table 3).

Besides the baryon asymmetry, it would be desirable to also account for the CDM. In the scenario of the lightest neutralino χ^0_1 as a CDM candidate, the CDM generation has a strong dependence on the mass ($m_{\chi^0_1}$) and composition of χ^0_1. Since $m_{\chi^0_1}$ is sensitive to the soft mass terms of H^0_d, H^0_u and S due to their roles in determining $\tan\beta$, we will consider EWBG with respect to γ in three cases first (cases a, b and c) which are specified by different $m^2_{H^0_d}$ values (see Table 3), and then discuss

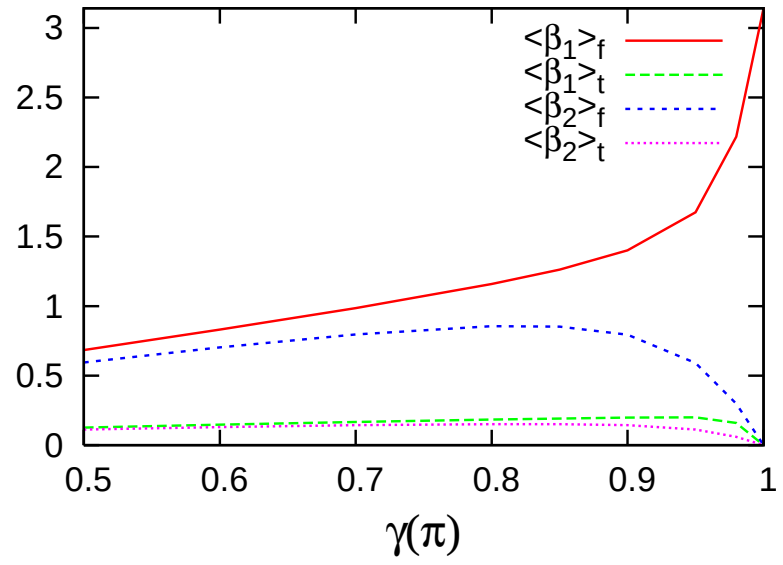

Figure 2: $\langle\beta_{1,2}\rangle_{f,t}$ vs. $\gamma(\pi)$, in case b.

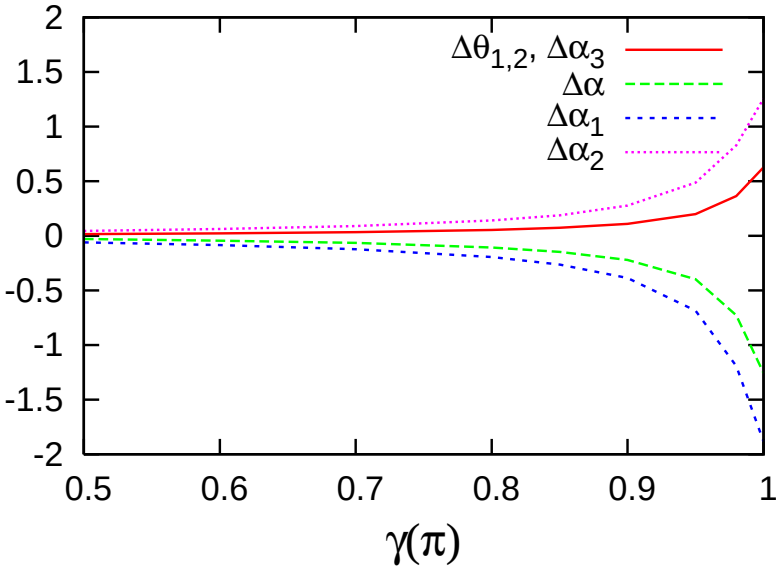

Figure 3: $\Delta\theta_{\phi_i}$ vs. $\gamma(\pi)$, in case b.

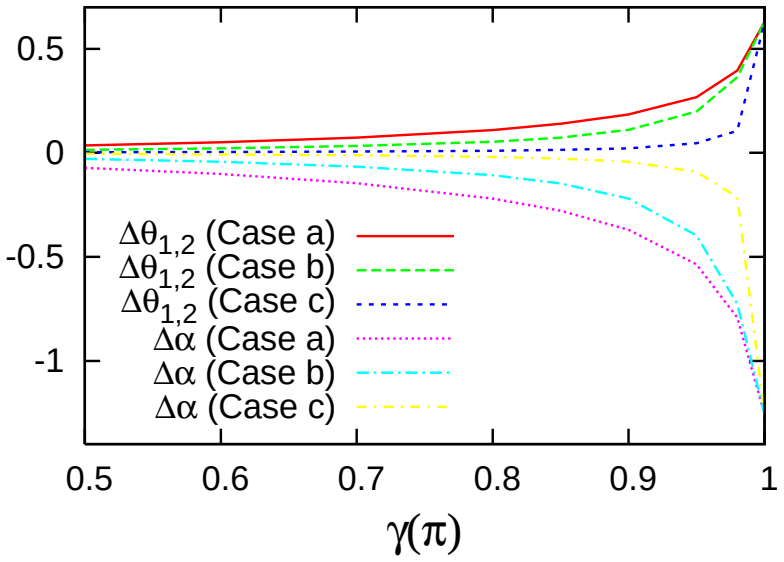

Figure 4: $\Delta\theta_{1,2}$, Δ_α vs. $\gamma(\pi)$, in cases a, b and c.

the continuous dependence of EWBG and the χ_1^0 relic density on $m^2_{H_d^0}$ for a given γ value. In Figure 4 we show the γ dependence of $\Delta\theta_1 = \Delta\theta_2$ and $\Delta\alpha$ in cases a, b and c (since the baryon asymmetry generation mainly couples to these three phases). From this figure we see that for a given γ value a larger $m^2_{H_d^0}$ value gives a smaller phase variation crossing the wall. This is because a large $m^2_{H_d^0}$ value make $|S|$ small in both vacua, which further leads to a small $\Delta|S|$ (or small $\Delta\beta_i$ due to Eq. (46)). As expected from the previous discussion, the large $|\Delta\theta_{\phi_i}|$ appears in the large γ region. For $\gamma = \pi$ there exists a Z_2 discrete symmetry in the neutral Higgs potential which might cause a dilution between matter and anti-matter bubbles for SCPV-induced EWBG (the explicit CP breaking from the fermion sector avoids problems with cosmological domain walls [106]). The vacua degeneracy is lifted as long as γ deviates from π. Because the nucleation rates of these two vacua are exponentially biased by the difference of their energy densities, a slight shift from π for γ can greatly diminish the dilution. In this article therefore we will choose $\pi/2 \leq \gamma < \pi$.

5.3 New Contributions to Electric Dipole Moments

In this subsection, let us discuss possible new contributions to the EDMs in the SCPV-induced baryogenesis (also see [70]). According to the discussions in the previous subsection, no CP violation occurs at zero temperature for $\gamma = 0, \pi$, so there is no EDM problem.

For $\gamma \neq 0, \pi$, the Higgs fields may obtain nonzero phases at zero temperature.

However, their contributions to the EDMs are highly suppressed. Among the four gauge independent phases, β_3 and β_4 are zero due to the A_h and A_λ terms, so there will be no phases entering the h and A_h terms after we do the field redefinitions. The only phases are associated with the $m^2_{SS_1}$ $m^2_{SS_2}$ and $m^2_{S_1S_2}$ terms. (The phases will enter the fermion Yukawa couplings also, but they only lead to overall phases in the mass matrices which do not affect the CKM matrix.) Therefore, the CP violation will only affect the Higgs sector.

The Feynman diagrams contributing to the electron and quark EDMs which are mediated by the Higgs fields involve two vertices containing the Yukawa couplings, and include a mass insertion on the fermion line to flip the chirality. The EDMs will therefore be proportional to the cube of Yukawa coupling, making it very small. The EDMs are also proportional to the CP violation term which comes from the secluded sector and couples very weakly to the ordinary fermions. In particular, if any of the three soft mass terms $m^2_{SS_1}$ $m^2_{SS_2}$ and $m^2_{S_1S_2}$ vanish, there will be no tree-level CP violation. Also, for the parameters that we consider, the imaginary part of $m^2_{S_1S_2}$ is very small. Combining all these effects, new EDM contributions from the Higgs sector are very small. Our numerical estimate shows that they are 6 to 7 orders smaller than the experimental upper limit.

6 Wall Thickness and Velocity

In the early Universe the first order EWPT is realized by nucleating bubbles of the broken phase. To calculate the baryon asymmetry, understanding the dynamical behavior of these bubbles, such as the nucleation rate, expansion velocity, and bubble wall profile, is important but analytically difficult. In this section, we will focus on the wall profile and wall velocity.

6.1 Wall Thickness

The kinetic Lagrangian for the complex scalar fields can be written as

$$\mathcal{L} \sim \sum_i \left(\frac{1}{2} \partial_\mu \phi_i \partial^\mu \phi_i + \frac{\phi_i^2}{2} \partial_\mu \theta_{\phi_i} \partial^\mu \theta_{\phi_i} \right) \ , \tag{47}$$

where ϕ_i and θ_{ϕ_i} collectively denote the magnitudes and phases of the Higgs fields, respectively. For the unitary gauge, we are left with 10 dynamical equations (with respect to 6 magnitudes and 4 gauge-invariant phase variables). Once the stationary solutions to these 10 equations are found, we can obtain the relevant physical information on the bubble wall, such as the wall thickness and velocity. However, these classical field equations are extremely complicated, so we have to solve them numerically.

A useful numerical method was devised in [72, 73, 74]. The basic idea [72] is that to solve the classical field equations one has to find the field configuration for

which

$$S_A = \int_{-\infty}^{+\infty} dz \left[\sum_i E_{\phi_i}(z)^2 + \frac{1}{T_c^2} \sum_j E_{\beta_j}(z)^2 \right] \equiv 0 \ , \tag{48}$$

where $E_{\phi_i}(z)$ and $E_{\beta_j}(z)$ are the relevant field equations under the planar wall approximation. ($E_{\beta_j}(z)$ is rescaled by a factor $\frac{1}{T_c}$, so that $E^i_{magnitude}(z)$ and $E^j_{phase}(z)$ have the same dimensions.) This can be achieved by searching for the absolute minimum of the action S_A. We need to find an appropriate ansatz satisfying the boundary conditions at infinity as a first step. The kink ansatz is especially suitable since it satisfies the boundary conditions very well and has a smooth, gradually changing behavior as one moves from negative infinity to positive infinity. Therefore, we will take the kink ansatz for the independent field variables

$$\begin{aligned} \phi_i(z) &= \frac{\langle\phi_i\rangle_t + \langle\phi_i\rangle_f}{2} + \frac{\langle\phi_i\rangle_t - \langle\phi_i\rangle_f}{2} \tanh(\frac{z}{\delta}) \ , \\ \beta_j(z) &= \frac{\langle\beta_j\rangle_t + \langle\beta_j\rangle_f}{2} + \frac{\langle\beta_j\rangle_t - \langle\beta_j\rangle_f}{2} \tanh(\frac{z}{\delta}) \ , \ j = 1, 2, 4 \end{aligned} \tag{49}$$

where the index "i" runs over the six complex neutral Higgs fields: H_d^0, H_u^0, S, S_1, S_2, S_3, and "t" and "f" denote the VEVs in the true and false vacua, respectively. In our convention the true vacuum is located at $z \to \infty$ and the false one is located at $z \to -\infty$. For simplicity, we assume that there are no off-sets which shift the fields against each other.

However, this assumption does not hold for β_3. From the A_h term in Eq. (39), it is easy to see that, as $\langle H_d^0\rangle$ and $\langle H_u^0\rangle$ become non-trivial crossing the bubble wall, $\langle\beta_3\rangle$ will be suppressed to zero quickly. So a good ansatz for β_3 should be

$$\beta_3(z) = \frac{\langle\beta_3\rangle_f}{2}[1 - \tanh(\frac{z+a}{\delta})] \ . \tag{50}$$

This is an anti-kink function and $a \geq \delta$. For simplicity, we set $a = \delta$, so all kink ansatzs are mediated by only one parameter – the wall thickness δ. This discussion does not contradict the assumption $\Delta\beta_3 = \beta(\infty) - \beta(-\infty) = 0$ in Subsection 5.2, since there we are analyzing the phase change crossing the wall while $\beta_3 \sim 0$ inside the wall.

Figure 5 describes the dependence of the wall thickness on γ ($\frac{\pi}{2} \leq \gamma < \pi$) by minimizing the action S_A over δ for the parameter sets in Table 3. Again, the three curves correspond to the three different $m^2_{H_d^0}$ values: 2, 4 and 6. These plots tell us that the wall thickness becomes larger as γ increases and reaches its peak value around $\gamma = \pi$. In the action S_A the kinetic terms and potential slope terms are proportional to δ^{-3} and δ, respectively. The wall thickness is a result of the balance between them. According to the discussions in Section 5, large γ induces large magnitudes for $\Delta\beta_j$ or $\Delta\theta_{\phi_i}$, which can increase the weight of the kinetic terms in S_A. The wall thickness therefore is an approximately monotonic increasing function with respect to γ. Numerical simulation shows that the wall thickness varies in the range $(3-30)T_c^{-1}$.

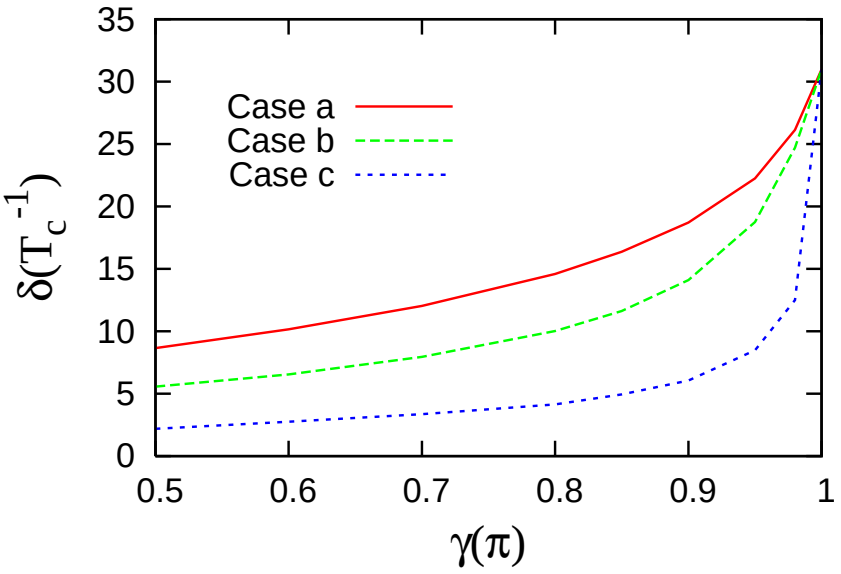

Figure 5: Wall thickness δ vs. $\gamma(\pi)$.

6.2 Wall Velocity

The velocity of the bubble wall also plays a crucial role in EWBG. As a technical requirement, the wall velocity cannot be smaller than 0.01. Otherwise, the effect of EW sphalerons and Higgs-mediated (in the thin wall regime) decay processes cannot be neglected while the CP-violating current is propagating in the false vacuum, and the new relaxation effect of EW sphalerons will appear before the wall recaptures the left-chiral particles composing the flux.

The wall velocity of a new-born bubble is mainly mediated by three kinds of forces: 1) the driving force (F_d) responsible for the bubbles' expansion; 2) the shrinking force (F_s) due to the surface tension of the bubbles (T_s); and 3) the friction coming from the plasma (F_f). Though some progress has been reported in the MSSM recently [91], a systematic study on the dynamics of the bubble wall is still absent in the sMSSM. In the following, we will argue that the wall velocity in these models should be comparable to or smaller than that in MSSM or NMSSM under the thin wall approximation [92][9].

Consider two bubbles from the sMSSM and MSSM, respectively, and assume that the energy density differences across the wall, $\varepsilon = V_{out} - V_{in}$, are the same for both bubbles. In this section, a prime will be used to denote the quantities from the sMSSM. The driving force per area acting on the walls is $F_d = \varepsilon$ and the shrinking force is $F_s = 2T_s/r$, so we can approximately estimate the critical radii for both kinds

[9]This "thin wall" is different from the one defined in next section in that the comparison scale is the bubble radius rather than the mean free path of the scattered particles.

of bubbles by employing the equation $F_d = F_s$, which gives

$$r_c = 2T_s/\varepsilon, \tag{51}$$
$$r'_c = 2T'_s/\varepsilon. \tag{52}$$

For $T'_s = aT_s$, we have $r'_c = ar_c$. Here $a \gg 1$ since the large VEVs of the Higgs fields in the secluded sector will contribute significantly to T'_s according to the second term of Eq. (47).

Now suppose that both bubbles sweep a distance Δr, *i.e.*, the bubble radii respectively increase to $r_c + \Delta r$ and $r'_c + \Delta r$, and that the wall tensions T_s and T'_s are left invariant during this process; then the shrinking forces due to the surface tension will become smaller. The net force for both bubbles are changed from zero to

$$\Delta F = F_d - F_s = \varepsilon - \frac{2T_s}{r_c + \Delta r}, \tag{53}$$
$$\Delta F' = F'_d - F'_s = \varepsilon - \frac{2T'_s}{r'_c + \Delta r}, \tag{54}$$

and

$$\Delta F - \Delta F' = 2T_s\left(\frac{-1}{r_c + \Delta r} + \frac{1}{r_c + \Delta r/a}\right) > 0. \tag{55}$$

That is, in the sMSSM the shrinking force decreases more slowly if there is no other physics involved (note that the driving forces stay unchanged during this process).

On the other hand, due to thermal scattering from particles in the hot plasma, the bubble wall will suffer friction or thermal pressure F_f during its expansion, where F_f is determined by the thermal environment and the wall velocity relative to the plasma. Now suppose that bubbles in both models expand at the same velocities, microscopically this thermal pressure is mainly induced by momentum transfer of the scattered particles, particularly those with

$$m(\infty) \gg m(-\infty), \frac{k_i.k_f}{|k_i||k_f|} < 0. \tag{56}$$

Besides the ones in the MSSM, the sMSSM contains extra light degrees of freedom, e.g., the singlets in the Higgs sector and the additional exotic particle species. We may well expect that in the sMSSM the thermal pressure is not smaller than that in the MSSM given $T_c = T'_c$ and $v_w = v'_w$. Therefore, the wall velocity in the sMSSM should be non-relativistic. In this article, we will set $v_w = 0.05$.

7 Non-local Electroweak Baryogenesis

In EWBG scenarios, the non-local baryogenesis or charge transport mechanism [75] refers to the case where particles have CP-violating interactions with a bubble wall.

These CP-violating interactions cause an asymmetry in some CP-odd quantum numbers or transport charges other than B carried by particle currents into the false vacuum. In front of the expanding bubble wall, where the thermal equilibrium is broken to some extent, the asymmetry of transport charges induces a non-vanishing number density for left-chiral particles carrying EW charges. This asymmetry is subsequently converted by the $B+L$-violating EW sphaleron processes, such as $t_{\overline{R}}t_{\overline{R}}b_{\overline{R}}\tau_{\overline{R}} \leftrightarrow 0$ and $t_{\overline{R}}b_{\overline{R}}b_{\overline{R}}\nu_{\overline{R}} \leftrightarrow 0$, into an asymmetry in baryon number. Some instant later the wall sweeps over the region. The generated net n_B is then frozen in the bubble due to the exponentially suppressed EW sphaleron effects. There are two typical regimes relevant to non-local baryogenesis, depending on the particles under consideration: the thin wall regime for $\delta/\Delta < 1$ and the thick wall region for $\delta/\Delta \geq 1$, where δ is the wall thickness and Δ is the particle's mean free path or propagation length.

For the thin wall regime [93, 94], the physical picture is relatively simple since we may neglect the damping effect on the CP-violating source caused by the self-energy thermal correction. The reflectivity and transmittivity of particle scattering can be calculated in quantum mechanics, where the fermions interacting with the bubble wall are treated as free particles with space-dependent masses, and the CP-violating source can be modeled as a delta function current.

For the thick wall regime, the effects of additional decay processes in the wall cannot be neglected, and hence modeling the CP-violating source will be very complicated. Generally, two parallel approaches are available: the semiclassical force method [95, 96] and spontaneous baryogenesis [97]. The first one is based on the fact that, under the WKB approximation ($p \gg \delta^{-1}$), a CP-violating mass term in the Lagrangian can induce a CP-violating shift in gradients of the dispersion relation at first order. This CP-violating source then appears in the diffusion equations, interpreted as one kind of "semi-classical" source. This approach has been applied to the MSSM [90] and the non-minimal NMSSM [45]. However, this approach neglects the contributions from the non-WKB region, which may greatly enhance the produced baryon asymmetry. The second approach is a little like the one used in the thin wall regime: the CP-violating source is the particle current reflected by the bubble wall, but the damping and multiple-scattering effects are included.

With CP-violating sources produced, the particles carrying the CP-odd transport charges will undergo a diffusion process outside the bubble. Dynamical baryogenesis requires a slight departure from thermal equilibrium in front of the wall, implying that not all particle "decay" processes (*i.e.*, those which affect the charge number density) are fast or adiabatic compared to the expanding velocity of the bubble wall. If

$$\frac{D\Gamma}{v_w^2} > 1 \tag{57}$$

with Γ being the decay rate and D the associated diffusion constant, the processes will be considered as fast, and vice versa. In our calculations, almost all processes included in the diffusion equations are fast, otherwise they will not have enough time to significantly affect the charge number density. The only exception is the EW

sphaleron process. We assume that they are slow during the diffusion and can be neglected in mediating the charge number density. We can therefore deal with the diffusion of the particles carrying transport charges and the generation of the net baryon number separately. We must then: (1) solve the diffusion equations of the particles carrying the transport charges, and find the number density of all left-chiral particles n_L which carry EW gauge charges; (2) insert n_L into the baryon diffusion equation, to find the generated baryon asymmetry. The description of the particle transport in front of the bubble wall by the diffusion equations is well-justified because $v_w \ll v_s$. Here $v_s = 1/\sqrt{3}$ is the sound speed in the plasma.

In the following, we will study the roles in EWBG played by different particles in the sMSSM. We will calculate the contributions from leptons in the thin wall regime, and the contributions from squarks, charginos and quarks in the thick wall regime by assuming the spontaneous baryogenesis mechanism.

7.1 The Lepton Contribution – Thin Wall Regime

In the supersymmetric extension of the SM, leptons generally have a mean free path in the thermal plasma much larger than the bubble wall thickness. To consider their contribution to EWBG, we can work in the relatively simple thin wall regime [93].In the thin wall regime, the scattering of particles by the bubble wall is described in terms of freely propagating particles with space-dependent masses, with the Lagrangian

$$\mathcal{L} \;=\; \overline{\psi}_L i\gamma^\mu \partial_\mu \psi_L + \overline{\psi}_R i\gamma^\mu \partial_\mu \psi_R - m(z)\overline{\psi}_L \psi_R \;-\; m^*(z)\overline{\psi}_R \psi_L \;\;, \tag{58}$$

with the mass term determined by the Yukawa coupling. For charged leptons it is

$$m_l(z) = y_l v_1(z) e^{i\theta_1(z)} \;. \tag{59}$$

Since the Yukawa coupling $y_\tau \gg y_{e,\mu}$, we will only study the contributions from τ leptons.

The CP-violating current in this case is produced by $\tau_R \to \tau_L$, where the CP-odd transport charge is axial τ number

$$\mathcal{Q}^\tau_{\tau_{L,R}} = \mathrm{Diag}(1,-1). \tag{60}$$

Explicitly solving the Dirac equation and only considering the contribution from the non-WKB momentum subspace ($k_i^z < \delta^{-1}$) as a conservative approximation, one obtains the CP-odd reflection asymmetry [93, 94]

$$\begin{aligned} \Delta R_{\tau_R \to \tau_L}(k_i, k_f) &= 4t_\phi(1-t_\phi^2)\int_{-\infty}^{\infty} dz\ \cos(2k_i^z z)\mathrm{Im}\left[m_\tau(z)\frac{m_\tau(\infty)^*}{|m_\tau(\infty)|}\right] \\ &= \frac{-\sqrt{\pi}}{2} m_\tau(\infty)^2 \delta\Delta\theta_1 \frac{e^{-(\delta k_i^z)^2}}{k_i^z}, \end{aligned} \tag{61}$$

where $t_\phi = \tanh\phi$ and $\tanh(2\phi) = |m_\tau(\infty)|/|k_i^z|$. In the second line, the kink ansatz defined by Eq. (49) and the assumption of $\Delta\theta_1/2$ as perturbative (it turns out that $\frac{1}{2}\Delta\theta_1 \lesssim 0.3$ in the parameter region we are interested in) have been used.

The axial τ current j_{τ_L} induced by the scattering of leptons is [93, 94]

$$j_{\tau_L} = \int_{k_i^z > m_\tau} \frac{d^3k_i}{(2\pi)^3} \frac{k_f^z}{E} (f_f^\tau(k_i^z) - f_t^\tau(-k_i^z)) \Delta R_{\tau_R \to \tau_L}(k_i, k_f) \mathcal{Q}_{\tau_L}^\tau \ . \tag{62}$$

Here f_t and f_f in Eq. (62) are the Fermi-Dirac distributions in the wall frame for the particles localized in and outside the bubble, respectively, given by

$$f^\tau(k_i^z) = \frac{\gamma_w^2 (1 - v_w \frac{k_i^z}{E})}{e^{\gamma_w (E - v_w k_i^z)/T_c} + 1} \ . \tag{63}$$

The chemical potential in the exponential factor is suppressed due to the large value of the critical temperature T_c. Similarly, due to the exponential suppression for $E > T_c$, we may only consider the contribution from the small energy region $E < T_c$ and make a perturbative expansion with respect to $\frac{E}{T_c}$, approximately yielding the formula for the injected CP-violating current

$$j_{\tau_L} = \frac{-m_\tau(\infty)^2 v_w \delta \Delta\theta_1}{(2\pi)^2} h(\delta, T_c) \ , \tag{64}$$

where

$$h(\delta, T_c) = \int_0^{T_c} dk_{i\perp} \int_0^{1/\delta} dk_i^z \frac{k_\perp}{\sqrt{k_\perp^2 + (k_i^z)^2}} \left(\left(\frac{\gamma_w k_i^z}{T_c} - \frac{k_i^z}{\sqrt{k_\perp^2 + (k_i^z)^2}} \right) + O[(\frac{E}{T_c})^3] \right) \tag{65}$$

is a function of the wall thickness and critical temperature. The first term in Eq. (65) exactly leads to Eq. (25) in Ref. [94] up to an ansatz-dependent factor after $h(\delta, T_c)$ is integrated out. The second term, which will suppress the injected chiral flux, is neglected in Ref. [94]. Note that the CP-violating current j_{τ_L} is proportional to $m_\tau(\infty)^2$. Given that the associated calculations can be applied to the other two families of leptons as well, we are justified to only consider the τ.

While propagating in the false vacuum, for a wall velocity that is not too large the behavior of the scattered leptons can be approximately described by diffusion processes. The injected current will lead to a "diffusion tail" of the particles in front of the moving wall. If this diffusion tail or persistence length ξ is much larger than the width of the wall, it will be a good approximation to describe the injected current as a delta-function-like source. While the current is propagating in the false vacuum, leptons will undergo some Higgs-mediated or chiral mixing decay processes which may have a negative effect on the CP-violating current amplitude. A reasonable assumption is that the characteristic decay time for leptons is much longer than the time it takes for the wall to recapture them. We can then neglect lepton decays or chiral mixing processes and only consider the left-chiral leptons propagating in the false vacuum. Furthermore, we also need to make an assumption that the EW sphaleron processes are too slow to alter the density in front of the wall significantly and thus can be neglected except for their role in generating baryons. These two

assumptions require $\frac{D\Gamma}{v_w^2} < 1$ for the associated processes. For τ leptons, they work well if $v_w > 0.01$ [93]. Neglecting these decay processes, the diffusion equation in the bubble wall frame can be rewritten as [93]

$$D_{\tau_L} n''_{\tau_L}(z) - v_w n'_{\tau_L}(z) + J_{\tau_L} = 0 \ , \tag{66}$$

with

$$\begin{aligned} n'_{\tau_L} &= \partial n_{\tau_L}(z)/\partial z \ , \\ J_{\tau_L} &= -\xi_{\tau_L} j_{\tau_L} \delta'(z) \ , \end{aligned} \tag{67}$$

where the persistence length ξ_{τ_L} is given by $\xi_{\tau_L} \sim 6 D_{\tau_L} \langle v_{\tau_L} \rangle$ [93], with $D_{\tau_L} \sim 100\, T_c^{-1}$ being the related diffusion constant [93] and $\langle v_{\tau_L} \rangle$ being the average velocity of the injected current relative to the wall; $\delta'(z) = \partial \delta(z)/\partial z$ and z is related to the coordinates in the plasma frame by $z = r + v_w t$. Solving Eq. (67) by combining with the boundary conditions

$$\lim_{|z| \to \infty} n_{\tau_L}(z) = 0 \ , \tag{68}$$

one obtains

$$n_{\tau_L}(z) = \begin{cases} \mathcal{C}_{\tau_L} e^{\frac{v_w}{D_{\tau_L}}(z)} & z < 0 \\ 0 & z > 0 \end{cases} \ , \tag{69}$$

with

$$\mathcal{C}_{\tau_L} = 6 \langle v_{\tau_L} \rangle j_{\tau_L}. \tag{70}$$

The baryon generation is described by the diffusion equation

$$D_L n''_B - v_w n'_B - n_f \Gamma_{ws} n_L = 0. \tag{71}$$

Here n_L is the net number density of left-chiral particles carrying EW charges. Only such particles are involved in the EW sphaleron processes and hence able to source the baryon generation. D_L is effective diffusion constant. In the thin wall region, the main contribution to n_L is from the scattering of τ leptons, so we have $n_L = n_{\tau_L}$ and $D_L = D_{\tau_L}$. Under the approximation ($\Theta(-z)$ is step function)

$$\begin{aligned} \Gamma_{ws}(z) &= \Theta(-z) \Gamma_{ws}(-\infty) \\ &= 6 \kappa \alpha_w^5 T_c \Theta(-z), \end{aligned} \tag{72}$$

with $\kappa \sim 21$ for $T_c > T_{EW} \sim 100$ GeV [98, 99], we find for $z \geq 0$

$$n_B = \frac{-n_f D_{\tau_L} \Gamma_{ws} \mathcal{C}_{\tau_L}}{v_w^2}. \tag{73}$$

Here the boundary condition $n_B(-\infty) = 0$ has been used. Then with $s = \frac{2\pi^2 g_* T_c^3}{45}$ the baryon asymmetry is solved to be

$$\frac{n_B}{s} = \frac{540\gamma_w^3 \langle v_{\tau_L}\rangle D_{\tau_L} m_\tau(\infty)^2 \delta \Delta\theta_1 h(\delta, T_c)\Gamma_{ws}}{(2\pi)^4 v_w g_* T_c^3}. \quad (74)$$

Eq. (74) tells us that in the thin wall regime of the non-local EWBG scenario, three model-dependent physical quantities play critical roles: the variation of the CP phase crossing the wall $\Delta\theta_1$, the wall thickness δ, and its velocity v_w. $\Delta\theta_1$ will bias the symmetry between the dynamical behaviors of particles and anti-particles. For the perturbative approximation in the non-WKB momentum region, *i.e.*, both $\Delta\theta_1$ and momentum are not large ($\Delta\theta_1/2 < 1$ and $k_i^z < \delta^{-1}$), the CP-violating current and baryon asymmetry are proportional to $\Delta\theta_1$. It turns out that the contribution from the thin wall regime is non-trivial compared to the ones from the thick wall regime. The wall configuration is also essential. It measures the size of the region in which the CP-violating current is generated, and it provides the p_z upper limit or definition standard of non-WKB particles. From Eqs. (64) and (74), the CP-violating current and baryon asymmetry are proportional to the wall thickness, and are also affected by the wall thickness through the integration upper limit on p_z. In addition, $1/v_w$ measures the time for which the EW sphaleron processes continue before the particles in the CP-violating current are recaptured by the bubble wall, so it is natural that the baryon produced asymmetry is inversely proportional to v_w.

7.2 The Squark, Chargino and Quark Contributions – Thick Wall Regime

In this subsection we will calculate the baryon asymmetry generated by squarks, charginos and quarks by employing the spontaneous baryogenesis mechanism. Compared to the thin wall regime, there are two new effects which are important for our understanding of the interactions between particles and the bubble wall:

(1) The effect of thermal scattering. This can lead to a self-energy correction to the particle propagators and hence suppress the CP-violating source (due to the shortened life-time of the particles), and will be taken into account by including the imaginary part of the fermion self-energy in the dispersion relation, *i.e.*,

$$[\omega(\mathbf{k}) + i\tilde{\gamma}]^2 = \mathbf{k}^2 + m^2, \quad (75)$$

where $\tilde{\gamma}$ is the associated damping rate. This immediately gives

$$|\Im(\mathbf{k})| = \frac{1}{\Delta}, \quad (76)$$

with

$$\Delta = \tau \left|\frac{\Re(\mathbf{k})}{\omega}\right|, \quad \tau = \frac{1}{\tilde{\gamma}}. \quad (77)$$

Since τ is the lifetime of the scattered particles, and $\Re(\mathbf{k})/\omega$ is their velocity, Δ defines the propagation length of the scattered particles in the wall. In addition, from Eq. (75), we have

$$\omega^2 \;=\; \Re(\mathbf{k})^{\mathbf{2}} + \mathbf{m^2} + \tilde{\gamma}^{\mathbf{2}}(\mathbf{1} - \frac{\omega^{\mathbf{2}}}{\Re(\mathbf{k})^{\mathbf{2}}}). \tag{78}$$

We will work in the limit $\tilde{\gamma}^2 \ll \Re(\mathbf{k})^{\mathbf{2}} + \mathbf{m^2}$, which gives the relation

$$\omega^2 \;=\; \Re(\mathbf{k})^{\mathbf{2}} + \mathbf{m^2}. \tag{79}$$

(2) The effect of multiple scattering by the wall. This effect can be interpreted as multiple insertions in a perturbation regime. Currently, there are two main insertion methods: mass insertion [76] and Higgs insertion [31, 77]:

Mass insertion assumes that the tree-level physics is described by kinetic energy terms and considers the space-dependent mass terms as a perturbation, which can be denoted by

$$\mathcal{L} = \mathcal{L}_{tree} + \mathcal{L}_{pert} = K - M, \tag{80}$$

where K is kinetic energy terms and M is mass terms. Since tree-level physics in the mass insertion regime is a Lorentz-invariant free theory of massless particles, this method is effective only if $K \gg M$. However, due to the Boltzmann factor suppression for the injected CP-asymmetric current, the main contribution to the CP-violating source comes from the non-WKB momentum region, which usually makes multiple mass insertions unstable.

Compared with mass insertions, Higgs insertion is more extensively assumed in the literature. Its starting point is to separate the mass terms into a free part and perturbative part, *i.e.*, [31]

$$\mathcal{L} = \mathcal{L}_{tree} + \mathcal{L}_{pert} = (K - M^0(z)) - \delta M(z, z_i)\ , \tag{81}$$

where z denotes the point where the CP-violating current is calculated, and also the mass eigenstates are defined, and z_i denotes the point where the scattering occurs. Using these local mass eigenstates as approximate asymptotic states, one can calculate the associated S matrix and the CP-violating source. If these local mass eigenstates are not the gauge eigenstates in the false vacuum, after the CP-violating source is found one needs to go back to the gauge eigenstates by taking an inverse unitary transformation to evaluate the diffusion equations in the false vacuum. This method is justified for any scattered particle species, but it requires that the Higgs field variations be small within a propagation length. This implies $\Delta \ll \delta$. This relation adds an upper bound on the particle momentum in the z direction. Numerically, its effect is weak, since the contributions from the small momentum region to

the CP-violating current are more important, due to Boltzmann factor suppression in the high momentum region.

We will use Higgs insertion method. For given momentum and energy, the CP-violating current at point "z" is mainly generated in the layer between z and $z+\Delta$. Since $\Delta \ll \delta$, at the lowest order we can use a formalism similar to that in the thin wall regime to approximately calculate the current. Then the generated baryon asymmetry can be solved by embedding this CP-violating source into the diffusion equations in the thick wall regime. This approximation is adequate for our purpose, *i.e.*, for presenting typical features of EWBG in the sMSSM.

(I) The squark sector

The mass square matrix of the up-type squark is

$$M_{\tilde{u}} = \begin{pmatrix} M^2_{\tilde{u}^i_L} & M^2_{\tilde{u}^i_{LR}} \\ M^2_{\tilde{u}^i_{RL}} & M^2_{\tilde{u}^i_R} \end{pmatrix}, \tag{82}$$

where the diagonal entries are defined by

$$\begin{aligned} M^2_{\tilde{u}^i_L} &= m^2_{\tilde{Q}_i} + m^2_{u_i} + \Delta_{\tilde{u}^i_L} + \Delta'_{\tilde{u}^i_L} \ , \\ M^2_{\tilde{u}^i_R} &= m^2_{\tilde{u}^i_R} + m^2_{u_i} + \Delta_{\tilde{u}^i_R} + \Delta'_{\tilde{u}^i_R} \ , \\ M^2_{\tilde{u}^i_{LR}} &= y_{u_i}(hsv_1 e^{i(\alpha+\theta_1)} - A_{h_{u_i}} v_2 e^{-i\theta_2}) \ , \\ M^2_{\tilde{u}^i_{RL}} &= y_{u_i}(hsv_1 e^{-i(\alpha+\theta_1)} - A_{h_{u_i}} v_2 e^{i\theta_2}) \ , \end{aligned} \tag{83}$$

with

$$\begin{aligned} m^2_{u_i} &= y^2_{u_i} v_1^2 \ , \\ \Delta_{\tilde{u}^i_L} &= (\frac{1}{2} - \frac{2}{3}\sin^2\theta_W)\cos(2\beta)\frac{G^2}{2}(v_1^2 + v_2^2) \ , \\ \Delta_{\tilde{u}^i_R} &= \frac{2}{3}\sin^2\theta_W \cos(2\beta)\frac{G^2}{2}(v_1^2 + v_2^2) \ , \\ \Delta'_{\tilde{u}^i_L} = \frac{1}{8}\Delta'_{\tilde{u}^i_R} &= \frac{-1}{4\sqrt{15}} g^2_{Z'}(v_1^2 - v_2^2) \ . \end{aligned} \tag{84}$$

$M_{\tilde{u}}$ can be perturbatively expanded at "z" as

$$\begin{aligned} M^0_{\tilde{u}} &= M_{\tilde{u}}(z) = \begin{pmatrix} M^2_{\tilde{u}^i_L}(z) & M^2_{\tilde{u}^i_{LR}}(z) \\ M^2_{\tilde{u}^i_{RL}}(z) & M^2_{\tilde{u}^i_R}(z) \end{pmatrix} \approx \begin{pmatrix} m^2_{\tilde{Q}_i} & 0 \\ 0 & m^2_{\tilde{u}^i_R} \end{pmatrix}, \\ \delta M^0_{\tilde{u}} &= \begin{pmatrix} M^2_{\tilde{u}^i_L}(z_i) - M^2_{\tilde{u}^i_L}(z) & M^2_{\tilde{u}^i_{LR}}(z_i) - M^2_{\tilde{u}^i_{LR}}(z) \\ M^2_{\tilde{u}^i_{RL}}(z_i) - M^2_{\tilde{u}^i_{RL}}(z) & M^2_{\tilde{u}^i_R}(z_i) - M^2_{\tilde{u}^i_R}(z) \end{pmatrix}. \end{aligned} \tag{85}$$

In the first line, we have made a first order approximation for $M^0_{\tilde{u}}$. In the second line, "z_i" denotes the space point where the particle scattering occurs.

According to the bilinear interactions, a CP-violating left-chiral squark current $j_{\tilde{u}^i_L}$ is produced through $\tilde{u}^i_R \to \tilde{u}^i_L$, where the CP-odd transport charge is axial top number

$$\mathcal{Q}^t_{\tilde{t}_{L,R}} = \mathrm{Diag}(1,-1). \tag{86}$$

Considering that this is mediated by the Yukawa couplings of the up-type quarks and that the Yukawa coupling of the top quark $y_t = y_{u_3}$ is much larger than the other two, *i.e.*, y_{u_1,u_2}, we neglect the contributions from the first two family squarks. After a field theory calculation (for details, see Appendix C), we find

$$\begin{aligned}
\Delta R_{\tilde{t}_R\to\tilde{t}_L}(k_i,k_f,z) &= \frac{-1}{4E_iE_f}\frac{1}{v_i^z v_f^z}\int_z^{z+\Delta(\tilde{\gamma}_{\tilde{t}})} dz_1 dz_2 \sin((k_i^z-k_f^z)(z_1-z_2)) \\
&\quad \{w_1(z_1)w_1(z_2)\sin(\theta_1'(z_1)-\theta_1'(z_2)) \\
&\quad +w_2(z_1)w_2(z_2)\sin(-\theta_2(z_1)+\theta_2(z_2)) \\
&\quad +w_1(z_1)w_2(z_2)\sin(\theta_1'(z_1)+\theta_2(z_2)) \\
&\quad +w_2(z_1)w_1(z_2)\sin(-\theta_2(z_1)-\theta_1'(z_2)) \\
&\quad -(z_1\to z)-(z_2\to z)\},
\end{aligned} \tag{87}$$

with

$$\begin{aligned}
E_i^2 = E_f^2 &= (k_i)^2 + m^2_{\tilde{t}_R} = (k_f)^2 + m^2_{\tilde{t}_L}, \\
v_i^z &= \frac{k_i^z}{E_i}, \quad v_f^z = \frac{k_f^z}{E_f}, \\
w_1(z) &= y_t h s(z) v_1(z), \\
w_2(z) &= -y_t A_{h_t} v_2(z), \\
\theta_1'(z) &= \alpha(z)+\theta_1(z), \\
\tilde{\gamma}_{\tilde{t}} &= \tilde{\gamma}_{\tilde{t}_R}+\tilde{\gamma}_{\tilde{t}_L}.
\end{aligned} \tag{88}$$

Here the indices "i" and "f" denote the initial and final states of the scattering, respectively; and $(z_i \to z)$ denotes terms similar to the first four ones in $\{\}$, but with z_i replaced by z. In this paper, we set the damping rates $\tilde{\gamma}_{\tilde{t}_R} = \tilde{\gamma}_{\tilde{t}_L} = 0.1T_c \sim \alpha_s T_c$ as an approximation, since an analytical calculation for them is still absent. $\Delta R_{\tilde{t}_R\to\tilde{t}_L}(k_i,k_f,z)$ is sensitive to the A_{h_t} soft parameter due to its dependence on w_2. This makes its contribution to EWBG very different for small and large A_{h_t} (EWPT is not sensitive to A_{h_t}, since it enters the neutral Higgs effective potential only at loop level). Particularly, this contribution can be quadratically enhanced by a large A_{h_t} through the w_2w_2 term. We will discuss more on these issues in the next subsection. Using these results, the space-dependent CP-violating current is solved to be

$$j_{\tilde{t}_L}(z) = \int_{k_i^z>0}\frac{d^3k_i}{(2\pi)^3}\frac{k_f^z}{E_f}\left(f_z^{\tilde{t}_R}(k_i^z) - f^{\tilde{t}_R}_{z+\Delta(\tilde{\gamma}_{\tilde{t}})}(-k_i^z)\right)\Delta R_{\tilde{t}_R\to\tilde{t}_L}(k_i,k_f,z)\mathcal{Q}^t_{\tilde{t}_L}. \tag{89}$$

Here $f_z^{\tilde{t}_R}(k_i^z)$ and $f_{z+\Delta}^{\tilde{t}_R}(-k_i^z)$ are the thermal distributions of $\tilde{t}_R$ in the wall frame at "z" and "$z+\Delta$", respectively. Compared to the one defined in Eq. (63), they have a factor 3 difference due to QCD color as well as a sign-flip for the second term in the denominator.

(II) The chargino sector

The chargino mass matrix is

$$M_{\tilde{\chi}^\pm} = \begin{pmatrix} M_2 & u_2 e^{-i\theta_2} \\ u_1 e^{-i\theta_1} & \mu e^{i\alpha} \end{pmatrix} , \tag{90}$$

with $u_i = g_2 v_i/\sqrt{2}$ and $\mu \equiv hs$. It can be perturbatively expanded around z as

$$\begin{aligned} M^0_{\tilde{\chi}^\pm} &= M_{\tilde{\chi}^\pm}(z), \\ \delta M_{\tilde{\chi}^\pm} &= \begin{pmatrix} 0 & u_2(z_i)e^{-i\theta_2(z_i)} - u_2(z)e^{-i\theta_2(z)} \\ u_1(z_i)e^{-i\theta_1(z_i)} - u_1(z)e^{-i\theta_1(z)} & \mu(z_i)e^{i\alpha(z_i)} - \mu(z)e^{i\alpha(z)} \end{pmatrix}. \end{aligned} \tag{91}$$

For the parameter values that we are using, $|u_{1,2}(z)| \ll M_2, |\mu(z)|$, so we simply neglect the off-diagonal elements in $M^0_{\tilde{\chi}^\pm}$. In this sector, the CP-violating Higgsino current is produced through $\tilde{W}^c \to \tilde{H}^c$, where the CP-odd transport charge is vector Higgs number [10]

$$\mathcal{Q}^H_{\tilde{W}^+,\tilde{H}^+,\bar{\tilde{W}}^+,\bar{\tilde{H}}^-} = \mathrm{Diag}(0,1,0,1). \tag{92}$$

After a field theory calculation (for details, see Appendix C), we find

$$\begin{aligned} \Delta R_{\tilde{W}^c\to\tilde{H}^c}(k_i,k_f,z) &= \frac{1}{E_i E_f}\frac{1}{v_i^z v_f^z}\int_z^{z+\Delta(\tilde{\gamma}_{\chi^c})} dz_1 dz_2 \sin((k_i^z - k_f^z)(z_1-z_2)) \\ &\{k_i^z k_f^z [u_1(z_1)u_1(z_2)\sin(\theta_1(z_1)-\theta_1(z_2)) \\ &+u_2(z_1)u_2(z_2)\sin(-\theta_2(z_1)+\theta_2(z_2))] + \\ &M_2\mu(z)[u_1(z_1)u_2(z_2)\sin(\theta_1(z_1)+\theta_2(z_2)+\alpha(z)) \\ &+u_2(z_1)u_1(z_2)\sin(-\theta_2(z_1)-\theta_1(z_2)-\alpha(z))] \\ &-(z_1\to z)-(z_2\to z)\}, \end{aligned} \tag{93}$$

where

$$\begin{aligned} E_i^2 = E_f^2 &= (k_i)^2 + M_2^2 = (k_f)^2 + \mu(z)^2, \\ v_i^z &= \frac{k_i^z}{E_i}, \quad v_f^z = \frac{k_f^z}{E_f}, \\ \tilde{\gamma}_{\chi^c} &= \tilde{\gamma}_{\tilde{W}^c} + \tilde{\gamma}_{\tilde{H}^c}. \end{aligned} \tag{94}$$

[10] In the chargino sector, the CP-odd transport charge can also be axial Higgs number. But this source usually is suppressed by a fast Higgsino violating process Γ_μ corresponding to the $h\langle S\rangle\widetilde{h}_1\widetilde{h}_2$ term in the Lagrangian [31]. We will therefore not consider it here.

For the damping rates, we will use the results in the MSSM, which are given by $\tilde{\gamma}_{\tilde{H}^c} = 0.025T_c$ and $\tilde{\gamma}_{\tilde{W}^c} = 0.065T_c$ [100]. The CP-violating current is solved to be

$$\begin{aligned} j_{\tilde{H}^c}(z) &= \int_{k_i^z>0} \frac{d^3k_i}{(2\pi)^3}\frac{k_f^z}{E_f} \\ &\quad \left(f_z^{\tilde{W}^c}(k_i^z) - f_{z+\Delta(\tilde{\gamma}_{\chi^c})}^{\tilde{W}^c}(-k_i^z)\right) \Delta R_{\tilde{W}^c\to\tilde{H}^c}(k_i,k_f,z)\mathcal{Q}^H_{\tilde{H}^+,\tilde{\bar{H}}^-}, \end{aligned} \tag{95}$$

where $f_z^{\tilde{W}^c}(k_i^z)$ and $f_{z+\Delta}^{\tilde{W}^c}(-k_i^z)$ are the thermal distributions of the charged gaugino $\tilde{W}^c$ in the wall frame, which have a factor 2 difference from that defined in Eq. (63) due to $\tilde{W}^c = \tilde{W}^c_L + \tilde{W}^c_R$.

(III) The quark sector

The top quark mass is

$$m_t = h_t v_2 e^{i\theta_2} \ . \tag{96}$$

which can be perturbatively expanded around z as

$$\begin{aligned} m_t^0 &= m_t(z), \\ \delta m_t &= h_t v_2(z_i) e^{i\theta_2(z_i)} - h_t v_2(z) e^{i\theta_2(z)}. \end{aligned} \tag{97}$$

In this sector, the CP-violating current is produced by $t_R \to t_L$, where the CP-odd transport charge is axial top number

$$\mathcal{Q}^t_{t_{L,R}} = \mathrm{Diag}(1,-1). \tag{98}$$

Then (for details, see Appendix C)

$$\begin{aligned} \Delta R_{t_R\to t_L}(k_i,k_f,z) &= \frac{1}{E_iE_f}\frac{1}{v_i^z v_f^z}\int_z^{\Delta(\tilde{\gamma}_t)} dz_1 dz_2 \sin((k_i^z-k_f^z)(z_1-z_2)) \\ &\quad \{h_t^2 k_i^z k_f^z v_2(z_1)v_2(z_2)\sin(\theta_2(z_1)-\theta_2(z_2)) \\ &\quad -(z_1\to z)-(z_2\to z)\}, \end{aligned} \tag{99}$$

where

$$\begin{aligned} E_i^2 = E_f^2 &= (k_i)^2 + |m_t^0(z)|^2 = (k_f)^2 + |m_t^0(z)|^2, \\ v_i^z &= \frac{k_i^z}{E_i}, \quad v_f^z = \frac{k_f^z}{E_f}, \\ \tilde{\gamma}_t &= \tilde{\gamma}_{t_R} + \tilde{\gamma}_{t_L}. \end{aligned} \tag{100}$$

Again, we approximate the damping rates by $\tilde{\gamma}_{t_L} = \tilde{\gamma}_{t_R} = 0.1T_c \sim \alpha_s T_c$. The trace in the S matrices of the chargino and top quark scattering gives an extra factor "4",

so the factor "4" in the denominator of Eq. (C.11) disappears in both Eq. (93) and Eq. (99). The CP-violating current is solved to be

$$j_{t_L}(z) = \int_{k_i^z>\Lambda_k^{t_L}} \frac{d^3k_i}{(2\pi)^3}\frac{k_f^z}{E_f} \left(f_z^{t_R}(k_i^z) - \frac{k_i^z}{\sqrt{k_i^{z\,2}-\Delta m_t^2}} f_{z+\Delta(\tilde{\gamma}_t)}^{t_R}(-k_i^z) \right) \Delta R_{t_R\to t_L}(k_i,k_f,z)\mathcal{Q}_{t_L}^t, \quad (101)$$

where $f_z^{t_R}(k_i^z)$ and $f_{z+\Delta}^{t_R}(-k_i^z)$ are the thermal distributions of the right chiral top quark in the wall frame, which have a factor 3 difference from that defined in Eq. (63) due to color,

$$\Delta m_t^2 = m_t^2(z+\Delta(\tilde{\gamma}_t)) - m_t^2(z) \quad (102)$$

is the difference of the quark mass square at z and $z+\Delta(\tilde{\gamma}_t)$, and

$$\Lambda_k^{t_L} = \sqrt{m_t^2(\infty) - m_t^2(z)} \quad (103)$$

is the momentum cutoff. The factor in front of $f_t^{t_L}(-k_i^z)$ in Eq. (101) is due to the large mass difference of the scattered particles inside and outside the bubble. For τ leptons, stops and charginos, this difference is small compared to T_c, so this factor is approximately equal to 1.

Before moving to the calculation of the produced baryon asymmetry, we have some comments on the CP-violating currents obtained from the lowest Higgs insertion. First, according to the discussions in Subsection 5.2, the single Higgs phases θ_{ϕ_i} are not physical since their values depend on two decoupled degrees of freedom: A and B. Indeed, though working in the θ_{ϕ_i} basis, from Eq. (87), Eq. (93) and Eq. (99) we see that all of these currents depend on some special linear combinations of θ_{ϕ_i}, where their dependences on A and B are cancelled and they are only sensitive to $\beta_i(z)$. Second, for the CP-violating currents from the stop and the chargino sectors, the terms $\propto \omega_1\omega_2$ and $\propto u_1u_2$ will be reduced to the $v_1\partial v_2 - v_2\partial v_1$ type sources in the MSSM if $\theta_{1,2}(z) = 0$ and $\alpha(z) =$ constant. Though in this limit these contributions are trivial for $\partial\tan\beta = 0$, they are not in Eq. (87) and Eq. (93) due to the space-dependence of $\theta_{1,2}$ in the wall. Third, the terms $\propto v_iv_i$ in Eq. (87) and Eq. (93) are zero in the limit $\theta_{1,2}(z) = 0$ and $\alpha(z) =$ constant. They therefore never appear in the MSSM currents and denote a new-type of CP-violating current in the stop and chargino sector. This is also the only type of CP-violating current at the leading order in the quark sector. The vector Higgsino current of the $v_1\partial v_2 + v_2\partial v_1$ type does not appear in our calculations since it denotes a resummation effect from higher order Higgs insertions [77, 31, 32]. Finally, we emphasize that all of these features are results of SCPV-driven EWBG, so they are not sensitive to the concrete embeddings of the sMSSM. (For different embeddings, the $U(1)_Y$ and $U(1)'$ gauge charges

in Eq. (43) and hence the formulas in Eq. (41) are different. However, we did not use these results when deriving the formulas of the CP-violating currents.)

The field theory calculations used in the thick wall regime cannot be directly applied to the thin wall regime. In the thin wall regime, the main contribution is from an interference effect between a CP and a non-CP term (see the Appendix of [94]). The non-CP term is induced by the effect that the fundamental solutions inside and outside the bubble are different due to the mixing between left- and right-chiral fermions. In the quantum mechanics calculations of the reflection and transmission coefficients, this effect is explicitly included. Its strength can be measured by the parameter t_ϕ which is defined in Subsection 7.1. In the thick wall regime, this effect is neglected in the field theory calculations. Instead we assume the same asymptotic states between the two sides of a layer inside the wall, which greatly simplifies the calculations. This assumption is justified by the fact that t_ϕ is approximately estimated to be

$$t_\phi \lesssim \frac{\Delta m(z)}{\overline{\Delta} m} \sim \frac{\Delta}{2\delta} \ll 1 \tag{104}$$

in the thick wall limit. Here $\Delta m(z) = m(z+\Delta) - m(z)$ is the mass difference of the incident particles between the two sides of the layer, $\overline{\Delta} m = m(\infty) - m(-\infty)$ is their mass variation crossing the wall, and Δ is the thickness of the layer (see Eq. (77)). The main contribution in the thick wall regime therefore is from an interference effect of the CP-violating terms. Actually, if we apply the field theory calculation to leptons (similar to what we did for quarks), we will get their subleading contribution, which is given in the Appendix of [94].

While these injected CP-violating Higgsino or squark currents propagate in the false vacuum, the original thermal equilibrium among different particle species is broken and these species may obtain nonvanishing net number densities due to the associated decay processes. In the thick wall regime, the main decay processes include [76]: (1) the Yukawa interaction Γ_{y_T} corresponding to all supersymmetric and soft trilinear interactions arising from the $y_T H_2 Q_L T_R$ term in the superpotential[11] (Q_L is the left-chiral superfield of the third family quarks and T_R is the right-chiral superfield of the top quark); (2) the Higgsino violating process Γ_μ corresponding to the $h\langle S\rangle \widetilde{h}_1 \widetilde{h}_2$ term in the Lagrangian and supergauge interaction Γ_g; (3) the axial top number violating process Γ_m and the Higgs-violating process Γ_h corresponding to top quark mass effects and Higgs self interactions, respectively; (4) the strong sphaleron process Γ_{ss} [101] and weak sphaleron process Γ_{ws}. Γ_m and Γ_h are suppressed in the false vacuum and Γ_{ws} is suppressed in the true vacuum (for a strong enough first order EWPT); all of the others can occur both inside and outside of the bubble. For simplicity, we neglect all processes with a singlet component involved in the current propagation. In the concrete calculations, further simplifications are also made [76].

[11] As a first order approximation, we neglect the tau and bottom Yukawa interactions. For relevant discussion, see [102].

(a) We assume fast enough Γ_g which thermally equilibrates n_q and $n_{\tilde{q}}$; thus we can describe the system by the densities $n_{Q_L} = n_{q_L} + n_{\tilde{q}_L}$, $n_{T_R} = n_{t_R} + n_{\tilde{t}_R}$, $n_{H_1} = n_{h_1} + n_{\tilde{H}_1}$ and $n_{H_2} = n_{h_2} + n_{\tilde{H}_2}$. (b) We assume fast enough Γ_μ; then we have $n_{H_1} = n_{H_2}$ and hence are able to simplify the two quantities n_{H_1} and n_{H_2} into one $n_H = n_{H_1} + n_{H_2}$. (c) We assume slow Γ_{ws}, which allows us to ignore leptons for the particle diffusion and the n_L generation. Under these approximations, the diffusion equations in the wall frame are[12] [76]

$$\begin{aligned}
v_\omega n'_{Q_L} &= D_{Q_L} n''_{Q_L} - \Gamma_{y_T}\left[\frac{n_{Q_L}}{k_{Q_L}} - \frac{n_{T_R}}{k_{T_R}} - \frac{n_H}{k_H}\right] - \Gamma_m\left[\frac{n_{Q_L}}{k_{Q_L}} - \frac{n_{T_R}}{k_{T_R}}\right] \\
&- 6\Gamma_{ss}\left[2\,\frac{n_{Q_L}}{k_{Q_L}} - \frac{n_{T_R}}{k_{T_R}} + 9\,\frac{n_{Q_L}+n_{T_R}}{k_{B_R}}\right] + J_{\tilde{t}_L} + J_{t_L}, \qquad (105)\\
v_\omega n'_{T_R} &= D_{Q_L} n''_{T_R} + \Gamma_{y_T}\left[\frac{n_{Q_L}}{k_{Q_L}} - \frac{n_{T_R}}{k_{T_R}} - \frac{n_H}{k_H}\right] + \Gamma_m\left[\frac{n_{Q_L}}{k_{Q_L}} - \frac{n_{T_R}}{k_{T_R}}\right] \\
&+ 3\Gamma_{ss}\left[2\,\frac{n_{Q_L}}{k_{Q_L}} - \frac{n_{T_R}}{k_{T_R}} + 9\,\frac{n_{Q_L}+n_{T_R}}{k_{B_R}}\right] - J_{\tilde{t}_L} - J_{t_L}, \qquad (106)\\
v_\omega n'_H &= D_H n''_H + \Gamma_{y_T}\left[\frac{n_{Q_L}}{k_{Q_L}} - \frac{n_{T_R}}{k_{T_R}} - \frac{n_H}{k_H}\right] - \Gamma_h\,\frac{n_H}{k_H} + J_{\tilde{H}^c}, \qquad (107)
\end{aligned}$$

with

$$\begin{aligned}
J_{\tilde{t}_L}(z) &= -\partial_z j_{\tilde{t}_L}(z) \sim \frac{\tilde{\gamma}_{\tilde{t}}}{\langle v_{\tilde{t}_L}\rangle} j_{\tilde{t}_L}(z), \\
J_{t_L}(z) &= -\partial_z j_{t_L}(z) \sim \frac{\tilde{\gamma}_t}{\langle v_{t_L}\rangle} j_{t_L}(z), \\
J_{\tilde{H}^c}(z) &= -\partial_z j_{\tilde{H}^c}(z) \sim \frac{\tilde{\gamma}_{\chi^c}}{\langle v_{\tilde{H}^c}\rangle} j_{\tilde{H}^c}(z), \qquad (108)
\end{aligned}$$

where $\langle v_{\tilde{t}_L, t_L, \tilde{H}^c}\rangle$ is average velocity of the scattered particles and $\{k_{Q_L}, k_{T_R}, k_{B_R}, k_H\}$ are statistical factors.

For light particles compared to T_c, their statistical factor is 2 for bosons and 1 for fermions. If these particles are very heavy, then their statistical factors are suppressed exponentially. Explicitly, this suppression factor is (e.g., see [103])

$$12\Big(\frac{m}{2\pi T_c}\Big)^{3/2} \exp\left(\frac{-m}{T_c}\right), \qquad (109)$$

with m being the particle mass. In this paper, we assume that all charginos and neutralinos are light for simplicity. As for squark masses, we take $m^2_{\tilde{Q}_3} = m^2_{\tilde{u}^3_R} = 8$ while keeping the other squark soft mass squares to be 25 (see Table 3). This soft

[12] These equations are only valid in the limit of non-relativistic wall velocity. This is also true for Eq. (67).

mass pattern is phenomenologically favored due to the large beta functions for $m^2_{\tilde{Q}_3}$ and $m^2_{\tilde{u}^3_R}$. According to Eq. (109), we immediately find[13]

$$k_{Q_L} \approx 10, \quad k_{T_R} \approx 5, \quad k_{B_R} \approx 3, \quad k_H \approx 12, \tag{110}$$

and

$$\begin{aligned} \bar{D} &= \frac{5}{28} D_{Q_L} + \frac{23}{28} D_H, \\ \bar{\Gamma} &= \frac{23}{336} (\Gamma_m + \Gamma_h), \\ \bar{J} &= \frac{23}{28} (J_{\tilde{t}_L} + J_{t_L} + J_{\tilde{H}^c}). \end{aligned} \tag{111}$$

Here $\bar{D}$, $\bar{\Gamma}$, and $\bar{J}$ are the effective diffusion constant, decay rate and CP-violating current (for their definition, see [76]). It has been implicitly assumed that the other Higgs singlets are not thermally equilibrated with the EW charged ones. Using $D_H \sim 110/T_c$ and $D_{Q_L} \sim 6/T_c$ [93], one finds $\bar{D} \sim 91/T_c$. This result further constrains the wall velocity: slow weak sphaleron processes require

$$\bar{D}\Gamma_{ws}/v_w^2 < 1, \tag{112}$$

or

$$v_w > 0.02. \tag{113}$$

As for $\bar{\Gamma}$, using the estimation for $\Gamma_m(z) + \Gamma_h(z)$ with $\tan\beta > 1$ in [76], we have

$$\bar{\Gamma}(\infty) \approx 10^{-2} T_c. \tag{114}$$

To solve Eq. (105-107), we further assume that Γ_{ss} and Γ_{y_T} are large, and approximate

$$\begin{aligned} \Theta(z)\bar{J}(z) &\rightarrow \bar{J}(z), \\ \Theta(z)\bar{\Gamma}(\infty) &\rightarrow \bar{\Gamma}(z), \end{aligned} \tag{115}$$

following [31, 76]. Then using the boundary conditions $n_L(\pm\infty) = 0$, we find

$$n_L = \sum_i (n_{q^i_L} + n_{\tilde{q}^i_L}) = \mathcal{C}_{Q_L} e^{z\, v_\omega/\bar{D}} \tag{116}$$

for $z < 0$, where

$$\mathcal{C}_{Q_L} = \frac{5}{46} \frac{1}{\bar{D}\lambda_+} \int_0^\infty d\zeta\ \bar{J}(\zeta)\ e^{-\zeta\lambda_+}, \tag{117}$$

[13] As an approximation, we use their soft masses as the squarks' physical masses.

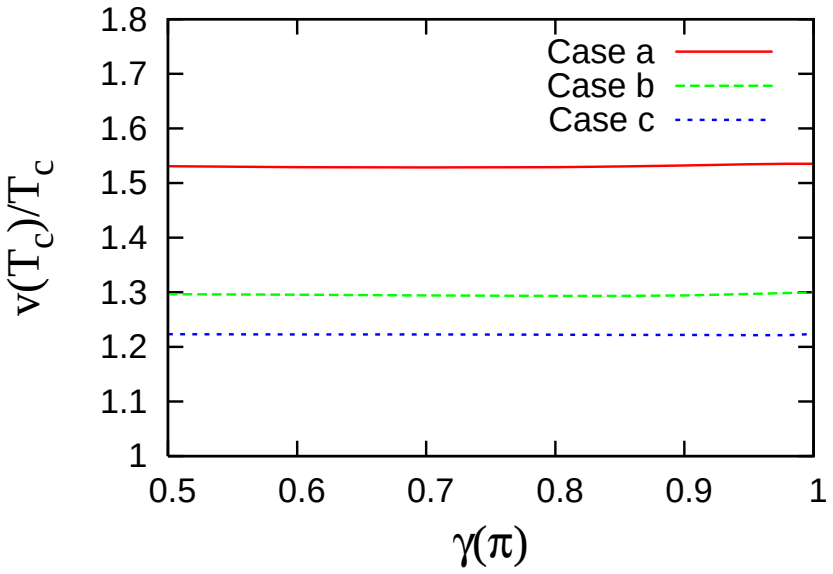

Figure 6: $\frac{v(T_c)}{T_c}$ vs. $\gamma(\pi)$ for cases a, b, and c defined in Table 3.

with

$$\lambda_+ = \frac{1}{2\bar{D}}\left\{v_\omega + \sqrt{v_\omega^2 + 4\bar{\Gamma}(\infty)\bar{D}}\right\} \approx 10^{-2} T_c. \tag{118}$$

This solution is the same as the MSSM one obtained in [31, 76] except the coefficient, which is caused by the difference of the $\{k_{Q_L}, k_{T_R}, k_{B_R}, k_H\}$ values. Solving the diffusion equation for n_B, which has exactly the same form as Eq. (71) with $D_L \to \bar{D}$ and $\mathcal{C}_L \to \mathcal{C}_{Q_L}$, we obtain the baryon number density for the $z \geq 0$ region

$$n_B = \frac{-n_f \bar{D}\Gamma_{ws}\mathcal{C}_{Q_L}}{v_w^2}, \tag{119}$$

and finally

$$\frac{n_B}{s} = -\frac{45}{2\pi^2 g_* T_c^3}\frac{15\Gamma_{ws}}{46 v_w^2 \lambda_+}\int_0^\infty d\zeta\ \bar{J}(\zeta)\ e^{-\zeta\lambda_+}. \tag{120}$$

7.3 Numerical Results of Non-local EWBG

According to the previous sections, the explicit CP phase, γ, plays a crucial role in mediating the EWBG. Both the spontaneous CP phases and the bubble wall physics show a strong dependence on it. There should be a similar γ dependence, therefore, for the generated baryon asymmetry.

Let us first consider the γ dependence of $v(T_c)/T_c$, the measure of the EWPT strength. Some related issues on EWBG have been discussed in Section 4 where no

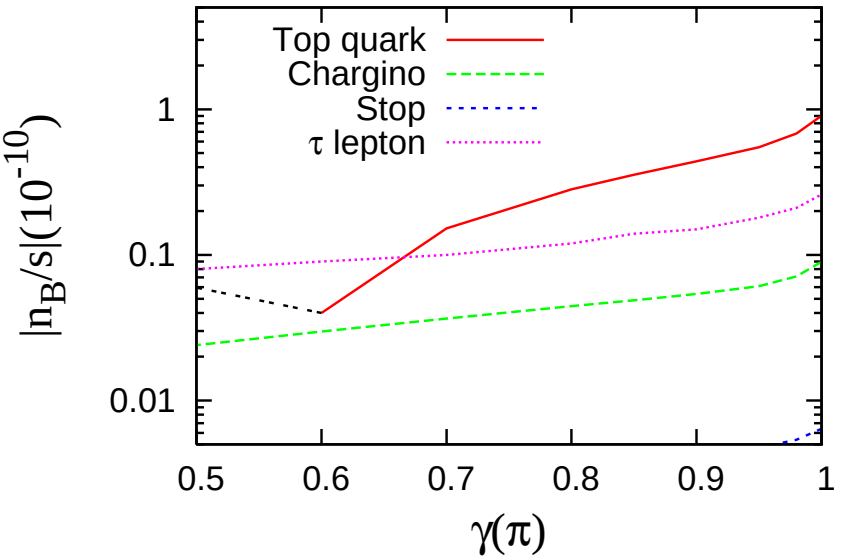

Figure 7: $\frac{n_B}{s}$ vs. $\gamma(\pi)$ for $v_w = 0.05$, in case a. There is a sign flip for n_B/s in the region denoted by black-dashed line for the top quark curve.

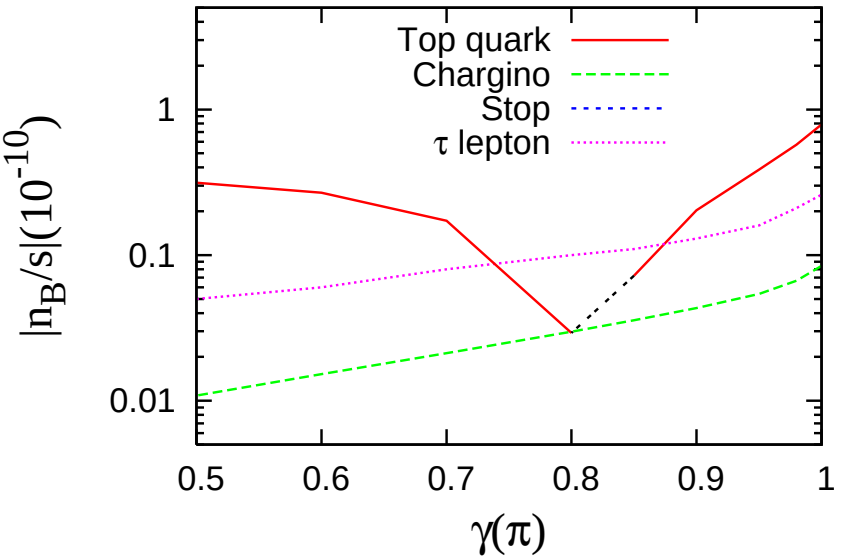

Figure 8: $\frac{n_B}{s}$ vs. $\gamma(\pi)$ for $v_w = 0.05$, in case b. There is a sign flip for n_B/s in the region denoted by black-dashed line for the top quark curve. The stop contribution is smaller than the scale of this figure.

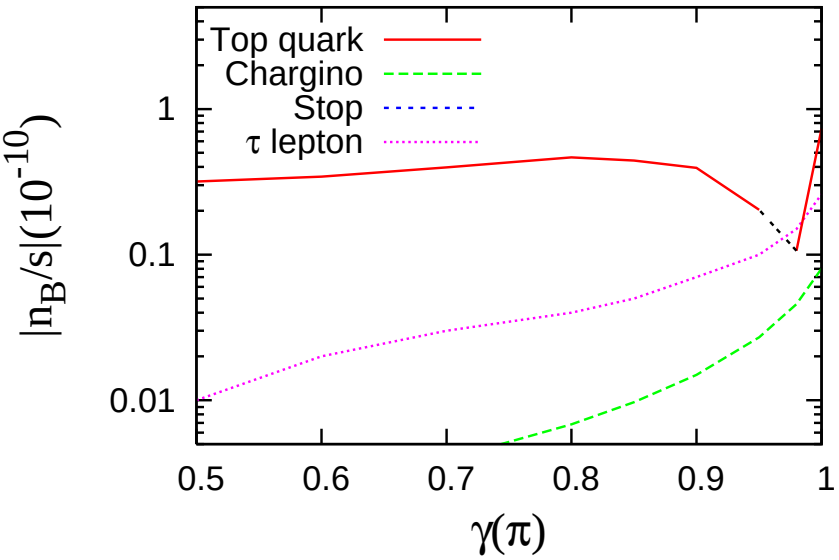

Figure 9: $\frac{n_B}{s}$ vs. $\gamma(\pi)$ for $v_w = 0.05$, in case c. There is a sign flip for n_B/s in the region denoted by black-dashed line for the top quark curve. The stop contribution is smaller than the scale of this figure.

ECPV is implicitly assumed. As expected, $v(T_c)/T_c$ shows a strong dependence on the soft SUSY breaking parameters $m^2_{\tilde{Q}_3}$, $m^2_{\tilde{u}^3_R}$ and A_h. In Figure 6, we illustrate the γ dependence of $v(T_c)/T_c$. The weak γ dependence is because γ is from the secluded sector of the neutral Higgs potential, which has no direct coupling to H^0_d and H^0_u. For all of the three cases a, b and c, the first order EWPT is strong enough for implementing the EWBG.

In Figure 7-9, we show the γ dependence of the baryon asymmetry $|n_B/s|$ produced by τ leptons, top squarks, charginos and top quarks[14]. We set $v_w = 0.05$. The produced baryon asymmetry is sensitive to γ. This is easy to understand since both the magnitude of SCPV and the bubble physics are sensitive to γ. Within theoretical uncertainties, the observed value $n_B/s = (8.82 \pm 0.23) \times 10^{-11}$ can be explained for a large range of γ values. Top quarks play a significant role in all three cases because of the top Yukawa coupling enhancement. In addition, due to the large change of the top quark mass crossing the bubble wall, the cancellation between $f^{t_R}_z(k^z_i)$ and $f^{t_R}_{z+\Delta}(-k^z_i)$ in Eq. (101) is relatively weak. The stop contribution depends on the magnitude of the soft parameter A_{h_t}. For a small A_{h_t}, it is dominated by the $w_1 w_1 \sim s^2 v_1^2$ term in Eq. (87). As $m^2_{H^0_d}$ increases, v_1 and s usually becomes smaller

[14]We did not consider the contribution from neutralinos. Since the relevant CP-violating sources and the interactions with the bubble wall are similar for neutralinos and charginos, their contributions are expected to be comparable with those from charginos. For relevant discussions in the MSSM, e.g., see [31].

and smaller. The stop contribution is then quartically suppressed. This explains why the stop contributions are smaller in case b and c than in case a, and also explains why the stop contribution is small for a small $m_{\chi_1^0}$ in Figure 15 of the next section (for all figures in this article, we chose $A_{h_t} = 0.1$). For a large A_{h_t}, the stop contribution is dominated by the $w_2 w_2 \sim A_{h_t}^2 v_2^2$ term in Eq. (87). It is not sensitive to the soft parameter $m_{H_d^0}^2$ and can be comparable with or even larger than the chargino contribution. Numerical results show that the stop contribution becomes comparable with the chargino one as A_{h_t} increases to $\sim T_c$ and with the top quark one as A_{h_t} increases to $\sim 4T_c$. As pointed out in the previous section, the $v_2 v_2$-type CP-violating current is absent at the leading order in the MSSM. Both the large contribution by top quarks and the enhancement effect of the stop contribution by a large A_{h_t} therefore are absent in the MSSM.

In addition to γ, there are two other important factors which can influence the produced baryon asymmetry. The first is v_w. One can see this from Eq. (74) and Eq. (119). A larger baryon asymmetry can be generated if the bubble wall is expanding at a more non-relativistic velocity; and vice versa. The second is the stop masses. In this paper we assume the stop soft mass $|m_{\tilde{Q}_3}| = |m_{\tilde{u}_R^3}|$ to be heavier than T_c, even though they are lighter than those of the other squarks and sleptons. If they (or more precisely, the stop physical masses) are light compared to T_c, then the associated statistical factors will be modified to [76]

$$k_{Q_L} \approx 18, \quad k_{T_R} \approx 9, \quad k_{B_R} \approx 3, \quad k_H \approx 12, \tag{121}$$

which gives an additional factor 3 in the numerator of Eq. (120).

8 Neutralino CDM and Non-local EWBG

Besides the baryon asymmetry, another mystery is dark matter (DM), which has been measured precisely by astrophysical and cosmological probes [104]:

$$\Omega_{\rm DM} h^2 = 0.106 \pm 0.008. \tag{122}$$

Given that supersymmetry with R-parity conservation could have a neutral LSP as a good candidate for the latter, e.g., the lightest neutralino χ_1^0, one naturally wants to know whether or not these two cosmological problems can be solved in the same framework.

To answer this question, we will not scan the whole space, since it is large. Instead, we vary parameters to which the neutralino DM relic density or $m_{\chi_1^0}$ is sensitive. From the discussions in the previous sections, $m_{H_d^0}^2$ can be such a parameter. Explicitly, we use parameter values given in Table 3, except that we vary $m_{H_d^0}^2$ between $10^4 \sim 5 \times 10^5$ GeV^2 and set $\gamma = 0.95\pi$. The relation between $m_{\chi_i^0}$ and $m_{H_d^0}^2$ is illustrated in Figure 10. As $m_{H_d^0}^2$ increases, $m_{\chi_i^0}$ decreases from more than 90 GeV to 35 GeV. This is because $m_{\chi_1^0} \sim h v_1$ in the limit of large $\langle S_{1,2,3} \rangle$ and $v_1 \ll v_2 \sim \langle S \rangle$ (see

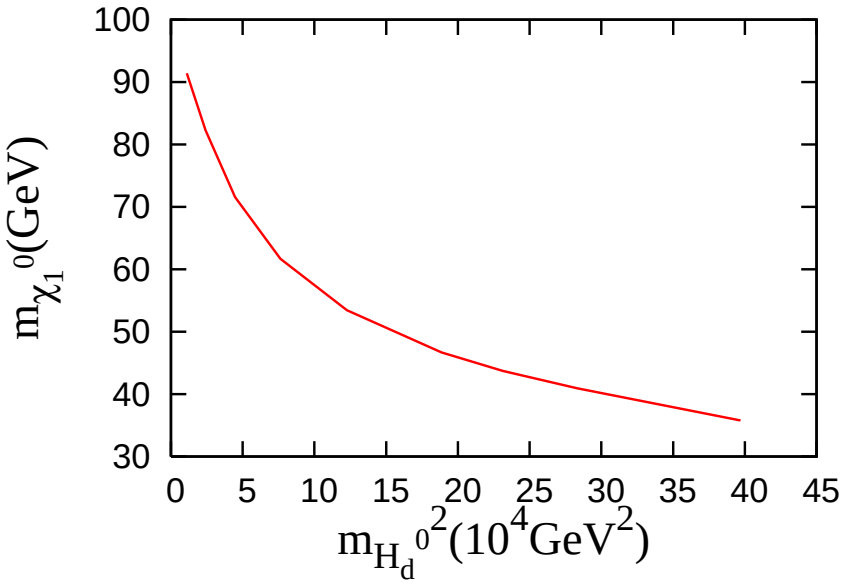

Figure 10: $m_{\chi_1^0}$ vs. $m^2_{H_d^0}$.

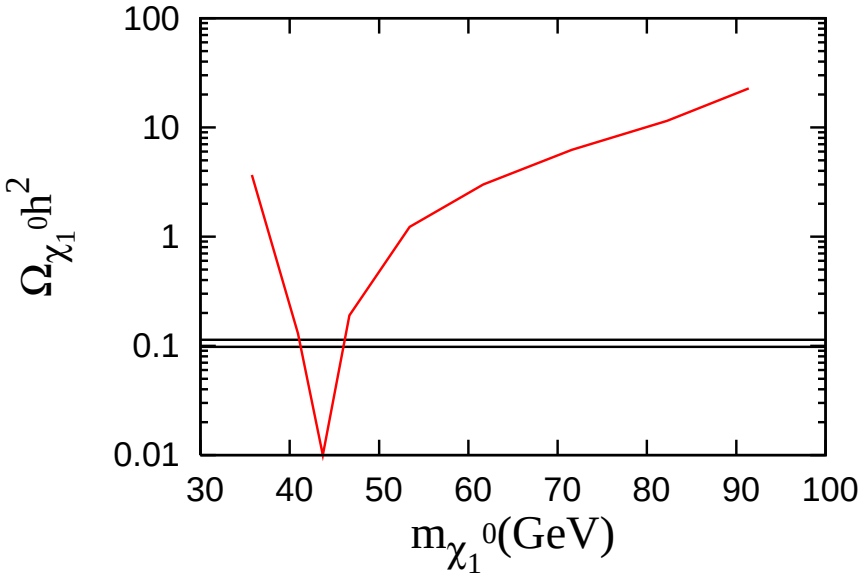

Figure 11: $\Omega_{\chi_1^0}h^2$ vs. $m_{\chi_1^0}$. The two black parallel lines give the upper and lower bounds on the DM relic density measured by astrophysical and cosmological probes [104].

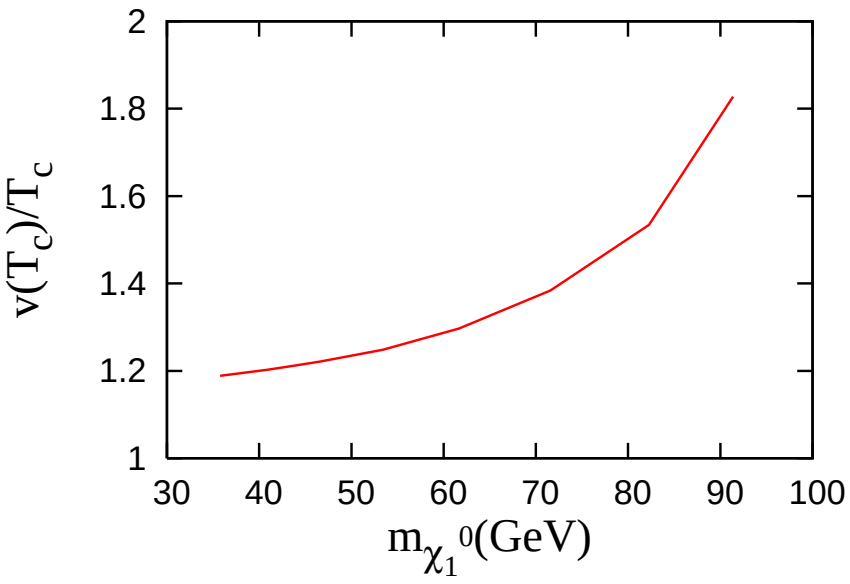

Figure 12: $\frac{v(T_c)}{T_c}$ vs. $m_{\chi_1^0}$.

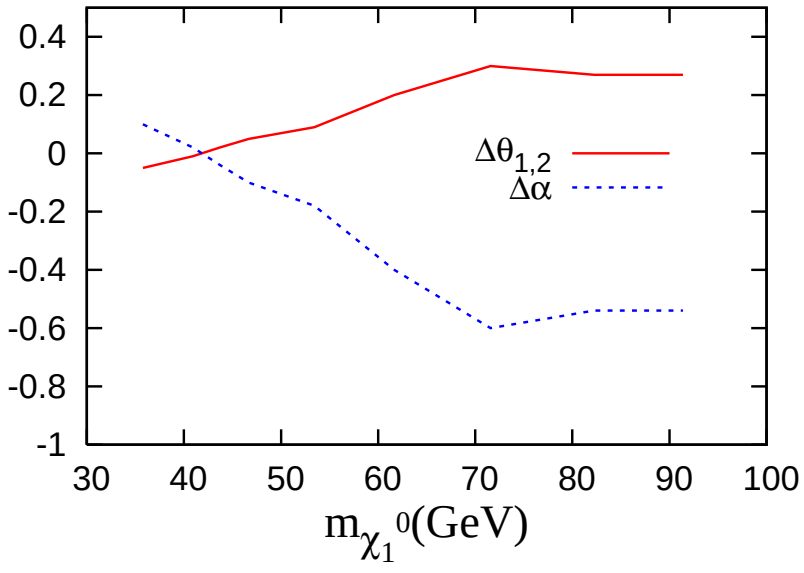

Figure 13: $\Delta\theta_{1,2}$ and $\Delta\alpha$ vs. $m_{\chi_1^0}$.

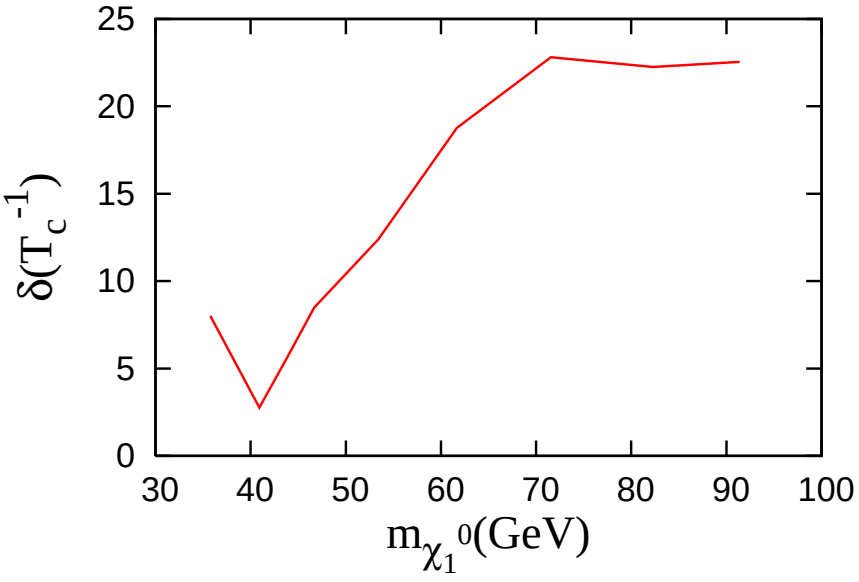

Figure 14: δ vs. $m_{\chi_1^0}$.

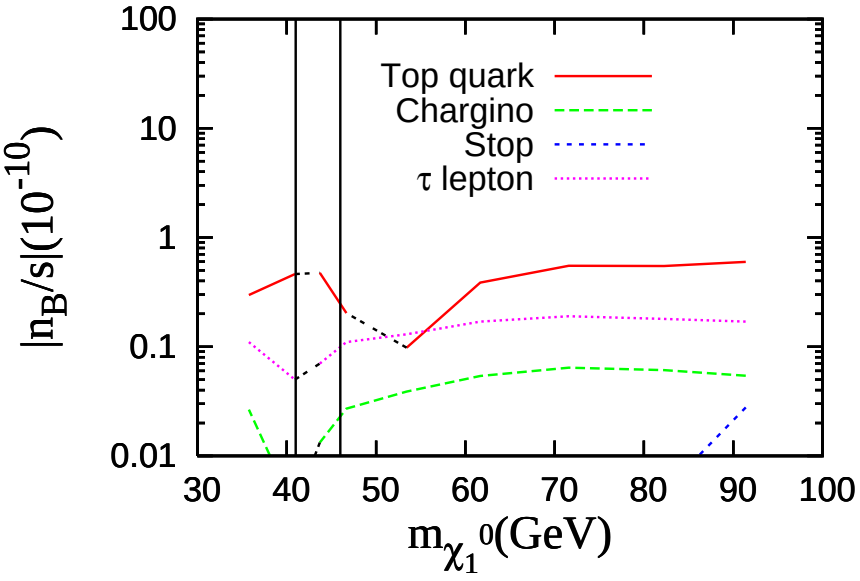

Figure 15: $\frac{n_B}{s}$ vs. $m_{\chi_1^0}$. There is a sign flip for n_B/s in the region denoted by black-dashed lines. The two black solid lines specify the $m_{\chi_1^0}$ values for which the observed dark matter relic density can be explained by χ_1^0.

Eqs. (A.25-A.27)) while a larger $m^2_{H^0_d}$ implies a smaller v_1. This feature is important for the DM relic density, since the Z pole region is covered. As is well-known, the relic density of neutralino CDM is usually overproduced. One way to reduce the abundance is from the Z-pole region, where we have $m_Z \sim 2m_{\chi^0_1}$ and the annihilation of two χ^0_1 through a Z boson is greatly enhanced. In this region, therefore, we can easily obtain an acceptable value for the χ^0_1 relic density. As a first-order approximation, we calculate the χ^0_1 relic density today, only counting in the processes mediated by gauge bosons (for general discussions on the relevant calculations, e.g., see [105]). The results are shown in Figure 11.

Let us come back to EWBG for this parameter region. With $m_{\chi^0_1}$ (or equivalently $m^2_{H^0_d}$) as a varying parameter, the strength of the EWPT, the magnitude of CP-violation, the thickness of the bubble wall and the produced baryon asymmetry by different particle species are shown in Figures 12-15. From Figure 12, it is easy to see that the measure of the EWPT strength $v(T_c)/T_c$ is always larger than 1.1. As $m_{\chi^0_1}$ increases or equivalently $m^2_{H^0_d}$ decreases, its value increases. This can be understood because a smaller scaled $m^2_{H^0_d}$ (the real $m^2_{H^0_d}$ value is also smaller) usually leads to a larger scaled $v_1(T_c)$ in the true vacuum, while keeping the scaled $v_2(T_c)$ and T_c almost invariant ($T_c \sim 1.4$ in our simulation). In Figure 13, we see that $\Delta\theta_{1,2}$ and $\Delta\alpha$ are close to zero around $m_{\chi^0_1} \approx 40$ GeV, which explains the small wall thickness in Figure 14 (recall that a large phase variation crossing the wall usually leads to a small wall thickness (see discussion in Subsection 6.1)) and a sign flip of n_B/s for the same $m_{\chi^0_1}$ value in Figure 14. Another sign flip for the top curve in Figure 14 is related to the ones shown in Figures 7-9, which is a result of balance between the contributions from the particle reflection and transmission. Finally, for most region of $m_{\chi^0_i} \sim 35 - 90$ GeV a strong enough first order EWPT and a reasonable baryon asymmetry can be obtained, and in the Z pole region the right χ^0_1 relic density can be produced (see Figure 15). The two cosmological mysteries, baryon asymmetry and DM, can therefore be explained simultaneously.

9 Some Other Cosmological Effects

9.1 Superconducting Cosmic Strings

There may exist phase transitions in the early Universe due to gauge symmetry breaking, and then topological defects, such as monopoles and/or cosmic strings, etc, can be produced [106, 107]. If the gauge group G is broken down to a subgroup H, we will have monopoles and cosmic strings if the homotopy group $\pi_2(G/H) \neq I$ and $\pi_1(G/H) = Z \neq I$, respectively, where Z is the group of integers. In particular, the cosmic strings may be superconducting because of the presence of a charged field condensate in the core of the string [108]. The gauge symmetry in the simplest cosmic string model is $U(1) \times U(1)'$ where the $U(1)'$ gauge symmetry is broken via the Higgs mechanism [108]. Note that $\pi_1(U(1)') = Z$, so we can have a topologically stable

cosmic string solution. Although the $U(1)$ symmetry is respected by the vacuum, it can be broken in the string core and then give rise to a bosonic condensate. Moreover, there may exist fermionic superconducting strings that have fermionic zero modes in its core [108]. These fermions can have non-zero $U(1)$ charges, and arise from Yukawa couplings to the scalar fields. In the non-supersymmetric models, we only need to introduce two complex scalar fields: one is charged under $U(1)$ while the other is charged under $U(1)'$ [108]. However, in order to have the bosonic superconductivity for cosmic strings in the supersymmetric $U(1) \times U(1)'$ model, one needs to introduce at least five chiral superfields [109]. Interestingly, one can realize the fermionic superconductivity in the simplest supersymmetric Abelian Higgs models [110].

In the sMSSM, we have the fermionic superconductivity, and supersymmetry is broken in the core of the cosmic strings (supersymmetry is not broken outside of the string core) which is similar to that in Ref. [110]. However, we do not have the bosonic superconductivity since all the Higgs fields are charged under the $U(1)'$ gauge symmetry. Because the $U(1)'$ gauge symmetry is broken around the TeV scale, the string tension $T_{\rm S}$ should be around the TeV scale as well. The gravitational effect of cosmic strings with $T_{\rm S}^2/M_{\rm Pl}^2 \sim 10^{-30}$ is extremely weak and is not within foreseeable detection capabilities. Interestingly, we can search for the signatures of particle emissions, such as positrons or other decaying particles produced where the current on the string quenches. Similar to the discussions in Ref. [111], which also has strings around 1 TeV, the sMSSM might explain the observed 511 keV emission from the electron-positron annihilation in the Galactic bulge [112, 113, 114].

9.2 Gravitational Waves

There are a few experiments under consideration that might detect for the first time a stochastic background of GWs, for example, the planned Laser Interferometer Space Antenna (LISA) [115], and the Big Bang Observer (BBO) [116], which is the follow-on mission to LISA. One of the well-motivated and convincing sources for GWs is inflation, and the discovery of a relic gravitational background could be a smoking gun signal from inflation. Another source of the stochastic GWs are strong first-order phase transitions. In contrast with the inflationary spectrum, the spectrum from a phase transition is not flat and has a characteristic peak related to the temperature at which the phase transition took place. Especially, LISA and BBO will have fairly good sensitivity at the frequencies that coincide with the redshifted spectrum of GWs produced during an electroweak phase transition at temperatures around 100 GeV. Thus, the GW observations will give us information about EWBG since the strong first-order electroweak phase transition is a necessary requirement.

There are two distinct mechanisms that can generate the GWs during a first-order electroweak phase transition: the bubble collisions [117, 118, 119, 120] and the turbulent motion of the primordial plasma [121, 122, 123, 124, 125]. The GWs from the electroweak phase transition have been studied in a model independent way in Refs. [126] and [127]. The results can be presented as a function of two main parameters: the typical size of the colliding bubbles and the available energy. It

was concluded that a sufficiently strong electroweak phase transition could lead to an observable GW signal at LISA. However, for a definite model, the bubble size and the available energy are correlated. Thus, it is still very important to study the concrete models in details.

It was found previously that in the MSSM the produced amount of GWs is orders of magnitude below the LISA sensitivity. The situation in the NMSSM seems much more promising because the trilinear term SH_dH_u can naturally lead to a much stronger electroweak phase transition [128]. Recently, it was pointed out that in Ref. [128] a rough approximation was used to calculate the bubble configurations, which overestimated the strength of the phase transition and the GW signal [129]. Moreover, in Refs. [129, 130] the nMSSM, which solves the μ problem and domain wall problem simultaneously, was considered. It was shown that the GW signals can be detected at BBO for part of parameter space, but cannot be observed at LISA [129, 130].

In the sMSSM the strong first-order electroweak phase transitions arises from the trilinear term SH_dH_u in the superpotential, which is similar to the NMSSM and nMSSM. The GW signals might therefore be detectable at BBO for part of the parameter space, but cannot be observed at LISA [129, 130]. As a side comment, the phase transition for the $U(1)'$ gauge symmetry breaking may not be strong first order since the coupling λ in the trilinear term $\lambda S_1 S_2 S_3$ is small, and one might not be able to observe the GWs from the $U(1)'$ gauge symmetry breaking.

10 Discussion and Conclusions

In this paper we discussed EWBG and its correlation with the neutralino CDM in the sMSSM. We first constructed two anomaly-free models. In Model I, we embedded the $SU(3)_C \times SU(2)_L \times U(1)_Y \times U(1)'$ gauge symmetry into a larger gauge symmetry, E_6, whose representations are anomaly-free. We considered three families of SM fermions and one pair of Higgs doublets arising from three E_6 fundamental representation **27**s. To include the SM singlet Higgs particles, achieve gauge coupling unification and cancel the $U(1)'$ anomaly, we assumed that three pairs of vector-like SM singlets and one pair of vector-like Higgs doublets from two pairs of **27** and $\mathbf{27}^*$ are light while the other particles in the two pairs of **27** and $\mathbf{27}^*$ are absent or very heavy. In Model II, we calculated the anomaly-free conditions, and added the minimal number of exotic particles to cancel the $U(1)'$ anomalies. We required that all the particles have rational $U(1)'$ charges. Although we had minimal exotic particles, we lost the gauge coupling unification. We also presented the general superpotential and the supersymmetry breaking soft terms in both models.

We discussed the one-loop effective potential at finite temperature in the 't Hooft-Landau gauge and in the $\overline{MS}$-scheme. We showed that there exists a strong enough first order EWPT because of the large trilinear term $A_h h S H_u H_d$ in the tree-level Higgs potential. Unlike the MSSM, the stop masses can be very heavy. The EWPT features in both models are quite similar because the exotic particles' contri-

butions to the one-loop effective potential at finite temperature are suppressed due to their heavy masses. We therefore restricted the detailed analysis to Model I.

In the early Universe the first order EWPT is realized by nucleating bubbles of the broken phase. Crossing the bubble walls, the VEVs of the Higgs fields (including their magnitudes and phases) are space-dependent. Because the dynamical behaviors of these bubbles, such as wall profile and expansion velocity, can have important influences on the production of the baryon asymmetry, we also studied their physics in detail. Numerical results show that the bubble wall thickness varies from $3 \sim 30\ T_c^{-1}$ as a monotonically increasing function of the phase changes of the Higgs fields. We also argued that the wall velocity in the sMSSM cannot be larger than that in the MSSM under the same phase transition condition and thus should be non-relativistic. This fact implies that EW sphaleron processes have more time to occur and hence will enhance the final baryon asymmetry.

We also discussed possible CP violation introduced by the extended Higgs sector. Unlike the MSSM, where there is no CP-violation at tree level in the Higgs sector, the CP symmetry can be broken spontaneously as well as explicitly. With loop corrections included, there may coexist vacua at finite temperature with broken and unbroken EW symmetry. The values of these spontaneous CP phases usually are different in these vacua. In our work, the SCPV provides a direct source for baryogenesis while its magnitude is mediated by an explicit one from the secluded sector. These new CP sources do not introduce significant new contributions to EDMs. After proper field redefinitions, the CP-violation phases will only appear in the Higgs mass matrix through soft masses associated with singlet components. Numerical results show that, for typical parameter values, their contributions to EDMs will be about six or seven orders smaller than the experimental upper limits. These contributions disappear completely in the limit with a trivial explicit CP phase, where the spontaneous CP phases are trivial in the true vacuum but not where EWBG occurs.

Subsequently, we systematically studied non-local EWBG in both the thin wall and thick wall regimes. We calculated the contribution from leptons in the thin wall regime, and the ones from squarks, charginos and quarks in the thick wall regime in terms of the profile of bubble wall. For leptons and quarks, the induced CP-violating currents outside the bubbles are proportional to Yukawa couplings squared, so we only considered the contributions from τ leptons and top quarks. We found that the CP-violating currents for stops and charginos are very different from those obtained in the MSSM. Due to the space-dependence of the relevant CP phases, they do not require a variation of $\tan\beta$ in the bubble wall to have a non-trivial structure at the lowest order of Higgs insertion. In addition, there exists a new type of CP-violating current at the leading order which can contribute to the generation of the baryon asymmetry. The CP-violating current of the new type has important influence on the EWBG. First, the stop contribution can be quadratically enhanced by a large A_{h_t}. Second, in addition to τ leptons, top squarks and charginos, top quarks can also play a significant role in the EWBG. We emphasize that all of these features are results of the SCPV-driven EWBG, so they are not sensitive to the concrete embeddings of the sMSSM. Numerical results show that the produced baryon asymmetry is large

enough to explain the cosmological observations.

After that, we studied the correlation between EWBG and neutralino CDM in the sMSSM. Though we did not scan the whole parameter space, we found that there exists a region where a strong enough first order EWPT, large CP phase variations crossing the bubble wall, a reasonable baryon asymmetry, as well as an acceptable neutralino LSP relic density can be achieved simultaneously. We also commented on possible cosmological signals of the model: superconducting cosmic strings and GWs. Particle emission from the decays of cosmic strings and GWs from EWPT could be observed within the foreseeable future.

The secluded $U(1)'$-breaking sector plays an essential role. It induces ECPV and SCPV at tree level in the Higgs sector, helping avoid significant new contributions to the EDMs which may hinder a successful EWBG in supersymmetric models, and also influences the bubble wall physics. It provides more degrees of freedom to drive the realization of EWBG, and makes the EWBG physics in the sMSSM very different from those in the MSSM and NMSSM. These differences make it interesting to further study the relevant collider implications for the LHC [64], which we will leave to future exploration.

Acknowledgments

We thank Michael Ramsey-Musolf and Carlos Wagner for fruitful discussions. The work of Paul Langacker is supported by the IBM Einstein Fellowship and by NSF grant PHY-0503584. The work of Tianjun Li is supported in part by the Natural Science Foundation of China under grant No. 10821504, by the DOE grant DE-FG03-95-Er-40917, and by the Mitchell-Heep Chair in High Energy Physics. The work of Tao Liu is supported by the Fermi-McCormick Fellowship and by the DOE through Grant No. DE-FG02- 90ER40560. This work was completed at the Aspen Center for Physics.

A Mass Matrices for the Particles in Model I

For the Higgs mass matrices, here we only present the results in the limit $m^2_{S_1S_2} = 0$, where there is no CP violation. It is not difficult to extend them to the general case with non-zero $m^2_{S_1S_2}$ and CP violation, as considered in the main text. Let us define

$$v_1 = \langle H_d^0 \rangle \ , \ v_2 = \langle H_u^0 \rangle \ , \ \tan\beta = \frac{v_2}{v_1} \ , \tag{A.1}$$

$$s = \langle S \rangle \ , \ s_i = \langle S_i \rangle \ . \tag{A.2}$$

Then the mass-square matrix for the CP-odd neutral Higgs particles in the basis $\{H_d^{0i} = Im(H_d^0), H_u^{0i}, S^{0i}, S_1^{0i}, S_2^{0i}, S_3^{0i}\}$ is

$$M^2_{A^0} = \begin{pmatrix} O_{A^0} & C_{A^0} \\ C^T_{A^0} & S_{A^0} \end{pmatrix} \ , \tag{A.3}$$

where

$$O_{A^0} = \begin{pmatrix} \beta^2_{H_d} & A_h h s & A_h h v_2 \\ A_h h s & \beta^2_{H_u} & A_h h v_1 \\ A_h h v_2 & A_h h v_1 & \beta^2_S \end{pmatrix} , \tag{A.4}$$

$$S_{A^0} = \begin{pmatrix} \beta^2_{S_1} & A_\lambda \lambda s_3 & A_\lambda \lambda s_2 \\ A_\lambda \lambda s_3 & \beta^2_{S_2} & A_\lambda \lambda s_1 \\ A_\lambda \lambda s_2 & A_\lambda \lambda s_1 & \beta^2_{S_3} \end{pmatrix} , \tag{A.5}$$

$$C_{A^0} = \begin{pmatrix} 0 & 0 & 0 \\ 0 & 0 & 0 \\ -m^2_{SS_1} & -m^2_{SS_2} & 0 \end{pmatrix} , \tag{A.6}$$

and

$$\beta^2_{H_d} = m^2_{H_d} + h^2(v_2^2 + s^2) + \frac{G^2}{4}(v_1^2 - v_2^2) + g^2_{Z'} Q_{H_d} \Delta \ , \tag{A.7}$$

$$\beta^2_{H_u} = m^2_{H_u} + h^2(v_1^2 + s^2) + \frac{G^2}{4}(v_2^2 - v_1^2) + g^2_{Z'} Q_{H_u} \Delta \ , \tag{A.8}$$

$$\beta^2_S = m^2_S + h^2(v_1^2 + v_2^2) + g^2_{Z'} Q_S \Delta \ , \tag{A.9}$$

$$\beta^2_{S_i} = m^2_{S_i} + \lambda^2 \sum_{j \neq i} s_j^2 + g^2_{Z'} Q_{S_i} \Delta \ , \tag{A.10}$$

where

$$\Delta \equiv Q_S s^2 + Q_{H_d} v_1^2 + Q_{H_u} v_2^2 + \sum_{i=1}^{3} Q_{S_i} s_i^2 \ . \tag{A.11}$$

Similarly, in the basis $\{H_d^{0r} = Re(H_d^0), H_u^{0r}, S^{0r}, S_1^{0r}, S_2^{0r}, S_3^{0r}\}$, the mass-square matrix for the CP-even neutral Higgs particles is

$$M_{H^0}^2 = \begin{pmatrix} O_{H^0} & C_{H^0} \\ C_{H^0}^T & S_{H^0} \end{pmatrix} \ , \tag{A.12}$$

where

$$O_{H^0} = \begin{pmatrix} \kappa_{H_d}^2 & \kappa_{H_d,H_u} & \kappa_{H_d,S} \\ \kappa_{H_d,H_u} & \kappa_{H_u}^2 & \kappa_{H_u,S} \\ \kappa_{H_d,S} & \kappa_{H_u,S} & \kappa_S^2 \end{pmatrix} , \tag{A.13}$$

$$S_{H^0} = \begin{pmatrix} \kappa_{S_1}^2 & \kappa_{S_1,S_2} & \kappa_{S_1,S_3} \\ \kappa_{S_1,S_2} & \kappa_{S_2}^2 & \kappa_{S_2,S_3} \\ \kappa_{S_1,S_3} & \kappa_{S_2,S_3} & \kappa_{S_3}^2 \end{pmatrix} , \tag{A.14}$$

$$C_{H^0} = \begin{pmatrix} \kappa_{H_d,S_1} & \kappa_{H_d,S_2} & \kappa_{H_d,S_3} \\ \kappa_{H_u,S_1} & \kappa_{H_u,S_2} & \kappa_{H_u,S_3} \\ \kappa_{S,S_1} + m_{S,S_1}^2 & \kappa_{S,S_2} + m_{S,S_2}^2 & \kappa_{S,S_3} \end{pmatrix} , \tag{A.15}$$

and

$$\kappa_{H_d}^2 = 2\left(\frac{G^2}{4} + g_{Z'}^2 Q_{H_d}^2\right) v_1^2 + m_{H_d}^2 + h^2(v_2^2 + s^2) + \frac{G^2}{4}(v_1^2 - v_2^2) + g_{Z'}^2 Q_{H_d} \Delta \ , \tag{A.16}$$

$$\kappa_{H_u}^2 = 2\left(\frac{G^2}{4} + g_{Z'}^2 Q_{H_u}^2\right) v_2^2 + m_{H_u}^2 + h^2(v_1^2 + s^2) + \frac{G^2}{4}(v_2^2 - v_1^2) + g_{Z'}^2 Q_{H_u} \Delta \ , \tag{A.17}$$

$$\kappa_S^2 = 2 g_{Z'}^2 Q_S^2 s^2 + m_S^2 + h^2(v_1^2 + v_2^2) + g_{Z'}^2 Q_S \Delta \ , \tag{A.18}$$

$$\kappa_{S_i}^2 = 2 g_{Z'}^2 Q_{S_i}^2 s_i^2 + m_{S_i}^2 + \lambda^2 \sum_{j \neq i} s_j^2 + g_{Z'}^2 Q_{S_i} \Delta \ , \tag{A.19}$$

$$\kappa_{H_d,H_u} = 2\left(h^2 - \frac{G^2}{4} + g_{Z'}^2 Q_{H_d} Q_{H_u}\right) v_1 v_2 - A_h h s \ , \tag{A.20}$$

$$\kappa_{H_i,S} = 2\left(h^2 + g_{Z'}^2 Q_{H_i} Q_S\right) v_i s - |\epsilon_{ij}| A_h h v_j \ , \tag{A.21}$$

$$\kappa_{H_i,S_j} = 2 g_{Z'}^2 Q_{H_i} Q_{S_j} v_i s_j \ , \ \kappa_{S,S_i} = 2 g_{Z'}^2 Q_S Q_{S_i} s s_i \ , \tag{A.22}$$

$$\kappa_{S_i,S_j} = 2(\lambda^2 + g_{Z'}^2 Q_{S_i} Q_{S_j}) s_i s_j - |\epsilon_{ijk}| A_\lambda \lambda s_k \ . \tag{A.23}$$

The charged Higgs mass is

$$M_{H^\pm}^2 = M_W^2 + \frac{2 A_h h s}{\sin 2\beta} - h^2(v_1^2 + v_2^2) \ , \tag{A.24}$$

where $M_W^2 = g_2^2(v_1^2 + v_2^2)/2$.

In the basis $\{\tilde{B}', \tilde{B}, \tilde{W}_3^0, \tilde{H}_d^0, \tilde{H}_u^0, \tilde{S}, \tilde{S}_1, \tilde{S}_2, \tilde{S}_3\}$, the neutralino mass matrix is

$$M_{\tilde{\chi}^0} = \begin{pmatrix} M_{\tilde{\chi}^0}(6,6) & M_{\tilde{\chi}^0}(6,3) \\ M_{\tilde{\chi}^0}(6,3)^T & M_{\tilde{\chi}^0}(3,3) \end{pmatrix} \ , \tag{A.25}$$

where

$$M_{\tilde{\chi}^0}(6,6) = \begin{pmatrix} M_1' & 0 & 0 & \Gamma_{H_d^0}^* & \Gamma_{H_u^0}^* & \Gamma_S^* \\ 0 & M_1 & 0 & -\frac{1}{\sqrt{2}} g_1 H_d^{0*} & \frac{1}{\sqrt{2}} g_1 H_u^{0*} & 0 \\ 0 & 0 & M_2 & \frac{1}{\sqrt{2}} g_2 H_d^{0*} & -\frac{1}{\sqrt{2}} g_2 H_u^{0*} & 0 \\ \Gamma_{H_d^0}^* & -\frac{1}{\sqrt{2}} g_1 H_d^{0*} & \frac{1}{\sqrt{2}} g_2 H_d^{0*} & 0 & hS & h H_u^0 \\ \Gamma_{H_u^0}^* & \frac{1}{\sqrt{2}} g_1 H_u^{0*} & -\frac{1}{\sqrt{2}} g_2 H_u^{0*} & hS & 0 & h H_d^0 \\ \Gamma_S^* & 0 & 0 & h H_u^0 & h H_d^0 & 0 \end{pmatrix} \tag{A.26}$$

and

$$M_{\tilde{\chi}^0}(3,3) = \begin{pmatrix} 0 & \lambda S_3 & \lambda S_2 \\ \lambda S_3 & 0 & \lambda S_1 \\ \lambda S_2 & \lambda S_1 & 0 \end{pmatrix} , \tag{A.27}$$

where $\Gamma_\phi \equiv \sqrt{2} g_{Z'} Q_\phi \phi$; and M_1', M_1 and M_2 are the gaugino masses for $U(1)'$, $U(1)$ and $SU(2)_L$, respectively. The first row of $M_{\tilde{\chi}^0}(6,3)$ is given by $\begin{pmatrix} \Gamma_{S_1}^* & \Gamma_{S_2}^* & \Gamma_{S_3}^* \end{pmatrix}$, while the other entries are zero.

The chargino mass matrix is

$$M_{\tilde{\chi}^\pm} = \begin{pmatrix} M_2 & \frac{g_2}{\sqrt{2}} H_u^{0*} \\ \frac{g_2}{\sqrt{2}} H_d^{0*} & hS \end{pmatrix} \ . \tag{A.28}$$

In contrast to the Higgs mass matrix, the neutralino and chargino mass matrices as well as the other ones in the following, are written in a general background with CP violation.

In the basis (B_μ, W^3_μ, Z'_μ), the mass matrix for the neutral gauge bosons is

$$M_{B,W^3,Z'} = \begin{pmatrix} M^{11}_{B,W^3,Z'} & M^{12}_{B,W^3,Z'} & M^{13}_{B,W^3,Z'} \\ M^{21}_{B,W^3,Z'} & M^{22}_{B,W^3,Z'} & M^{23}_{B,W^3,Z'} \\ M^{31}_{B,W^3,Z'} & M^{32}_{B,W^3,Z'} & M^{33}_{B,W^3,Z'} \end{pmatrix}, \tag{A.29}$$

where

$$M^{11}_{B,W^3,Z'} = \frac{1}{2} g_1^2 [|H_u^0|^2 + |H_d^0|^2] \ , \tag{A.30}$$

$$M^{12}_{B,W^3,Z'} = M^{21}_{B,W^3,Z'} = -\frac{1}{2} g_1 g_2 [|H_u^0|^2 + |H_d^0|^2] \ , \tag{A.31}$$

$$M^{13}_{B,W^3,Z'} = M^{31}_{B,W^3,Z'} = g_1 g_{Z'} [Q_{H_u} |H_u^0|^2 - Q_{H_d} |H_d^0|^2] \ , \tag{A.32}$$

$$M^{22}_{B,W^3,Z'} = \frac{1}{2} g_2^2 [|H_u^0|^2 + |H_d^0|^2] \ , \tag{A.33}$$

$$M^{23}_{B,W^3,Z'} = M^{32}_{B,W^3,Z'} = g_2 g_{Z'} [Q_{H_d} |H_d^0|^2 - Q_{H_u} |H_u^0|^2] \ , \tag{A.34}$$

$$M^{33}_{B,W^3,Z'} = 2 g_{Z'}^2 (Q_S^2 |S|^2 + Q_{H_u}^2 |H_u^0|^2 + Q_{H_d}^2 |H_d^0|^2 + \sum_{i=1}^{3} Q_{S_i}^2 |S_i|^2) \ . \tag{A.35}$$

In addition, for a scalar ϕ, we define

$$\Delta_\phi \equiv [T_3^\phi - Q_{EM}^\phi \sin^2 \theta_W] M_Z^2 \cos(2\beta) \ , \tag{A.36}$$

$$\Delta'_\phi \equiv Q'_\phi g_{Z'}^2 [Q_{H_u} |H_u^0|^2 + Q_{H_d} |H_d^0|^2 + Q_S |S|^2 + \sum_{i=1}^{3} Q_{S_i} |S_i|^2] \ . \tag{A.37}$$

The up-type squark mass matrix is

$$M_{\tilde{u}} = \begin{pmatrix} M^2_{\tilde{u}^i_L} & h^*_{u_i} (h S H_d^0 - A^*_{h_{u_i}} H_u^{0*}) \\ h_{u_i} (h^* S^* H_d^{0*} - A_{h_{u_i}} H_u^0) & M^2_{\tilde{u}^i_R} \end{pmatrix}, \tag{A.38}$$

where

$$M^2_{\tilde{u}^i_L} = m^2_{\tilde{Q}_i} + m^2_{u_i} + \Delta_{\tilde{u}^i_L} + \Delta'_{\tilde{u}^i_L} \ , \tag{A.39}$$

$$M^2_{\tilde{u}^i_R} = m^2_{\tilde{u}^i_R} + m^2_{u_i} + \Delta_{\tilde{u}^i_R} + \Delta'_{\tilde{u}^i_R} \ , \tag{A.40}$$

while the down-type matrix is obtained by $u \leftrightarrow d$. The mass matrices for the sleptons and exotic scalars are similar.

B $\Pi_\Phi(T)$ for Scalar Particles in Model I

The $\Pi_\Phi(T)$s for the Higgs doublets are

$$\Pi_{H_d}(T) = \frac{3}{8}g_2^2T^2 + \frac{1}{8}g_1^2T^2 + \frac{1}{2}g_{Z'}^2Q_{H_d}^2T^2 + \sum_{i=1}^{3}\left(\frac{3}{4}h_{d_i}^2 + \frac{1}{4}h_{e_i}^2\right)T^2 + \frac{1}{4}h^2T^2 \ , \quad \text{(B.1)}$$

$$\Pi_{H_u}(T) = \frac{3}{8}g_2^2T^2 + \frac{1}{8}g_1^2T^2 + \frac{1}{2}g_{Z'}^2Q_{H_u}^2T^2 + \sum_{i=1}^{3}\frac{3}{4}h_{u_i}^2T^2 + \frac{1}{4}h^2T^2 \ . \quad \text{(B.2)}$$

For the SM singlets:

$$\begin{aligned}\Pi_S(T) &= \frac{1}{2}g_{Z'}^2Q_s^2T^2 + \frac{1}{4}\alpha^2T^2 + \frac{1}{2}h^2T^2 + \sum_{i=1}^{3}\frac{3}{4}(\alpha_i^D)^2T^2 \\ &\quad + \sum_{k=1}^{2}\frac{1}{2}(\alpha_k^{H'})^2T^2 + \sum_{i=1}^{3}\frac{1}{4}(\alpha_i^N)^2T^2 \ , \end{aligned} \quad \text{(B.3)}$$

$$\Pi_{S_i}(T) = \frac{1}{2}g_{Z'}^2Q_{S_i}^2T^2 + \frac{1}{4}\lambda^2T^2 \ . \quad \text{(B.4)}$$

For the longitudinal components of the $SU(3)_C \times SU(2)_L \times U(1)_Y \times U(1)'$ gauge bosons, g, W, B and Z':

$$\Pi_{g_L}(T) = 6g_3^2T^2 \ , \ \ \Pi_{W_L}(T) = 6g_2^2T^2 \ , \quad \text{(B.5)}$$

$$\Pi_{B_L}(T) = 8g_1^2T^2 \ , \ \ \Pi_{Z'_L}(T) = \frac{619}{2}g_{Z'}^2T^2 \ . \quad \text{(B.6)}$$

For $\tilde{\tilde{N}}_i$ and S_L^i:

$$\Pi_{\tilde{\tilde{N}}_i}(T) = \frac{1}{2}g_{Z'}^2Q_{N_i}^2T^2 + \frac{1}{4}(\alpha_i^N)^2T^2 \ , \quad \text{(B.7)}$$

$$\Pi_{S_L^i}(T) = \frac{1}{2}g_{Z'}^2Q_{S_L^i}^2T^2 + \frac{1}{4}(\alpha_i^N)^2T^2 \ . \quad \text{(B.8)}$$

For $\tilde{X}$ and $\tilde{X}_3$:

$$\Pi_{\tilde{X}}(T) = \frac{1}{2}g_{Z'}^2Q_X^2T^2 + \frac{1}{4}\alpha^2T^2 \ , \quad \text{(B.9)}$$

$$\Pi_{\tilde{X}_3}(T) = \frac{1}{2} g_{Z'}^2 Q_{X_3}^2 T^2 + \frac{1}{4}\alpha^2 T^2 \ . \tag{B.10}$$

For $\tilde{D}_i$ and $\bar{\tilde{D}}_i$:

$$\Pi_{\tilde{D}_i}(T) = \frac{2}{3} g_3^2 T^2 + \frac{1}{18} g_1^2 T^2 + \frac{1}{2} g_{Z'}^2 Q_{D_i}^2 T^2 + \frac{1}{4}(\alpha_i^D)^2 T^2 \ , \tag{B.11}$$

$$\Pi_{\bar{\tilde{D}}_i}(T) = \frac{2}{3} g_3^2 T^2 + \frac{1}{18} g_1^2 T^2 + \frac{1}{2} g_{Z'}^2 Q_{\bar{D}_i}^2 T^2 + \frac{1}{4}(\alpha_i^D)^2 T^2 \ . \tag{B.12}$$

For $H_u'^k$ and $H_d'^k$:

$$\Pi_{H_u'^k}(T) = \frac{3}{8} g_2^2 T^2 + \frac{1}{8} g_1^2 T^2 + \frac{1}{2} g_{Z'}^2 Q_{H_u'^k}^2 T^2 + \frac{1}{4}(\alpha_k^{H'})^2 T^2 \ , \tag{B.13}$$

$$\Pi_{H_d'^k}(T) = \frac{3}{8} g_2^2 T^2 + \frac{1}{8} g_1^2 T^2 + \frac{1}{2} g_{Z'}^2 Q_{H_d'^k}^2 T^2 + \frac{1}{4}(\alpha_k^{H'})^2 T^2 \ . \tag{B.14}$$

For H_u' and $\bar{H}_u'$:

$$\Pi_{H_u'}(T) = \frac{3}{8} g_2^2 T^2 + \frac{1}{8} g_1^2 T^2 + \frac{1}{2} g_{Z'}^2 Q_{H_u'}^2 T^2 \ , \tag{B.15}$$

$$\Pi_{\bar{H}_u'}(T) = \frac{3}{8} g_2^2 T^2 + \frac{1}{8} g_1^2 T^2 + \frac{1}{2} g_{Z'}^2 Q_{\bar{H}_u'}^2 T^2 \ . \tag{B.16}$$

For the superpartners of the SM fermions:

$$\Pi_{\tilde{Q}_i}(T) = \frac{2}{3} g_3^2 T^2 + \frac{3}{8} g_2^2 T^2 + \frac{1}{72} g_1^2 T^2 + \frac{1}{2} g_{Z'}^2 {Q_{Q_i}}^2 T^2 + \frac{1}{4}\left(h_{u_i}^2 + h_{d_i}^2\right) T^2 \ , \tag{B.17}$$

$$\Pi_{\tilde{u}_R^i}(T) = \frac{2}{3} g_3^2 T^2 + \frac{2}{9} g_1^2 T^2 + \frac{1}{2} g_{Z'}^2 {Q_{\bar{u}_i}}^2 T^2 + \frac{1}{2} h_{u_i}^2 T^2 \ , \tag{B.18}$$

$$\Pi_{\tilde{d}_R^i}(T) = \frac{2}{3} g_3^2 T^2 + \frac{1}{18} g_1^2 T^2 + \frac{1}{2} g_{Z'}^2 {Q_{\bar{d}_i}}^2 T^2 + \frac{1}{2} h_{d_i}^2 T^2 \ , \tag{B.19}$$

$$\Pi_{\tilde{L}_i}(T) = \frac{3}{8} g_2^2 T^2 + \frac{1}{8} g_1^2 T^2 + \frac{1}{2} g_{Z'}^2 {Q_{L_i}}^2 T^2 + \frac{1}{4} h_{e_i}^2 T^2 \ , \tag{B.20}$$

$$\Pi_{\tilde{e}_R^i}(T) = \frac{1}{2} g_1^2 T^2 + \frac{1}{2} g_{Z'}^2 {Q_{\bar{e}_i}}^2 T^2 + \frac{1}{2} h_{e_i}^2 T^2 \ . \tag{B.21}$$

C Derivation of ΔR in the Thick Wall Regime

ΔR is the reflectivity asymmetry between the particle and antiparticle scatterings. It is crucial for the calculation of the CP-violating current in the EWBG. In the following, we will show how ΔR is calculated in the thick wall regime. We will explicitly calculate $\Delta R_{\tilde{W}^c\to\tilde{H}^c}(k_i,k_f,z)$ (see Eq. (93)) as an illustration. The calculations for $\Delta R_{\tilde{t}_R\to\tilde{t}_L}(k_i,k_f,z)$ and $\Delta R_{t_R\to t_L}(k_i,k_f,z)$ (see Eq. (87) and Eq. (99)) are similar, so we will not present their details.

The general formula for the probability calculation in quantum field theory is (eg. see [131])

$$\begin{aligned} P(\psi_i\to\psi_f) &= \int\frac{d^3p_f}{(2\pi)^3}\frac{1}{2E_f}|\langle p_f|\psi_i\rangle|^2 \\ &= \int\frac{d^3p_f}{(2\pi)^3}\frac{1}{2E_f}\int\frac{d^3p_i}{(2\pi)^3}\frac{\psi_i(p_i)}{\sqrt{2E_i}}\int\frac{d^3\tilde{p}_i}{(2\pi)^3}\frac{\psi_i^*(\tilde{p}_i)}{\sqrt{2\tilde{E}_i}}\langle p_f|p_i\rangle\langle p_f|\tilde{p}_i\rangle^*. \end{aligned} \tag{C.1}$$

Here the subscripts "i" and "f" denote initial and final states, respectively. Given that in the model the Langrangian is approximately invariant under the translations in the x, y and t directions, it is natural to define

$$\begin{aligned} \langle p_f|p_i\rangle &= \langle p_f|i\int d^4x\mathcal{L}(z)|p_i\rangle \\ &= iM(p_i\to p_f)(2\pi)^3\delta(E_i-E_f)\delta(p_i^x-p_f^x)\delta(p_i^y-p_f^y), \end{aligned} \tag{C.2}$$

with

$$M = \langle p_f^z|\int dz\mathcal{L}(z)|p_i^z\rangle. \tag{C.3}$$

Embedding Eq. (C.2) into Eq. (C.1), we find

$$P(\psi_i\to\psi_f)=\frac{1}{4E_iE_f}\frac{1}{v_i^zv_f^z}|M(k_i^z\to k_f^z)|^2, \tag{C.4}$$

where k, E and v are particle momentum, energy and velocity, respectively. For a given particle with mass m, all of the quantities are functions of k_i^z.

For the scattering process $\tilde{W}^c\to\tilde{H}^c$ in the chargino sector, $M(k_i^z,k_f^z,z)$ is

$$\begin{aligned} M(k_i^z,k_f^z,z) &= \int_z^{z+\Delta(\tilde{\gamma}_{\tilde{\chi}^c})}dz_1\exp(i(k_i^z-k_f^z)z_1) \\ &\quad (A(k_i^z,k_f^z,z_1)-A(k_i^z,k_f^z,z_1\to z)), \end{aligned} \tag{C.5}$$

with

$$\begin{aligned} A(k_i^z,k_f^z,z_1) &= \bar{u}_{\tilde{H}^c}(k_f^z)[(u_1(z_1)\exp(-i\theta_1(z_1)-u_1(z)\exp(-i\theta_1(z))P_L \\ &\quad +(u_2(z_1)\exp(i\theta_2(z_1)-u_2(z)\exp(i\theta_2(z))P_R]u_{\tilde{W}^c}(k_i^z), \end{aligned} \tag{C.6}$$

where $P_{L,R}$ denote chirality projection operators. Then,

$$\begin{aligned}\Delta|M(k_i^z,k_f^z,z)|^2 &= |M(k_i^z,k_f^z,z)|^2-(CP\text{ Conjugate})\\ &= \Delta\mathcal{A}(k_i^z,k_f^z,z_1,z_2)+\Delta\mathcal{A}(k_i^z,k_f^z,z_1\to z,z_2\to z)\\ &\quad -\Delta\mathcal{A}(k_i^z,k_f^z,z_1\to z,z_2)-\Delta\mathcal{A}(k_i^z,k_f^z,z_1,z_2\to z),\end{aligned}\quad (C.7)$$

with

$$\begin{aligned}\Delta\mathcal{A}(k_i^z,k_f^z,z_1,z_2) &= \int_z^{z+\Delta(\tilde{\gamma}_{\tilde{\chi}^c})} dz_1dz_2\exp(i(k_i^z-k_f^z)(z_1-z_2))\\ &\quad [A(k_i^z,k_f^z,z_1)A(k_i^z,k_f^z,z_2)^*-(CP\text{ Conjugate})].\end{aligned}\quad (C.8)$$

For the other $\Delta\mathcal{A}$s, only "z_1" or "z_2" or both in the *second* line of Eq. (C.8) are replaced by "z". It is easy to calculate

$$\begin{aligned}\Delta\mathcal{A}(k_i^z,k_f^z,z_1,z_2) &= \int_z^{z+\Delta(\tilde{\gamma}_{\tilde{\chi}^c})} dz_1dz_2\sin((k_i^z-k_f^z)(z_1-z_2))\\ &\quad \{k_i^zk_f^z[u_1(z_1)u_1(z_2)\sin(\theta_1(z_1)-\theta_1(z_2))\\ &\quad +u_2(z_1)u_2(z_2)\sin(-\theta_2(z_1)+\theta_2(z_2))]+\\ &\quad M_2\mu(z)[u_1(z_1)u_2(z_2)\sin(\theta_1(z_1)+\theta_2(z_2)+\alpha(z))\\ &\quad +u_2(z_1)u_1(z_2)\sin(-\theta_2(z_1)-\theta_1(z_2)-\alpha(z))]\},\end{aligned}\quad (C.9)$$

which implies

$$\Delta\mathcal{A}(k_i^z,k_f^z,z_1\to z,z_2\to z)\equiv 0. \quad (C.10)$$

Finally, embedding Eq. (C.9) into Eq. (C.7), we obtain Eq. (93) according to the relation

$$\Delta R_{\tilde{W}^c\to\tilde{H}^c}(k_i,k_f,z)=\frac{1}{4E_iE_f}\frac{1}{v_i^zv_f^z}\Delta|M(k_i^z,k_f^z,z)|^2. \quad (C.11)$$

D More Results at $T=0$ K in Model I

Additional $T=0K$ results in the sMSSM with both ECPV and SCPV turned on are presented in Figure 16 - Figure 20. These results include the γ dependences of $\tan\beta$, $m_{\chi_1^c}$ and $m_{\chi_1^0}$ in cases a, b and c, and the correlations between $\tan\beta$, $m_{\chi_1^c}$ and $m_{\chi_1^0}$ due to the variance of $m^2_{H_d^0}$. For discussions on the phenomenology in a similar framework, also see [132].

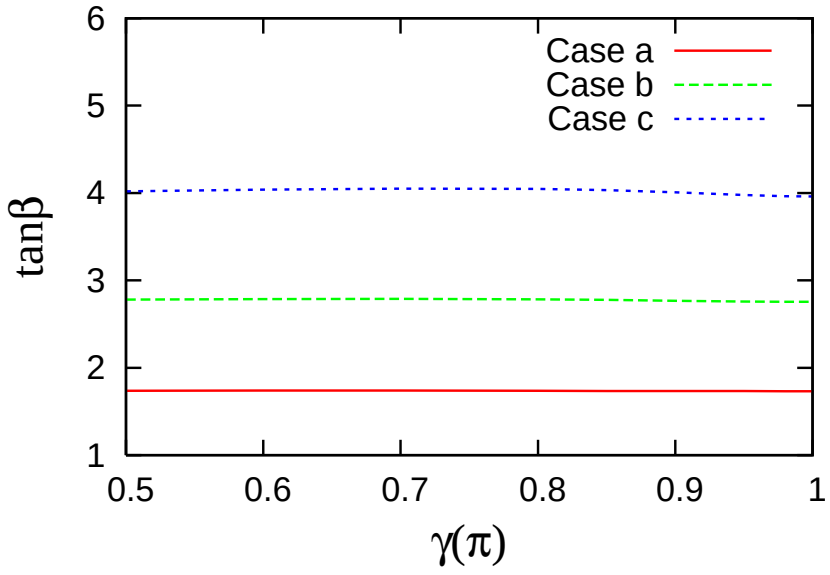

Figure 16: $\tan\beta$ vs. $\gamma(\pi)$.

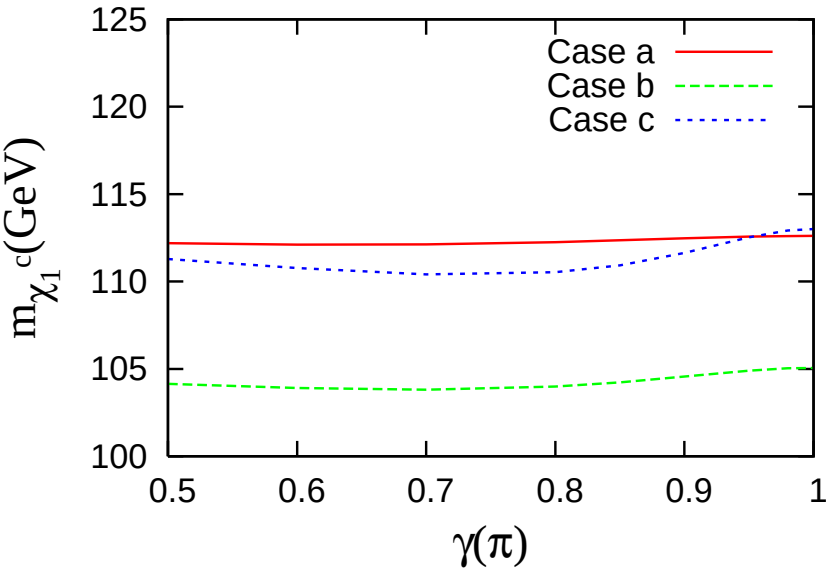

Figure 17: $m_{\chi_1^c}$ vs. $\gamma(\pi)$.

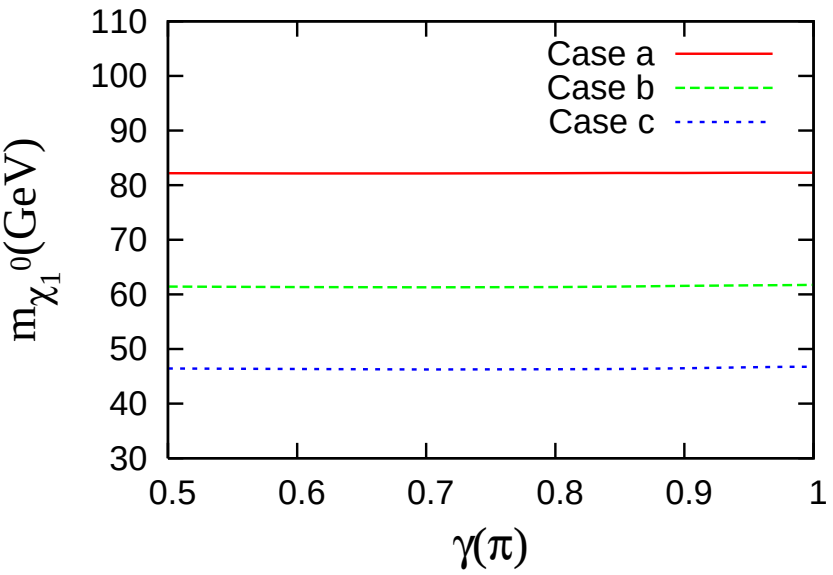

Figure 18: $m_{\chi_1^0}$ vs. $\gamma(\pi)$.

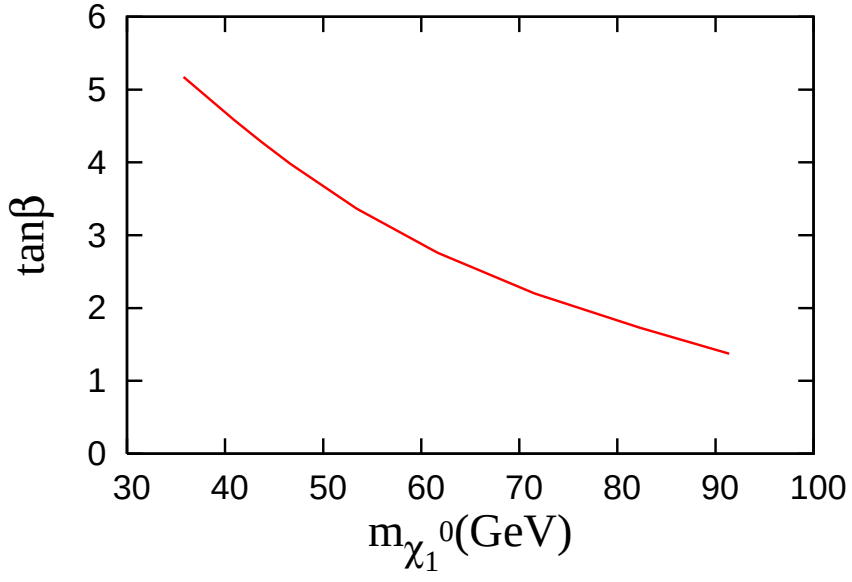

Figure 19: $\tan\beta$ vs. $m_{\chi_1^0}$.

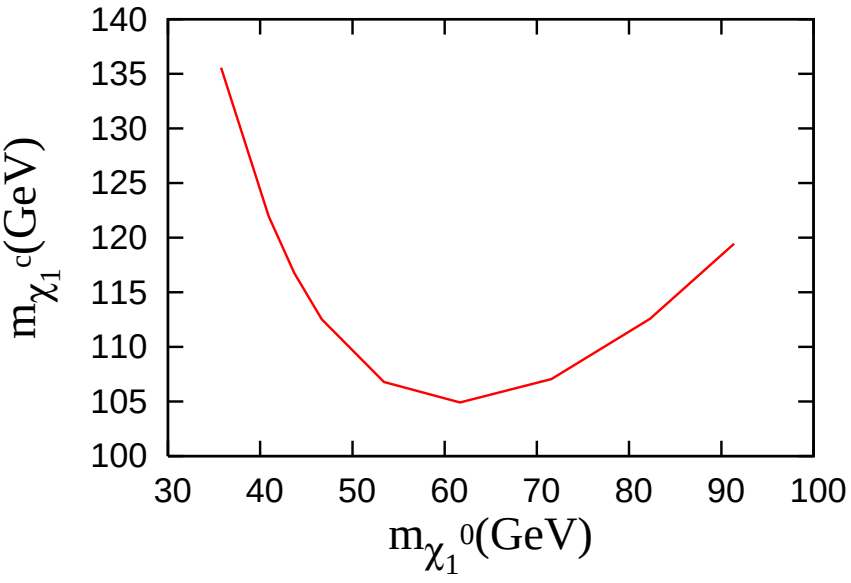

Figure 20: $m_{\chi_1^c}$ vs. $m_{\chi_1^0}$.

References

[1] E. Komatsu *et al.* [WMAP Collaboration], Astrophys. J. Suppl. **180**, 330 (2009).

[2] C. Amsler *et al.* [Particle Data Group], Phys. Lett. B **667**, 1 (2008).

[3] A. D. Sakharov, JETP Lett. **5**, 24 (1967).

[4] M. Yoshimura, Phys. Rev. Lett. **41**, 281 (1978) [Erratum-ibid. **42**, 746 (1979)].

[5] S. Dimopoulos and L. Susskind, Phys. Rev. D **18**, 4500 (1978).

[6] S. Weinberg, Phys. Rev. Lett. **42**, 850 (1979).

[7] I. Affleck and M. Dine, Nucl. Phys. B **249**, 361 (1985).

[8] M. Fukugita and T. Yanagida, Phys. Lett. B**174**, 45 (1986).

[9] W. Buchmuller and M. Plumacher, Int. J. Mod. Phys. A **15**, 5047 (2000), and references therein.

[10] V. A. Kuzmin, V. A. Rubakov and M. E. Shaposhnikov, Phys. Lett. B **155**, 36 (1985); **191**, 171 (1987).

[11] A. G. Cohen, D. B. Kaplan and A. E. Nelson, Ann. Rev. Nucl. Part. Sci. **43**, 27 (1993).

[12] V. A. Rubakov and M. E. Shaposhnikov, Usp. Fiz. Nauk **166**, 493 (1996) [Phys. Usp. **39**, 461 (1996)].

[13] M. Trodden, Rev. Mod. Phys. **71**, 1463 (1999).

[14] A. Riotto and M. Trodden, Ann. Rev. Nucl. Part. Sci. **49**, 35 (1999).

[15] W. Bernreuther, Lect. Notes Phys. **591**, 237 (2002), hep-ph/0205279.

[16] M. Dine and A. Kusenko, Rev. Mod. Phys. **76**, 1 (2004).

[17] G. 't Hooft, Phys. Rev. Lett. **37**, 8 (1976); Phys. Rev. **D14**, 3432 (1976) .

[18] F. R. Klinkhamer and N. S. Manton, Phys. Rev. D **30**, 2212 (1984).

[19] S. Y. Khlebnikov and M. E. Shaposhnikov, Nucl. Phys. B **308**, 885 (1988); J. A. Harvey and M. S. Turner, Phys. Rev. D **42**, 3344 (1990).

[20] R. Barate *et al.*, Phys. Lett. B **565**, 61 (2003).

[21] S. Profumo, M. J. Ramsey-Musolf and G. Shaughnessy, JHEP **0708**, 010 (2007); V. Barger, P. Langacker, M. McCaskey, M. Ramsey-Musolf and G. Shaughnessy, Phys. Rev. D **79**, 015018 (2009).

[22] J. R. Espinosa, Nucl. Phys. B **475**, 273 (1996).

[23] B. de Carlos and J. R. Espinosa, Nucl. Phys. B **503**, 24 (1997).

[24] M. Laine and K. Rummukainen, Phys. Rev. Lett. **80**, 5259 (1998); Nucl. Phys. B **535**, 423 (1998).

[25] A. Riotto, Phys. Rev. D **58**, 095009 (1998).

[26] J. M. Cline and K. Kainulainen, Phys. Rev. Lett. **85**, 5519 (2000).

[27] J. M. Cline, M. Joyce and K. Kainulainen, JHEP **0007**, 018 (2000).

[28] M. S. Carena, M. Quiros and C. E. M. Wagner, Phys. Lett. B **380**, 81 (1996) [arXiv:hep-ph/9603420].

[29] M. S. Carena, M. Quiros, A. Riotto, I. Vilja and C. E. M. Wagner, Nucl. Phys. B **503**, 387 (1997).

[30] M. Carena, M. Quiros and C. E. M. Wagner, Nucl. Phys. B **524**, 3 (1998).

[31] M. Carena, J. M. Moreno, M. Quiros, M. Seco and C. E. M. Wagner, Nucl. Phys. B **599**, 158 (2001).

[32] M. Carena, M. Quiros, M. Seco and C. E. M. Wagner, Nucl. Phys. B **650**, 24 (2003).

[33] M. Carena, G. Nardini, M. Quiros and C. E. M. Wagner, JHEP **0810**, 062 (2008) M. Carena, A. Freitas and C. E. M. Wagner, JHEP **0810**, 109 (2008) M. Carena, G. Nardini, M. Quiros and C. E. M. Wagner, Nucl. Phys. B **812**, 243 (2009)

[34] V. Cirigliano, S. Profumo and M. J. Ramsey-Musolf, JHEP **0607**, 002 (2006);

[35] V. Cirigliano, Y. Li, S. Profumo and M. J. Ramsey-Musolf, arXiv:0910.4589 [hep-ph].

[36] D. J. H. Chung, B. Garbrecht, M. J. Ramsey-Musolf and S. Tulin, Phys. Rev. Lett. **102**, 061301 (2009).

[37] Y. Li, S. Profumo and M. Ramsey-Musolf, Phys. Lett. B **673**, 95 (2009); V. Cirigliano, Y. Li, S. Profumo and M. J. Ramsey-Musolf, arXiv:0910.4589 [hep-ph].

[38] A. Menon and D. E. Morrissey, Phys. Rev. D **79**, 115020 (2009).

[39] K. Funakubo and E. Senaha, Phys. Rev. D **79**, 115024 (2009).

[40] K. Kainulainen, T. Prokopec, M. G. Schmidt and S. Weinstock, JHEP **0106**, 031 (2001).

[41] K. Kainulainen, T. Prokopec, M. G. Schmidt and S. Weinstock, Phys. Rev. D **66**, 043502 (2002).

[42] J. Ellis, J. F. Gunion, H. E. Haber, L. Roszkowski, and F. Zwirner, Phys. Rev. D **39**, 844 (1989); and references therein. Recent references may be found in U. Ellwanger, J. F. Gunion, and C. Hugonie, hep-ph/0111179.

[43] M. Pietroni, Nucl. Phys. **B402**, 27 (1993).

[44] A. T. Davies, C. D. Froggatt and R. G. Moorhouse, Phys. Lett. B **372**, 88 (1996).

[45] S. J. Huber and M. G. Schmidt, Eur. Phys. J. **C10**, 473 (1999); Nucl. Phys. B **606**, 183 (2001).

[46] J. M. Cline, S. Kraml, G. Laporte and H. Yamashita, JHEP **0907**, 040 (2009).

[47] J. E. Kim and H. P. Nilles, Phys. Lett. B **138**, 150 (1984).

[48] T. Liu and C. E. M. Wagner, JHEP **0806**, 073 (2008); Z. Komargodski and N. Seiberg, JHEP **0903**, 072 (2009); J. D. Mason, Phys. Rev. D **80**, 015026 (2009).

[49] S. A. Abel, S. Sarkar and P. L. White, Nucl. Phys. B **454**, 663 (1995); J. Bagger, E. Poppitz and L. Randall, Nucl. Phys. B **455**, 59 (1995), and references theirin.

[50] C. Panagiotakopoulos and K. Tamvakis, Phys. Lett. B **446**, 224 (1999).

[51] C. Panagiotakopoulos and K. Tamvakis, Phys. Lett. B **469**, 145 (1999) ; C. Panagiotakopoulos and A. Pilaftsis, Phys. Rev. D **63**, 055003 (2001) ; A. Dedes, C. Hugonie, S. Moretti and K. Tamvakis, Phys. Rev. D **63**, 055009 (2001) .

[52] A. Menon, D.E. Morrissey and C.E.M. Wagner, Phys. Rev. D **70** 035005 (2004).

[53] C. Balazs, M. S. Carena, A. Freitas and C. E. M. Wagner, JHEP **0706**, 066 (2007) [arXiv:0705.0431 [hep-ph]].

[54] E. Accomando *et al.*, arXiv:hep-ph/0608079; V. Barger, P. Langacker and G. Shaughnessy, New J. Phys. **9**, 333 (2007).

[55] For a review, see, P. Langacker, arXiv:0801.1345 [hep-ph].

[56] M. Cvetič and P. Langacker, Phys. Rev. D **54**, 3570 (1996) and Mod. Phys. Lett. A **11**, 1247 (1996).

[57] For a review, see, M. Cvetič and P. Langacker, in *Perspectives on supersymmetry*, ed. G. L. Kane (World, Singapore, 1998), p. 312.

[58] For a review, see C. T. Hill and E. H. Simmons, Phys. Rept. **381**, 235 (2003).

[59] N. Arkani-Hamed, A.G. Cohen and H. Georgi, Phys. Lett. B 513, 232 (2001): N. Arkani-Hamed, A.G. Cohen, E. Katz and A. E. Nelson, JHEP 0207, 034 (2002); T. Han, H.E. Logan, B. McElrath, L.T. Wang, Phys. Rev. D 67, 095004 (2003).

[60] D. Suematsu and Y. Yamagishi, Int. J. Mod. Phys. A **10**, 4521 (1995).

[61] M. Cvetič, D. A. Demir, J. R. Espinosa, L. L. Everett and P. Langacker, Phys. Rev. D **56**, 2861 (1997) [Erratum-ibid. D **58**, 119905 (1997)]. For the case of gauge mediated symmetry breaking, see P. Langacker, N. Polonsky and J. Wang, Phys. Rev. D **60**, 115005 (1999).

[62] A. Vilenkin, Phys. Rept. **121**, 263 (1985).

[63] L. Durand and J. L. Lopez, Phys. Lett. B **217**, 463 (1989); M. Drees, Int. J. Mod. Phys. A **4**, 3635 (1989); M. Cvetič et al, ref. [61]. Other references are given in [57].

[64] T. Han, P. Langacker and B. McElrath, Phys. Rev. D **70**, 115006 (2004).

[65] V. Barger, P. Langacker, H. S. Lee and G. Shaughnessy, Phys. Rev. D **73**, 115010 (2006).

[66] J. Erler, Nucl. Phys. B **586**, 73 (2000).

[67] F. Abe et al. [CDF Collaboration], Phys. Rev. Lett. **79**, 2192 (1997); CDF Collaboration: D. E. Acosta et al., Phys. Rev. D **71**, 052002 (2005); CDF Collaboration: T. Aaltonen et al., Phys. Rev. Lett. **102**, 091805 (2009); CDF Collaboration: T. Aaltonen et al., Phys. Rev. Lett. **102**, 031801 (2009); D0 Collaboration: V. M. Abazov et al., Phys. Rev. Lett. **101**, 191801 (2008); D0 Collaboration: D0 Note 5923-Conf (2009), `http://www-d0.fnal.gov/Run2Physics/WWW/results/prelim/NP/N66`.

[68] J. Erler, P. Langacker, S. Munir and E. R. Pena, arXiv:0906.2435 [hep-ph], and references therein.

[69] J. Erler, P. Langacker, T. Li, Phys. Rev. D**66**, 015002 (2002).

[70] J. Kang, P. Langacker, T. j. Li and T. Liu, Phys. Rev. Lett. **94**, 061801 (2005).

[71] P. Langacker and J. Wang, Phys. Rev. D **58**, 115010 (1998).

[72] J. M. Moreno, M. Quiros and M. Seco, Nucl. Phys. B **526**, 489 (1998).

[73] P. John, Phys. Lett. B **452**, 221 (1999).

[74] J. M. Cline, G. D. Moore and G. Servant, Phys. Rev. D **60**, 105035 (1999).

[75] A. Cohen, D. Kaplan and A. Nelson, Nuc. Phys. B **349**, 727 (1991).

[76] P. Huet and A. E. Nelson, Phys. Rev. D **53**, 4578 (1996).

[77] N. Rius and V. Sanz, Nucl. Phys. B **570**, 155 (2000).

[78] See, for example, G. Cleaver, M. Cvetic, J. R. Espinosa, L. L. Everett, P. Langacker and J. Wang, Phys. Rev. D **59**, 055005 (1999).

[79] P. Langacker, G. Paz and I. Yavin, Phys. Lett. B **671**, 245 (2009) [arXiv:0811.1196 [hep-ph]].

[80] S. F. King, S. Moretti and R. Nevzorov, Phys. Rev. D **73**, 035009 (2006); R. Howl and S. F. King, JHEP **0801**, 030 (2008).

[81] R. Slansky, Phys. Rept. **79**,1 (1981).

[82] J. L. Hewett and T. G. Rizzo, Phys. Rept. **183**, 193 (1989).

[83] L. Wolfenstein and D. Wyler, Nucl. Phys. B **218**, (1983) 205; R. N. Mohapatra and J. W. F. Valle, Phys. Rev. D **34**, 1642 (1986); S. Nandi and U. Sarkar, Phys. Rev. Lett. **56**, 564 (1986).

[84] J. h. Kang, P. Langacker and T. j. Li, Phys. Rev. D **71**, 015012 (2005).

[85] J. Kang, P. Langacker and B. D. Nelson, Phys. Rev. D **77**, 035003 (2008).

[86] M. Quiros, hep-ph/9901312.

[87] G. W. Anderson and L. J. Hall, Phys. Rev. D **45**, 2685 (1992).

[88] D. Comelli and J. R. Espinosa, Phys. Rev. D **55**, 6253 (1997).

[89] S. W. Ham and S. K. Oh, Phys. Rev. D **76**, 095018 (2007); S. W. Ham, E. J. Yoo and S. K. Oh, Phys. Rev. D **76**, 075011 (2007).

[90] S. J. Huber and M. G. Schmidt, Nucl. Phys. B **606**, 183 (2001); S. J. Huber, P. John and M. G. Schmidt, Eur. Phys. J. C **20**, 695 (2001); S. J. Huber, P. John, M.Laine and M. G. Schmidt, Phys. Lett. B **475**, 104 (2001).

[91] G. D. Moore, JHEP **0003**, 006 (2000); P. John and M. G. Schmidt, Nucl. Phys. B **598**, 291 (2001) [Erratum-ibid. B **648**, 449 (2003)]; A. Megevand and A. D. Sanchez, arXiv:0908.3663 [hep-ph].

[92] A. D. Linde, Phys. Lett. B **70**, 306 (1977); Nucl. Phys. B **216**, 421 (1983).

[93] M. Joyce, T. Prokopec and N. Turok, Phys. Lett. B **338**, 269 (1994)

[94] M. Joyce, T. Prokopec and N. Turok., Phys. Rev. D **53**, 2930 (1996).

[95] M. Joyce, T. Prokopec and N. Turok, Phys. Rev. Lett. **75**, 1695 (1995) [Erratum-ibid. **75**, 3375 (1995)]

[96] M. Joyce, T. Prokopec and N. Turok, Phys. Rev. D **53**, 2958 (1996) [arXiv:hep-ph/9410282].

[97] A. G. Cohen, D. B. Kaplan and A. E. Nelson, Phys. Lett. B **263**, 86 (1991).

[98] D. Bödeker, G. D. Moore and K. Rummukainen, Phys. Rev. D **61**, 056003 (2000).

[99] G. D. Moore, Phys. Rev. D **62**, 085011 (2000).

[100] P. Elmfors, K. Enqvist, A. Riotto and I. Vilja, Phys. Lett. B **452**, 279 (1999)

[101] R. N. Mohapatra and X. m. Zhang, Phys. Rev. D **45**, 2699 (1992); G. F. Giudice and M. E. Shaposhnikov, Phys. Lett. B **326**, 118 (1994).

[102] D. J. H. Chung, B. Garbrecht, M. J. Ramsey-Musolf and S. Tulin, arXiv:0908.2187 [hep-ph]; D. J. H. Chung, B. Garbrecht, M. J. Ramsey-Musolf and S. Tulin, arXiv:0905.4509 [hep-ph].

[103] E. W. Kolb and M. S. Turner, *The Early Universe*, Addison-Wesley, (1994).

[104] C. Amsler *et al.* [Particle Data Group], Phys. Lett. B **667**, 1 (2008).

[105] G. Bertone, D. Hooper and J. Silk, Phys. Rept. **405**, 279 (2005); G. Jungman, M. Kamionkowski and K. Griest, Phys. Rept. **267** (1996) 195.

[106] A. Vilenkin, Phys. Rept. **121**, 263 (1985).

[107] A. Vilenkin and E. P. S. Shellard, *Cosmic Strings and Other Topological Defects* (Cambridge University Press, Cambridge, England, 1994).

[108] E. Witten, Nucl. Phys. B **249**, 557 (1985).

[109] J. R. Morris, Phys. Rev. D **53**, 2078 (1996).

[110] S. C. Davis, A. C. Davis and M. Trodden, Phys. Lett. B **405** (1997) 257.

[111] F. Ferrer and T. Vachaspati, Phys. Rev. Lett. **95**, 261302 (2005).

[112] P. A. Milne, J. D. Kurfess, R. L. Kinzer and M. D. Leising, New Astron. Rev. **46**, 553 (2002).

[113] P. Jean *et al.*, Astron. Astrophys. **407**, L55 (2003).

[114] J. Knodlseder *et al.*, Astron. Astrophys. **411**, L457 (2003).

[115] `http://lisa.jpl.nasa.gov/.`

[116] `http://universe.nasa.gov/program/vision.html.`

[117] A. Kosowsky, M. S. Turner and R. Watkins, Phys. Rev. D **45**, 4514 (1992).

[118] A. Kosowsky, M. S. Turner and R. Watkins, Phys. Rev. Lett. **69**, 2026 (1992).

[119] A. Kosowsky and M. S. Turner, Phys. Rev. D **47**, 4372 (1993).

[120] M. Kamionkowski, A. Kosowsky and M. S. Turner, Phys. Rev. D **49**, 2837 (1994).

[121] A. Kosowsky, A. Mack and T. Kahniashvili, arXiv:astro-ph/0102169.

[122] A. Kosowsky, A. Mack and T. Kahniashvili, Phys. Rev. D **66**, 024030 (2002).

[123] A. D. Dolgov, D. Grasso and A. Nicolis, Phys. Rev. D **66**, 103505 (2002).

[124] C. Caprini and R. Durrer, Phys. Rev. D **74**, 063521 (2006).

[125] G. Gogoberidze, T. Kahniashvili and A. Kosowsky, Phys. Rev. D **76**, 083002 (2007).

[126] A. Nicolis, Class. Quant. Grav. **21**, L27 (2004).

[127] C. Grojean and G. Servant, Phys. Rev. D **75**, 043507 (2007).

[128] R. Apreda, M. Maggiore, A. Nicolis and A. Riotto, Nucl. Phys. B **631**, 342 (2002).

[129] S. J. Huber and T. Konstandin, JCAP **0805**, 017 (2008).

[130] S. J. Huber and T. Konstandin, arXiv:0806.1828 [hep-ph].

[131] M. E. Peskin and D. V. Schroeder, *An Introduction to Quantum Field Theory*, Addison-Wesley, (1995).

[132] C. W. Chiang and E. Senaha, JHEP **0806**, 019 (2008).